ELECTROCHEMICAL DETECTION OF MODULATION OF EXOCYTOSIS FROM CHROMAFFIN CELLS MONITORED WITH AMPEROMETRY

Melissa Villanueva

A dissertation submitted to the faculty of the University of North Carolina at Chapel Hill in partial fulfillment of the requirements for the degree of Doctor of Philosophy in the Department of Chemistry

Chapel Hill

2006

Approved by
Advisor: Professor R. Mark Wightman
Reader: Professor James W. Jorgenson
Reader: Professor Paul B. Manis

ABSTRACT

MELISSA VILLANUEVA: Electrochemical Detection of Modulation of Exocytosis from Chromaffin Cells Monitored with Amperometry (Under the direction of Dr. R. Mark Wightman)

Biological intercellular communication necessitates rapid and efficient processes. Cells must be able to relay and receive messages rapidly and this is accomplished readily through exocytosis. Chemical messengers are packaged into membrane-bound organelles known as vesicles or granules, which fuse with the outer plasma membrane upon an increase in intracellular [Ca^{2+}] caused by influx from the extracellular space or from intracellular stores. Ca^{2+} increases can be effected through membrane depolarization or through receptor activation. The chemical messengers are then extruded into the extracellular space where they can bind to target cells and initiate a response. Because of the timescale of vesicular release and Ca^{2+} influx, it is necessary to utilize detection techniques that have sufficient temporal resolution. Additionally, the minute amounts that are secreted from these vesicles, whose dimensions are characteristically at the nanometer level, require a technique that possesses sensitivity sufficient to detect them. The electrochemical technique, constant potential amperometry, used in conjunction with carbon-fiber microelectrodes, offers excellent temporal and spatial resolution as well as sensitivity for electroactive chemical messengers. Moreover, the use of a fluorescent dye, fura-2 allows study of the Ca^{2+} dynamics occurring during exocytosis. Both amperometry and fluorescence measurements via fura-2 allow for the characterization of exocytosis in bovine and murine chromaffin cells.

Amperometry has been advantageous in studies involving chromaffin cells. Using this technique, an autoreceptor effect that causes facilitation in bovine chromaffin cells was revealed. Since this autoreceptor effect appears to occur on very rapid timescales, the exquisite temporal resolution of amperometry has permitted the observation and manipulation of this effect with minimal perturbation of the cells under study. In experiments involving genetically altered mice, amperometry revealed aspects of the exocytotic process that may be affected by specific proteins. In studies conducted on R6/2 mice that serve as models for Huntington's Disease, it was noted that vesicular quanta was significantly diminished. Also, in other experiments conducted in mice that lack the intracellular phosphoprotein, synapsin, vesicular release frequency was significantly enhanced. The studies mentioned demonstrate that amperometry with carbon-fiber microelectrodes is a powerful tool in studying exocytotic processes.

I dedicate this work to my family, especially to my parents, Federico Obach Villanueva, Jr. and Lorna Lacerna Villanueva, and to my sister, Samantha Lacerna Villanueva, who have always shown me extraordinary love and support.

ACKNOWLEDGMENTS

I would like to acknowledge the network of people who have helped me complete the work contained in this dissertation. I would like to thank Jorge Fuentealba for providing the protocol for the murine chromaffin cell preparation, which allowed for experiments to be done on cells from transgenic mice. I thank Dr. Michael A. Johnson for introducing me to work being done involving exocytosis and Huntington's Disease as well as Dr. Christy L. Haynes for data and the accompanying analysis of amperometric pre-spike features in that project. For the work done on synapsin, we collaborated with Dr. George J. Augustine and his group; I would particularly like to thank Dr. Qing Cheng, for providing transgenic mice and the plasmid used for transfection experiments. I also thank Dr. Wallace Ambrose for assistance in obtaining the electron micrographs of carbon-fiber microelectrodes. In obtaining data from adrenal slices, I thank Dr. Michael A. Johnson, Charles Miller, and Margie Ream. Finally, I thank Charles Miller, Jelena Petrovic, and Wendy Salmon for assistance in obtaining confocal images of adrenal slices.

TABLE OF CONTENTS

LIST OF TABLES

LIST OF FIGURES

LIST OF ABBREVIATIONS AND SYMBOLS

3-NP	3-nitropropionic acid
αMPT	α-methyl-*p*-tyrosine
ACh	acetylcholine
aCSF	artificial cerebrospinal fluid
Ag/AgCl	silver/silver chloride reference electrode
ATP	adenosine triphosphate
BSA	bovine serum albumin
CaMKI	calcium calmodulin-dependent kinase I
CaMKII	calcium calmodulin-dependent kinase II
CCD	charge-coupled device
CFME	carbon-fiber microelectrode
DAT	dopamine transporter
DMEM	Dulbecco's modified Eagle's medium
DMSO	dimethyl sulfoxide
EGFP	enhanced green fluorescent protein
EM	electron micrograph
EP	electropaint-insulated
EPI	epinephrine
EPSC	excitatory postsynaptic current
f_s	sampling frequency
FEEP	flame-etched electropaint-insulated
FSCV	fast scan cyclic voltammetry

GnRH	gonadotropin releasing hormone
HD	Huntington's disease
HEPES	N-[2-hydroxyethyl]piperazine-N'-[2-ethanesulfonic acid] buffer
hPLAP	human placental alkaline phosphatase
HPLC	high performance liquid chromatography
METH	methamphetamine
OT	oxytocin
OTLC	open tubular liquid chromatography
PAAH	polyacrylamide
PKA	cyclic AMP-dependent protein kinase
PLAP	placental alkaline phosphatase
Q	charge calculated from amperometric spike area
R6/2	transgenic mouse model line for Huntington's disease
S2/S1	second stimulus divided by first stimulus
SCH-23390	dopaminergic D1 receptor antagonist
SEM	standard error of the mean
SKF-38393	dopaminergic D1 receptor agonist
SNARE	soluble *N*-ethyl maleimide sensitive factor attachment protein receptor
$t_{1/2}$	halfwidth or width at half height of an amperometric spike
TH	tyrosine hydroxylase
TKO	triple (synapsin) knockout
VMAT1	vesicular monoamine transporter 1
WT	wildtype

CHAPTER ONE

MONITORING VESICLE MOBILIZATION DURING EXOCYTOSIS

INTRODUCTION

Exocytosis as a means of intercellular communication is active in many cell types such as neurons of the central and peripheral nervous systems, neuroendocrine cells, and mast cells. Tight regulation of exocytosis permits a highly efficient process. Neurotransmitters and other chemical messengers are packaged in membrane-bound organelles called secretory vesicles, which prevent inactivation of the chemical messengers and sustain a sufficient amount for rapid extrusion to the cell exterior. Chromaffin cells are often used as a model for studying exocytosis because of their robust nature; their shared precursors with neurons also allow for elucidation of some of the shared basic exocytotic mechanisms between the two cell types. Various techniques have been used to determine catecholamine content in chromaffin cells such as radioligand assays, liquid chromatography, patch clamp electrophysiology, and electrochemical techniques. A brief overview of these techniques will follow along with a brief description of some intracellular proteins that have been implicated in vesicle mobilization, which is one aspect of exocytotic regulation.

TECHNIQUES TO DETECT NEUROTRANSMITTERS AND EXOCYTOSIS

Radioligand assays

Various techniques have been employed to monitor vesicular release in secretory cells, particularly chromaffin cells of the adrenal medulla. Release assays utilizing isotopes

are also used to monitor exocytosis from a collection of cells. Such a release assay typically involves labeling cells with the tritiated analyte, e.g., [^{3}H]norepinephrine, treatment to induce exocytosis, and collection of samples to quantify using a scintillation counter (Trifaro and Lee, 1980). This method is useful to detect exocytosis over a population of cells.

Liquid chromatography

Separations methods such as HPLC can also detect species released from populations of lysed cells. HPLC provides good selectivity with the ability to detect multiple analytes and can be used to identify different analytes at one time from a particular population of cells depending on the nature of the detector. Electrochemical detectors rely on the redox properties of the analytes while UV and fluorescence detectors depend on their optical properties. Liquid chromatography has not only been useful in monitoring exocytosis from populations of cells, but it has been used to make measurements at single cells. With this method, an individual cell is generally lysed, an internal standard is introduced, and the supernatant is injected onto a column. Open tubular liquid chromatography (OTLC) has been used to analyze single neurons in the land snail, *Helix aspersa* (Kennedy and Jorgenson, 1989). The electrochemical detector used demonstrated a lower limit of 0.1 fmol in the voltammetric mode and 1 amol in the amperometric mode, exhibiting excellent sensitivity. To analyze chromaffin cells, the use of OTLC is not optimal as polar compounds such as norepinephrine are not sufficiently retained on the column. Instead, reversed-phase microcolumn chromatography coupled with electrochemical detection has been used to detect an average of 150 fmol catecholamine content from an individual chromaffin cell (Cooper et al., 1992). This technique demonstrates sufficient sensitivity and selectivity to

detect the epinephrine and norepinephrine molecules that are contained within chromaffin cells.

Patch clamp electrophysiology

Other techniques have been utilized to investigate more closely what occurs at an individual cell during exocytosis, such as patch clamp electrophysiology, fast-scan cyclic voltammetry (FSCV), and constant potential amperometry. The first technique, patch clamp electrophysiology, provides information about exocytosis occurring across the entirety of the cell. This technique detects exocytotic events as increases in the total capacitance arising from the plasma membrane. The cell is voltage clamped, and the capacitance value is extracted from current responses to voltage stimuli. Typically, the capacitance rises in a step-wise fashion, indicating the fusion of individual vesicles to the plasma membrane. A chromaffin cell has a typical resting capacitance of 5 pF (Neher and Marty, 1982); a dense core vesicle approximately 250-300 nm in diameter contributes an estimated 2.5 fF after fusion with the plasma membrane (Gillis, 1995). In the same vein, endocytosis of vesicular membrane can be detected as step-wise decreases in total capacitance. The ability to detect endocytosis leads to a potential problem in underestimating the amount of exocytosis that has occurred since endocytosis can convolute exocytotic information.

Fast-scan cyclic voltammetry, FSCV

FSCV used with carbon-fiber microelectrodes is a technique that can be used to monitor exocytosis from individual cells or from intact tissue. During FSCV, the potential range is scanned as a triangle waveform. Catecholamines can be detected by this technique

as they are oxidized and reduced during the potential scan. A plot of current versus potential, the cyclic voltammogram, can display the characteristic oxidation and reduction peaks of the analyte and can provide some selectivity in detection. For catecholamines detected at carbon-fiber microelectrodes, the oxidation peak is typically at +0.6 V and the reduction peak appears at -0.2 V (vs. a Ag/AgCl reference). FSCV is useful in identifying different analytes, but due to its limitations in selectivity, it is necessary to have knowledge of the tissue being tested to corroborate FSCV results. Additionally, different parameters such as treatment of the electrode surface, frequency of the waveform application to the electrode, and range of the potentials scanned can modify the sensitivity and the selectivity of FSCV. FSCV is also limited in its temporal resolution; when the identity of the analyte is of secondary importance and improved temporal resolution is sought, amperometry is used to monitor vesicular release.

The following text will concentrate on amperometry, an electrochemical technique used to monitor vesicular release, and fluorescent detection of intracellular Ca^{2+} dynamics that occur during exocytosis. There will also be a brief overview of vesicle mobilization: a few proteins implicated in reserve pool maintenance will be addressed along with facilitation of vesicular release achieved through a possible autoreceptor effect.

Constant potential amperometry

Exocytotic cellular signaling has been studied with the electrochemical technique, constant potential amperometry, at various cell types such as adrenal medullary chromaffin cells, beta cells of the pancreas, peritoneal mast cells, and retinal neurons. Because amperometry exhibits poor selectivity, general knowledge of anatomy and cell morphology is

necessary to reasonably identify the analyte of interest. If the tissue displays a high degree of heterogeneity, fluorescent labeling of proteins uniquely associated with the cells under study can be useful.

In spite of its poor selectivity, amperometry offers the advantage of excellent temporal resolution, which permits kinetic studies of vesicular content extrusion. Because the electrode sensor used in amperometry is held at a constant potential that is sufficient to oxidize the analyte molecule, the oxidation of a vesicle's contents is shown to correspond to an amperometric current spike (Figure 1.1). The area, Q, of such an amperometric spike is proportional to the number of molecules oxidized as defined by Faraday's law, $Q = nFm$, where Q is the charge in coulombs, n is the number of electrons involved in the redox reaction per molecule, F is Faraday's constant, and m is the number of moles of analyte. Chromaffin cells typically contain approximately 0.5 M catecholamine within a single vesicle, which corresponds to an estimated 3×10^6 molecules. Another spike parameter that provides information about extrusion time is the halfwidth or $t_{1/2}$. The characteristic halfwidth for an amperometric spike obtained from an exocytosing chromaffin cell demonstrates an extrusion time on the order of milliseconds. Amperometry not only demonstrates the ability to probe current spike parameters that are related to vesicular content extrusion characteristics such as Q and $t_{1/2}$, but amperometry can also be employed to study vesicle mobilization through spike frequency. The total number of events elicited from a particular stimulus or the frequency of an exocytotic burst can reveal aspects of the interplay between vesicle pools.

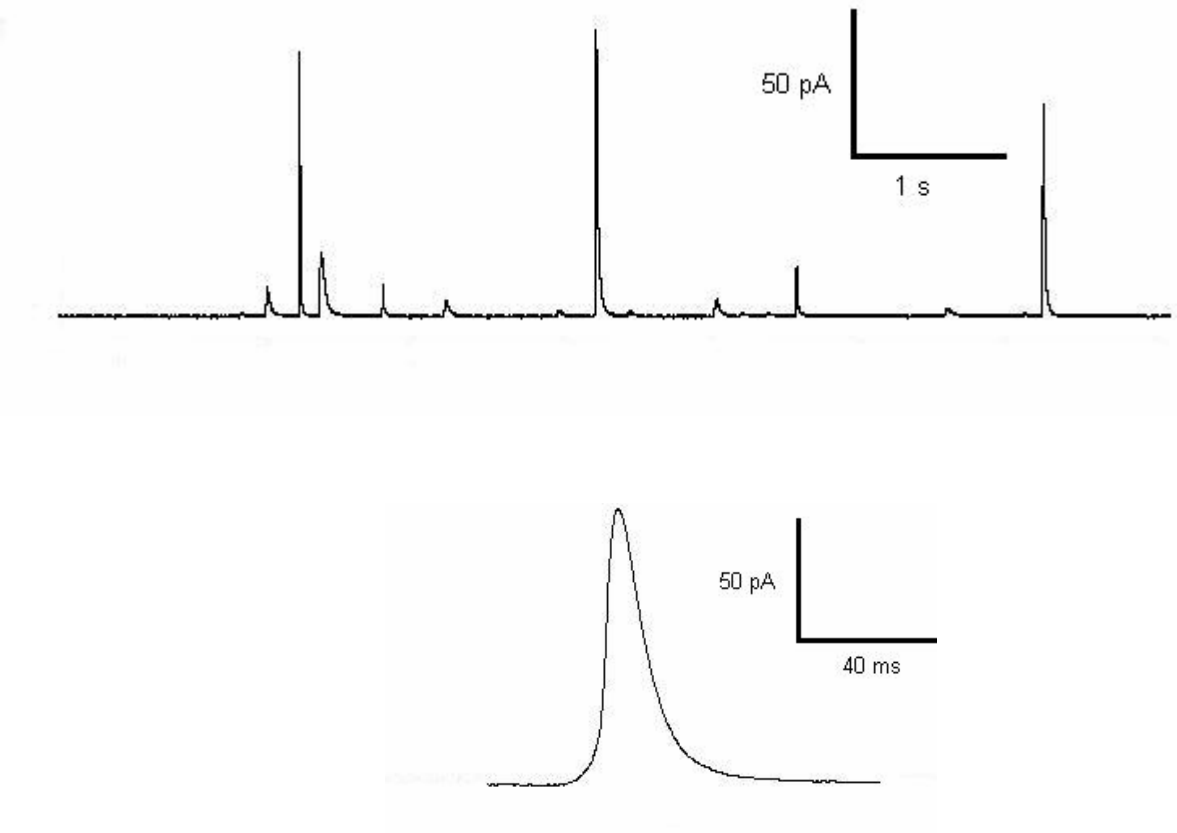

Figure 1.1. Amperometric recording of vesicular release. (A) An amperometric recording of vesicular release events at a bovine chromaffin cell. Each current spike corresponds to a vesicle release event. (B) A larger view of an individual amperometric spike.

Amperometric spike characteristics

As described earlier, amperometry is able to detect vesicle extrusion events with superior temporal resolution. Upon stimulation with high K^+ to depolarize the membrane and open voltage-gated channels, Ca^{2+} enters the cell and triggers exocytosis. Vesicular release events are stochastic. The distribution of the integrated areas of amperometric spikes that signal the extrusion of vesicular contents is not Gaussian. Instead, the integrated spike area, Q, and the width at half maximum, $t_{1/2}$, follow a skewed distribution (Figure 1.2), skewing the distribution toward smaller Q and $t_{1/2}$ values. Because Q can be related to the number of molecules in a discrete volume, $Q^{1/3}$ can be correlated to the radius of the vesicle. Plotting a histogram of $Q^{1/3}$ can then yield a Gaussian distribution (Wightman et al., 1995a). Moreover, plotting the cube root of $t_{1/2}$ can also yield a Gaussian distribution. Using both the cube roots of both Q and $t_{1/2}$ allows for the calculation of mean values that can be compared across experimental groups.

Instrumentation

Because amperometry is being used to probe vesicular release at the single cell level, excellent instrumentation and data collection techniques are sought. It is necessary that the experimental setup is maintained in a Faraday cage with proper grounding to further reduce noise. A low-noise potentiostat is also crucial for these measurements. As signals at individual chromaffin cells are recorded in the range of pA to hundreds of pA, a high signal-to-noise ratio is vital. The potentiostat used (Axopatch 200B, Axon Instruments, Union City,

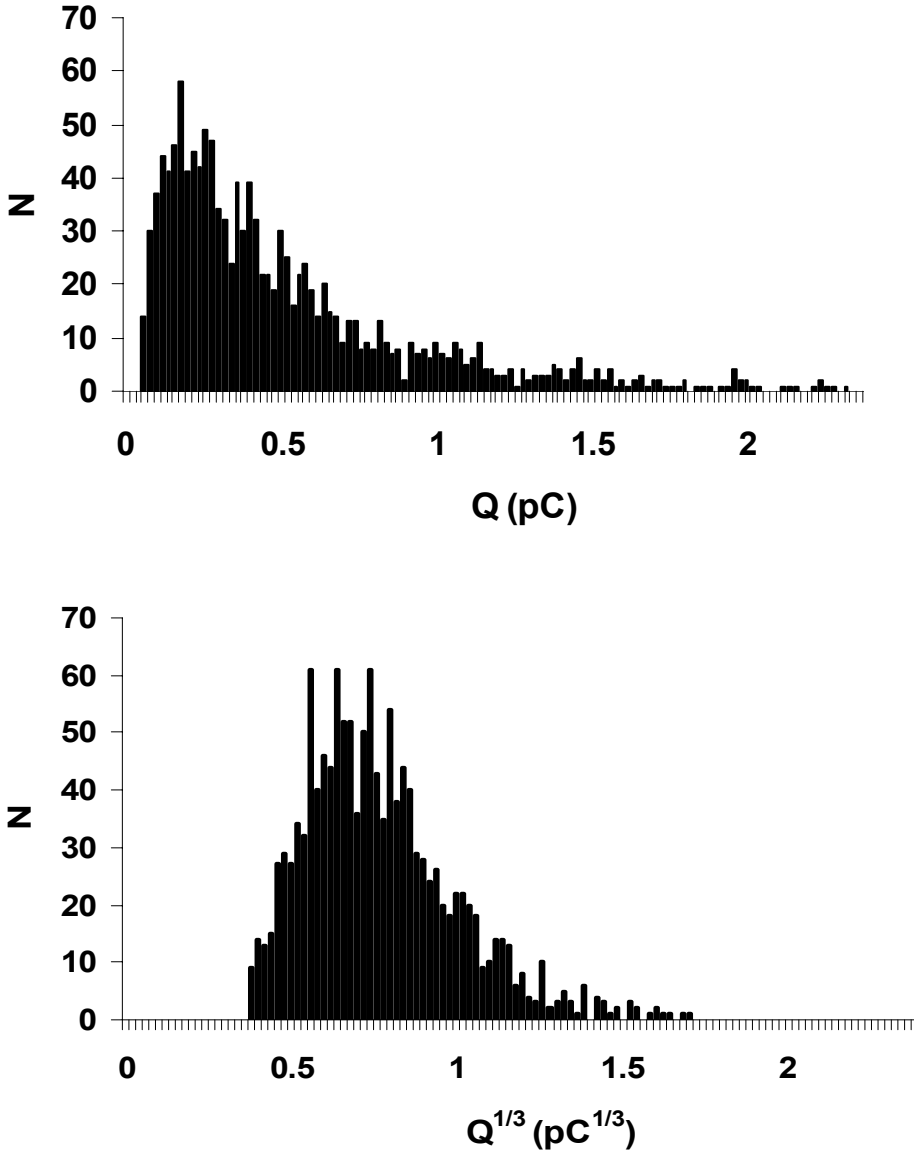

Figure 1.2. Distribution of Q and $Q^{1/3}$. (A) Distribution of Q from current spikes; note the skew in the distribution (B) Distribution of $Q^{1/3}$ displays a more Gaussian shape.

CA) must generate minimal noise. In the experiments presented, the resistive mode of feedback is used in the amplifier. The potentiostat generates minimal noise such that it is limited mainly to thermal noise and the noise arising from individual components such as the electrode itself. Additionally, filtering prior to digitization is necessary to prevent noise that arises from aliasing. Digital filters cannot remove aliasing effects once they are introduced into the signal. Frequencies equal to or greater than one half the sampling rate, f_s, must be eliminated. Thus, the analog signal is filtered with a low-pass Bessel filter at 5 kHz and digitized at a sufficiently high collection rate (f_s = 10 kHz).

Analog data that has been filtered and digitized is filtered again using a digital Gaussian low-pass filter. Data obtained for the experiments listed in this document using chromaffin cells have been filtered at 400 Hz. Filtering is desired to increase the signal-to-noise ratio and increase the number of events detected, but overfiltering can distort the resulting signal: the amplitude of the amperometric spike is decreased and the halfwidth is increased (Figure 1.3) (Hochstetler et al., 2000). Therefore, a balance is sought between enhancement of the signal and reduction of signal distortion. Lower cutoff frequencies are typically used with amperometric recordings obtained with neurons in order to maximize the detection of individual current spikes as the signals are lower than those obtained from chromaffin cells.

Electrode fabrication

Since spatial resolution is also vital to making measurements at single cells, fabrication of electrodes of micron dimensions is desired. Traditionally, carbon-fiber disk electrodes were fabricated with T-650 fibers and beveled to create a 45º angled surface,

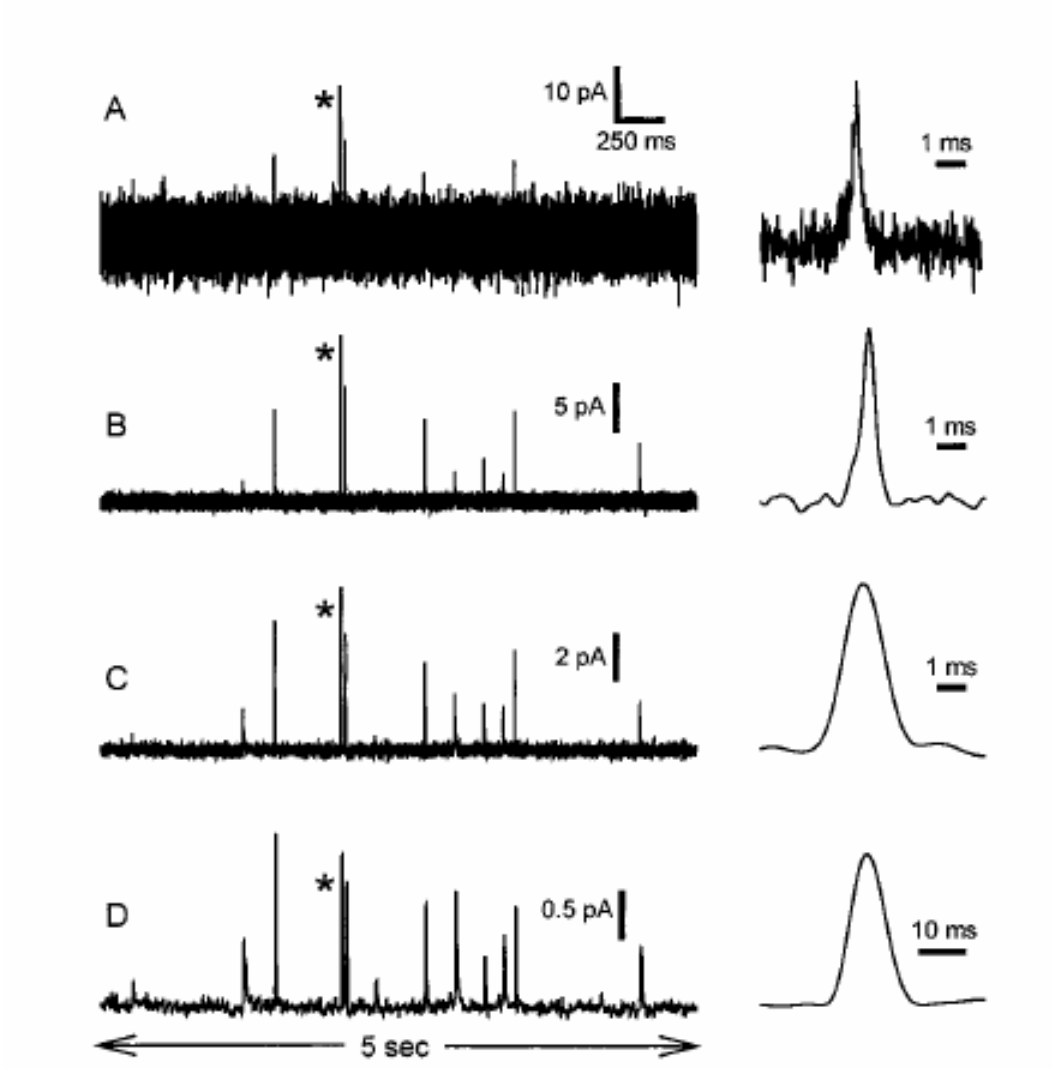

Figure 1.3. Effects of low pass filtering on current spikes. A trace collected from a dopamine cell filtered at (A) 10 kHz (analog 4-pole Bessel) (B) 1 kHz (digital 8-pole Bessel) (C) 200 Hz (digital 8-pole Bessel) (D) 40 Hz (digital 8-pole Bessel) (Hochstetler et al., 2000)

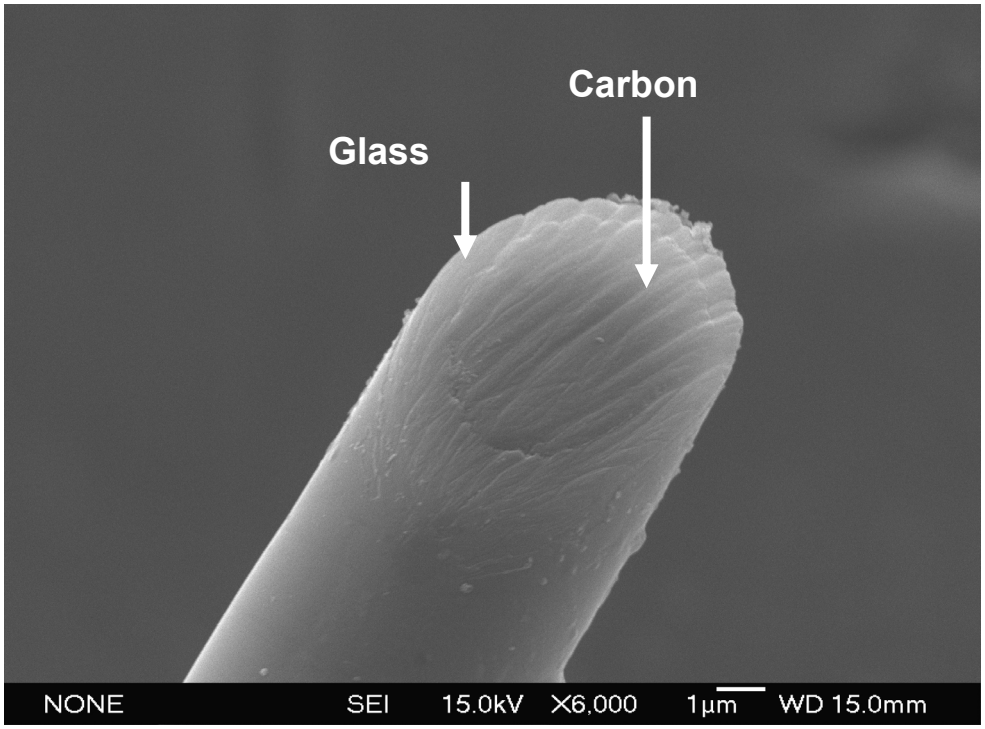

Figure 1.4. A scanning electron micrograph a disk electrode. A T-650 carbon-fiber microelectrode disk with an insulating layer of glass. Its diameter is ~ 6 microns.

which is ideal for placing in direct apposition to a cell. These microelectrodes are 6 μm in diameter and sample approximately 6% of the cellular surface (Figure 1.4). Other techniques to reduce the dimensions of the disk electrode have been investigated. In place of the glass insulation proximal to the sensing surface, another insulating coating, such as electropaint, may be used to provide thinner insulation. The insulating layer of electropaint is applied to the electrode by electrodeposition (Schulte and Chow, 1996). Anodic electrophoretic paint (PPG, ZQ84-3225) is used to coat the electrode. The paint is composed of polyacrylamide (PAAH) and excess base in order to render it soluble in water. In order to deposit the polyacrylamide onto the electrode surface, a positive DC potential is applied to the carbon-fiber electrode, which will oxidize water in the immediate vicinity (Eqn 1).

$$2H_2O \leftrightarrow O_2 + 4H^+ + 4e^- \qquad \textbf{Eqn 1.1.}$$

The result is a shift in the pH to a more acidic value, which subsequently shifts the polyacrylamide equilibrium such that the insoluble form of polyacrylamide is favored (Eqn 2) (Conyers and White, 2000).

$$PAA^- + H^+ \leftrightarrow PAAH \qquad \textbf{Eqn. 1.2.}$$

In addition to a thinner insulating layer, the carbon fiber itself may be etched, either by flame or by electrochemical means (Schulte and Chow, 1998), to decrease its dimensions. Combining both an etched carbon fiber with a slim layer of insulation allows for sensing at specific regions of the cell and can identify exocytotic "hotspots" (Schroeder et al., 1994). Though etched electrodes may provide greater spatial resolution, the sensitivity of the electrode is also compromised and must be taken into account. Etched and electropainted disk electrodes may potentially allow for measurements with greater spatial resolution to be

taken at nerve terminals in perfused brain tissue in conjunction with fluorescent labeling to clearly identify the nerve terminals of interest.

Fluorescent detection of intracellular Ca^{2+} dynamics

Use of the fluorescent dye, fura-2

Because exocytosis is Ca^{2+} dependent, a fluorescent Ca^{2+} dye has proven useful in monitoring Ca^{2+} dynamics that accompany vesicular release (Grynkiewicz et al., 1985). Fura-2 has been used to study changes in intracellular [Ca^{2+}] during exocytosis (Figure 1.5; (Grynkiewicz et al., 1985). Typically, this dye is used to obtain ratiometric measurements in order to correct for cell-to-cell differences. Excitation of the Ca^{2+}-bound fura-2 is accomplished at 340 nm while free and unbound fura-2 is excited at 380 nm; emission is measured at 510 nm. Use of these two excitation wavelengths gives the maximal dynamic range for Ca^{2+} measurements within the cell. Ratiometric measurements also allow for detection of [Ca^{2+}] within the cell independent of cell thickness, dye concentration, intensity of the excitation source, and sensitivity of the camera used (Moore et al., 1990). Fura-2 also has a dissociation constant, K_d, of 0.15 μM, which makes this dye appropriate for studying Ca^{2+} dynamics within the cell. Intracellular [Ca^{2+}] from resting levels (~100 nM) to exocytotic levels (approximating 1 μM) can be detected with confidence; concentrations much greater than 1 μM cannot be monitored as measurements with fura-2 depart from the linear relationship. Because of this departure from linearity, global cellular changes in [Ca^{2+}] are monitored using fura-2 as opposed to the isolated sites proximal to the plasma membrane as local [Ca^{2+}] may approach much higher values (Neher and Zucker, 1993; Aharon et al., 1994).

Fura-2 binds to Ca^{2+} in a 1:1 ratio, which simplifies calibration. The equation listed below is used to convert ratiometric measurements to $[Ca^{2+}]$.

$$[Ca^{2+}] = K_d \frac{(R - R_{\min})}{(R_{\max} - R)} * \frac{F_{380\max}}{F_{380\min}} \qquad \textbf{Eqn. 1.3}$$

The variables crucial to this calibration are K_d, which is the dissociation constant of fura-2; R, which is the ratio value obtained from the raw data; R_{min}, which is the ratio measured with no free Ca^{2+} present in the solution; R_{max}, which is the ratio measured in a solution of saturating $[Ca^{2+}]$; F_{380max}, which is the fluorescence observed with 380 nm excitation with no free Ca^{2+} present in solution; and F_{380min}, which is the fluorescence observed with 380 nm excitation in a solution containing saturating $[Ca^{2+}]$. This calculation, however, includes several assumptions. First, it is assumed that the fura-2 molecules that have entered the cell are completely de-esterified. Second, fura-2 is assumed to remain in the cytosol and not become compartmentalized in the organelles. The third assumption is that the fluorescent properties of the molecule remain the same in the cytosol of the cell as in the calibrating solution; the K_d value is also unaffected by intracellular factors such as viscosity. The fourth assumption is that any observed fluorescence originates solely from de-esterified fura-2 molecules.

Measurements using fura-2 do have limitations. Fura-2 molecules can become compartmentalized in extracytosolic space such as in mitochondria (Moore et al., 1990). Use of high concentrations of fura-2 (> 100 μM) can also affect calcium buffering within the cell. Leakage of the dye from the cell can also lead to higher background fluorescence.

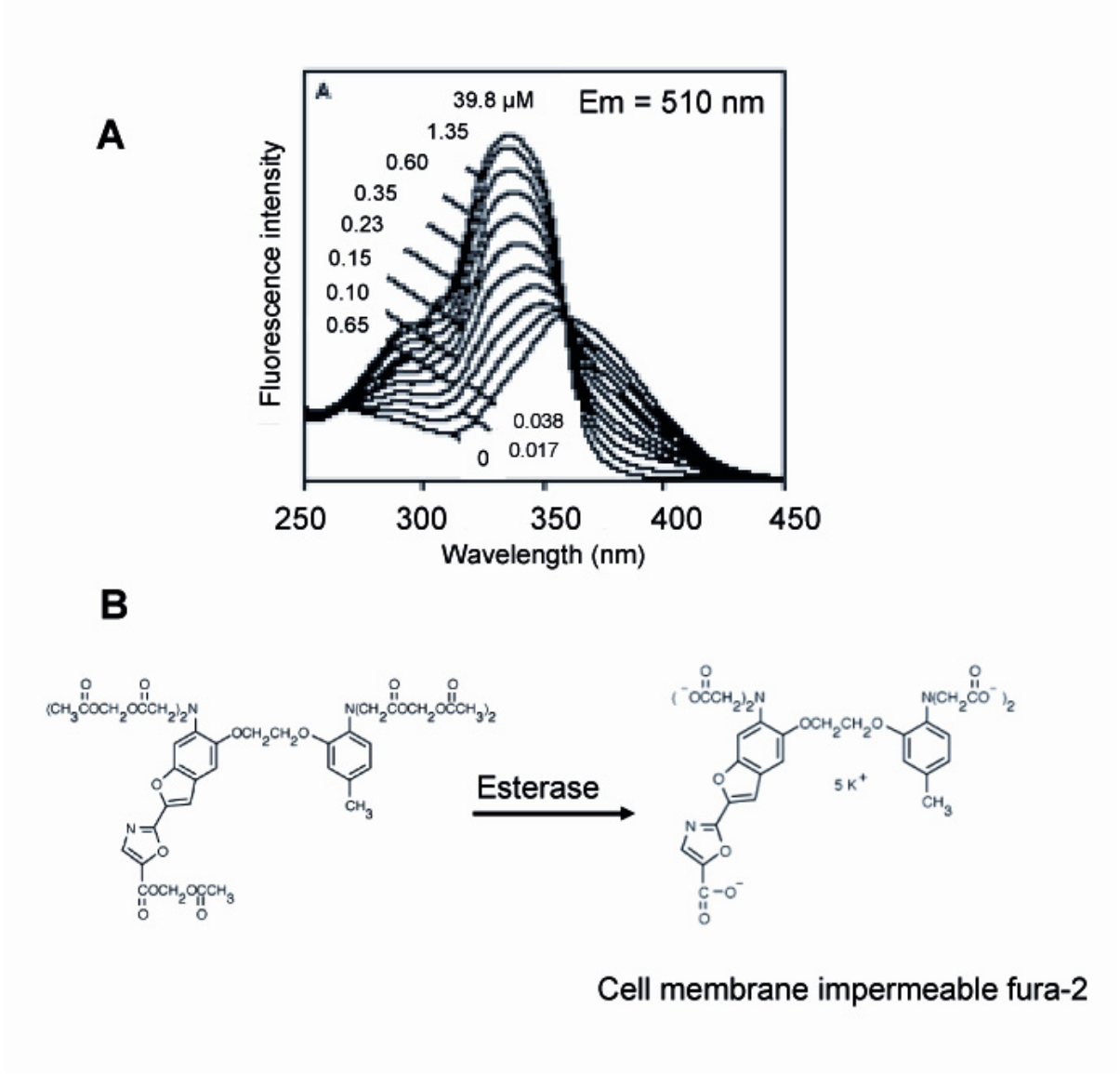

Figure 1.5. Excitation spectra and molecular structure of fura-2. (A) Excitation spectra of fura-2 over different [Ca2+] Emission is measured at 510 nm (B) Molecular structure of esterified fura-2 and its de-esterified form (Grynkiewicz et al., 1985).

Inevitably, it will be impossible to completely prevent these problems, but if the appropriate concentration of fura-2 is used, they can be minimized.

Instrumentation

Ratiometric fura-2 measurements are obtained on an epifluorescence system mounted on an inverted microscope. Dual excitation is achieved by software control of a galvanometer, which directs the light from a xenon arc lamp source via two mirrors alternately through the 340 nm and 380 nm filters. Emission is measured at 510 nm using a CCD digital camera, which provides high quantum efficiency, high signal-to-noise, and high dynamic range.

Conclusion

Techniques have been developed to examine processes that occur during exocytosis in order to better understand this process of intercellular communication. Improvements in sensitivity have permitted progress from measurements of exocytosis at cell populations to observations at single cells and allowed for greater understanding of individual components of the exocytotic process. Such aspects such as how the vesicle pools are mobilized and regulated can be studied in greater detail.

VESICLE POOL REGULATION

Vesicle mobilization is regulated by the maintenance of different vesicle pools. Vesicle pools have been studied in neurons and chromaffin cells. The total number of vesicles contained in the typical chromaffin cell is approximately 10,000 (Figure 1.6A)

(Ungar and Phillips, 1983). There have been three vesicle pools defined (Figure 1-6B) (Voets et al., 1999; Rizzoli and Betz, 2005). Roughly 1% of the vesicles is located at the plasmalemma and constitutes the readily releasable pool. This pool contains vesicles that fuse immediately upon the exocytotic trigger of sufficient Ca^{2+} influx. The second vesicle pool is the recycling pool. This pool contains vesicles that have been retrieved from the plasmalemma by fast endocytosis and constitutes up to 10% of the total number of vesicles. The recycling pool incorporates vesicles into the cell membrane after exocytosis and retrieves them through fast endocytosis as opposed to the slow clathrin-coated endocytosis that also recovers vesicular membranes from the plasmalemma. The third vesicle pool is the reserve pool, which contains an estimated 90% of the vesicles contained within the cell. These vesicles are presumed to be at a distance of 150-200 nm from the plasmalemma and replenish the readily releasable and recycling pools as they are depleted. It is interesting to note that the reserve pool is believed to contain the older vesicles while newer vesicles constitute the readily releasable pool (Wiegand et al., 2003). It would be reasonable to assume that the principal means of controlling vesicle mobilization is through the reserve pool. By selectively permitting vesicles to replenish the readily releasable and recycling pools, overall regulation of exocytosis is readily achieved.

Proteins implicated in reserve pool maintenance

F-actin and scinderin

In chromaffin cells, the cell cortex, which contains F-actin filaments, forms a barrier that precludes granules from reaching exocytotic sites (Burgoyne and Cheek, 1987). The F-

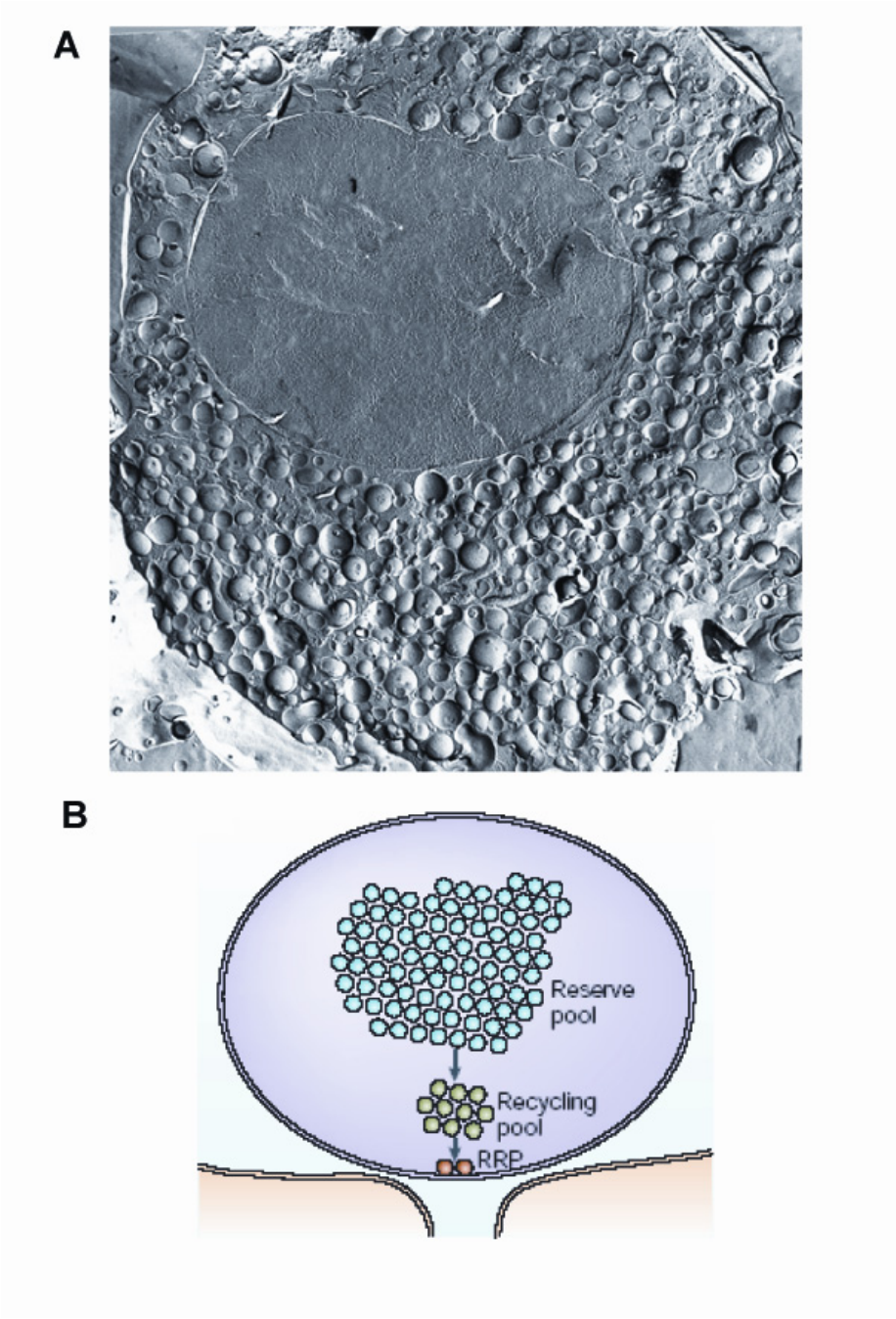

Figure 1.6. Vesicle pools. (A) Electron micrograph of a chromaffin cell, which contains approximately 10,000 vesicles (Image by Wolfgang Schmidt of the University of Innsbruck). (B) Diagram of synaptic vesicle pools. The readily releasable pool (RRP) constitutes ~1% of total vesicles and is located at the plasma membrane. The recycling pool contains ~10% of vesicles and is quickly recycled back into the RRP. The reserve pool contains the vast majority of vesicles, which are sequestered by the actin cytoskeleton (Rizzoli and Betz, 2005).

actin network is believed to be the principal means of sequestering the reserve pool of vesicles. Disruption of this network would allow vesicles to be mobilized to the plasmalemma to dock, prime, and fuse with the plasmalemma upon the exocytotic trigger.

Scinderin is a protein that has been implicated in severing actin filaments (Rodriguez et al. 1990). It is believed to be a Ca^{2+}-dependent molecular switch in the machinery of vesicle mobilization because it possesses three actin binding sites, two of which are implicated in actin disassembly (Marcu et al., 1994), and the third of which promotes association of actin (Marcu et al., 1998). In experiments where full length recombinant scinderin was introduced to chromaffin cells, F-actin disassembly was augmented; peptides derived from these two actin binding sites were then introduced and inhibited release (Zhang et al., 1996). Experiments in which full length recombinant scinderin or the peptide only containing the third F-actin binding site were introduced to cells, actin nucleation accelerated significantly compared to experiments lacking these peptides (Marcu et al., 1998). Moreover, experiments in which cells were incubated with recombinant scinderin, which was truncated to lack the first two actin-binding sites, showed no increase in catecholamine release in digitonin-permeabilized cells (Zhang et al. 1996). The severing activity of scinderin is also Ca^{2+}-dependent as it increases with Ca^{2+} concentration (Vitale et al., 1991). The nucleation activity of scinderin, conversely, is Ca^{2+}-independent (Marcu et al., 1998). This interplay between Ca^{2+} dependence and independence may serve as the mechanism by which scinderin acts as a molecular switch. During the influx of Ca^{2+} that occurs during exocytosis, the Ca^{2+}-dependent severing activity of scinderin may be dominant. As the Ca^{2+} levels are buffered and returned to near resting level, the Ca^{2+}-independent nucleation activity becomes the prevailing action of scinderin.

Vesicular tethers in chromaffin cells: α-actinin and α-fodrin

There have been several proteins believed to be involved in maintaining the reserve pool in chromaffin cells. Other proteins, which have been considered to be candidates as vesicular tethers between secretory vesicles and the actin network in chromaffin cells, are α-actinin (Jockusch et al., 1977; Aunis et al., 1980) and α-fodrin (Perrin and Aunis, 1985; Perrin et al., 1987). Introduction of antibodies against α-fodrin into permeabilized bovine chromaffin cells partially inhibited Ca^{2+}-dependent catecholamine vesicular release suggesting a role played by α-fodrin in maintaining vesicles to the actin cytoskeleton and presumably sequestering vesicles in the reserve pool compartment (Perrin et al., 1987).

Synapsin

In neurons, the protein implicated in sequestering vesicles in the reserve pool is synapsin, which has a putative role in tethering vesicles to the actin cytoskeleton. This protein associates with the cytoplasmic surface of synaptic vesicles (De Camilli et al., 1983). There are three isoforms of synapsin: I, II, and III. Increased phosphorylation of synapsin accompanies Ca^{2+}-dependent vesicular release. Synapsin I and II are physiological substrates for cyclic AMP-dependent protein kinase (PKA) and calcium calmodulin-dependent kinase I (CaMKI) while only synapsin I is a physiological substrate for calcium calmodulin-dependent kinase II (CaMKII) (Greengard et al., 1993). The PKA and CaMKI phosphorylation site is also present in synapsin III (Hosaka et al., 1999); this isoform also possesses similar sites that may be phosphorylated by CaMKII, but accessibility for phosphorylation is uncertain (Hilfiker et al., 1999). Synapsin phosphorylation at the PKA/CaMKI site, which is conserved among all of the known synapsins (Hilfiker et al.,

1999), may dissociate synapsin from synaptic vesicles (Hosaka et al., 1999). A role for this site is not clearly known as other work has shown that introduction of a peptide that derived from the domain containing this site, inhibited release in a phosphorylation-dependent manner while having no effect on synapsin-actin and synapsin-vesicle interactions (Hilfiker et al., 2005).

Recent *in vivo* studies done on mice in which all three isoforms had been deleted (TKO) have shown that cocaine, in addition to its traditional function as a dopamine transporter (DAT) inhibitor, is able to increase dopamine release by mobilizing the synapsin-dependent reserve pool (Venton et al., 2006). In order to isolate cocaine-induced release from the readily releasable pool, long depolarizing trains were applied following administration of α-methyl-*p*-tyrosine (αMPT) to inhibit dopamine synthesis that would maintain the readily releasable pool. The readily releasable pool was reduced to 25% of the pre-cocaine value. Shorter depolarizing trains were then applied to probe the effect of cocaine on release from the reserve pool. WT mice showed enhanced release with cocaine. Conversely, TKO mice showed an inability to recover release upon the shorter depolarizing trains.

Most of the studies on synapsin have been done with the isoform synapsin I and its role in vesicular release. Experiments in the squid giant axon showed that introduction of dephosphorylated synapsin I decreased transmitter release while introduction of CaMKII increased release (Llinas et al., 1991). CaMKII promotes the phosphorylation of synapsin I, which allows the protein to release the vesicles to move freely to the plasma membrane for fusion upon exocytotic stimuli. Additionally, introduction of a peptide derived from domain E of squid synapsin I into a squid giant axon exhibits disruption of synapsin I function

(Hilfiker et al., 1998). This treatment reduces the number of synaptic vesicles available in the cytoplasm presumably because synapsin I that is bound to vesicles is unable to associate with the actin cytoskeleton (Hilfiker et al., 2005). Interestingly, domain E is conserved among the "a"-type isoforms (Hilfiker et al., 1999), and may have an important role in vesicle mobilization as well. Synapsin I has also been found in the rat adrenal medulla, but only in acetylcholine (ACh) nerve terminals that form synapses with chromaffin cells (Senda et al., 1991). Synapsin I, therefore, appears only to associate with synaptic vesicles.

Synapsin III is the most recently identified isoform and is believed to be found solely in nerve terminals as well. This isoform is assumed to have a unique function from the synapsin I and II isoforms. Feng et al. showed that synapsin III appears to modify release by limiting the size of the recycling pool while leaving priming unperturbed (Feng et al., 2002).

The only isoform that has been found in chromaffin cells, synapsin II (previously named protein III) (Browning et al., 1987), has also been implicated in vesicle mobilization. Synapsin II is the only member of the synapsin family that appears to associate with dense-core granules. In response to depolarizing secretagogues such as acetylcholine, potassium, veratridine, and barium, bovine chromafffin cells exhibited increased phosphorylation of synapsin II (Haycock et al., 1988). Studies conducted by Firestone and Browning also showed that nicotinic and histaminergic stimulation of bovine chromaffin cells increased synapsin II phosphorylation along with catecholamine release (Firestone and Browning, 1992).

Facilitation of vesicular release via an autoreceptor

Work has also been done addressing a natural facilitation of vesicular release that occurs at short intervals in bovine chromaffin cells. This may be the result of D1-like autoreceptor activation. Artalejo et al. demonstrated the facilitation of Ca^{2+} current in bovine chromaffin cells as a result of D1 receptor activation (Artalejo et al., 1990). It was then postulated that facilitation induced in Ca^{2+} current could also cause facilitation in vesicular release. Data showing D1 agonist-induced facilitation in bovine chromaffin cells, as well as inhibition of this effect using a D1 antagonist, is shown in chapter two. Catecholamine binding to the D1 receptor is able to act on short timescales, effecting facilitation.

Conclusion

Exocytosis is a complex process which requires many proteins and other components to mediate regulation. One aspect of exocytotic regulation, vesicle pool mobilization, is regulated by various proteins. The intricate interplay between these components promotes the efficiency of exocytosis. Methods to monitor vesicular release and Ca^{2+} dynamics allow us to probe further into the exocytotic process in order to gain a clearer understanding of intercellular communication.

THESIS OVERVIEW

Chapter 2 will address the autoreceptor effects observed in bovine adrenal medullary chromaffin cells. There is also an extensive comparison of temperature and chemical stimulation conditions in order to determine the optimal experimental conditions for use in the subsequent autoreceptor studies. Traditionally, room temperature (25ºC) and longer

stimuli (3-5 s) were used in experiments on chromaffin cells. Paired pulse stimuli were applied to the cells and compared at 25ºC and at 37ºC. Effects of chemical stimuli with durations shorter than those used previously were also studied. The subsequent autoreceptor studies have been conducted in order to determine whether the D1 receptor-mediated facilitation of Ca^{2+} influx seen in earlier work by Artalejo et al. also mediates facilitation in catecholamine release (Artalejo et al., 1990). The use of physiological temperature and shorter chemical stimuli revealed a naturally occurring facilitation present in bovine chromaffin cells, which was then used to explore the effects of D1 agonists and antagonists on effecting or inhibiting facilitation.

Chapter 3 will focus on the studying the release characteristics in chromaffin cells of a transgenic mouse model for Huntington's disease. In brain slices of R6/2 mice, it had been demonstrated that dopaminergic release was diminished as compared to their wildtype littermates (Johnson et al. 2006). The work presented in chapter 3 examined catecholaminergic release in chromaffin cells of both R6/2 and wildtype mice. The vesicular release characteristics were studied using constant potential amperometry. In chromaffin cells obtained from R6/2 mice, vesicular content appeared diminished whereas release frequency was not compared to their WT littermates. In order to elucidate a mechanism for the decrease in exocytotic release, a mitochondrial toxin, 3-nitropropionic acid (3-NP), was also applied to R6/2 and WT chromaffin cells in order to probe the hypothesis that impairment of ATP production was the principal mechanism behind the diminished release.

Chapter 4 will examine the role of the intracellular phosphoprotein, synapsin, in vesicular release. Synapsin is believed to be a vesicular tether to the actin cytoskeleton. For these studies, genetically altered mice were used in which the three known isoforms of

synapsin had been knocked out (TKO). These experiments also utilized chromaffin cells, which are known to express only synapsin II. The work presented here showed no difference in vesicular extrusion characteristics as revealed by amperometry. However, upon stimulation with high K^+, chromaffin cells from TKO mice released a significantly higher number of vesicles compared to chromaffin cells of their WT littermates. Since synapsin is believed to have a role in regulating vesicle mobilization by controlling sequestration of the reserve pool, it is reasonable to assume that the absence of this protein would not interfere with vesicular release characteristics but would instead increase the number of vesicles that are free to move to the plasma membrane of the cell.

REFERENCES

Aharon S, Parnas H, Parnas I (1994) The magnitude and significance of Ca^{2+} domains for release of neurotransmitter. Bulletin of Mathematical Biology 56:1095-1119.

Artalejo CR, Ariano MA, Perlman RL, Fox AP (1990) Activation of facilitation calcium channels in chromaffin cells by D_1 dopamine receptors through a cAMP/protein kinase A-dependent mechanism. Nature 348:239-242.

Aunis D, Guerod B, Bader M-F, Cieselski-Treska J (1980) Immunocytochemical and biochemical demonstration of contractile proteins in chromaffin cells in culture. Neuroscience 5:2277.

Bath BD, Michael DJ, Trafton BJ, Joseph JD, Runnels PL, Wightman RM (2000) Subsecond adsorption and desorption of dopamine at carbon-fiber microelectrodes. Analytical Chemistry 72:5994-6002.

Browning MD, Huang C-K, Greengard P (1987) Similarities between Protein IIIa and Protein IIIb, two prominent synaptic vesicle-associated phosphoproteins. Journal of Neuroscience 7:847-856.

Burgoyne RD, Cheek TR (1987) Reorganisation of peripheral actin filaments as a prelude to exocytosis. Bioscience Reports 7:281-288.

Conyers JL, White HS (2000) Electrochemical characterization of electrodes with submicrometer dimensions. Analytical Chemistry 72:4441-4446.

Cooper BR, Jankowski JA, Leszczyszyn DJ, Wightman RM, Jorgenson JW (1992) Quantitative determination of catecholamines in individual bovine adrenomedullary cells by reversed-phase microcolumn liquid chromatography with electrochemical detection. Analytical Chemistry 64:691-694.

De Camilli P, Harris SMJ, Huttner WB, Greengard P (1983) Synapsin I (Protein I), a nerve terminal-specific phosphoprotein. II. Its specific association with synaptic vesicles demonstrated by immunocytochemistry in agarose-embedded synaptosomes. Journal of Cell Biology 96:1355-1373.

Feng J, Chi P, Blanpied TA, Xu Y, Magarinos AM, Ferreira A, Takahashi RH, Kao H-T, McEwen BS, Ryan TA, Augustine GJ, Greengard P (2002) Regulation of neurotransmitter release by synapsin III. Journal of Neuroscience 22:4372-4380.

Firestone J, Browning M (1992) Synapsin II phosphorylation and catecholamine release in bovine adrenal chromaffin cells: additive effects of histamine and nicotine. Journal of Neurochemistry 58:441-447.

Gillis KD (1995) Techniques for membrane capacitance measurements. In: Single-channel Recording, 2nd Edition (Sakmann B, Neher E, eds). New York: Plenum Press.

Greengard P, Valtorta F, Czernik AJ, Benfenati F (1993) Synaptic vesicle phosphoproteins and regulation of synaptic function. Science 259:780-785.

Grynkiewicz G, Poenie M, Tsien RY (1985) A new generation of Ca^{2+} indicators with greatly improved fluorescence properties. Journal of Biological Chemistry 260:3440-3450.

Haycock JW, Greengard P, Browning MD (1988) Cholinergic regulation of protein III phosphorylation in bovine adrenal chromaffin cells. Journal of Neuroscience 8:3233-3239.

Hilfiker S, Schweizer FE, Kao H-T, Czernik AJ, Greengard P, Augustine GJ (1998) Two sites of action for synapsin domain E in regulating neurotransmitter release. Nature Neuroscience 1:29-35.

Hilfiker S, Pieribone VA, Czernik AJ, Kao H-T, Augustine GJ, Greengard P (1999) Synapsins as regulators of neurotransmitter release. Philosophical transactions of the Royal Society of London Series B, Biological sciences 354:269-279.

Hilfiker S, Benfenati F, Doussau F, Nairn AC, Czernik AJ, Augustine GJ, Greengard P (2005) Structural domains involved in the regulation of transmitter release by synapsins. Journal of Neuroscience 25:2658-2669.

Hochstetler SE, Puopolo M, Gustincich S, Raviola E, Wightman RM (2000) Real-time amperometric measurements of zeptomole quantities of dopamine released from neurons. Analytical Chemistry 72:489-496.

Hosaka M, Hammer RE, Sudhof TC (1999) A phospho-switch controls dynamic association of synapsins with synaptic vesicles. Neuron 24:377-387.

Jockusch BM, Burger MM, Da Prada M, Richards JG, Chaponnier C, Gabbiani G (1977) α–Actinin attached to membranes of secretory vesicles. Nature 270:628-629.

Kennedy RT, Jorgenson JW (1989) Quantitative analysis of individual neurons by open tubular liquid chromatography with voltammetric detection. Analytical Chemistry 61:436-441.

Llinas R, Gruner JA, Sugimori M, McGuinness TL, Greengard P (1991) Regulation by synapsin I and Ca^{2+}-calmodulin-dependent protein kinase II of transmitter release in squid giant synapse. Journal of Physiology 436:257-282.

Marcu MG, Rodriguez del Castillo A, Vitale ML, Trifaro J-M (1994) Molecular cloning and functional expression of chromaffin cell scinderin indicates that it belongs to the family of Ca^{2+}-dependent F-actin severing proteins. Molecular and Cellular Biochemistry 141:153-165.

Marcu MG, Zhang L, Elzagallaai A, Trifaro J-M (1998) Localization by segmental deletion analysis and functional characterization of a third actin-binding site in domain 5 of scinderin. Journal of Biological Chemistry 273:3661-3668.

Moore EDW, Becker PL, Fogarty KE, Williams DA, Fay FS (1990) Ca^{2+} imaging in single living cells: Theoretical and practical issues. Cell Calcium 11:157-179.

Neher E, Marty A (1982) Discrete changes of cell membrane capacitance observed under conditions of enhanced secretion in bovine adrenal chromaffin cells. Proceedings of the National Academy of Science 79:6712-6716.

Neher E, Zucker RS (1993) Multiple calcium-dependent processes related to secretion in bovine chromaffin cells. Neuron 10:21-30.

Perrin D, Aunis D (1985) Reorganization of α-fodrin induced by stimulation in secretory cells. Nature 315:589-592.

Perrin D, Langley OK, Aunis D (1987) Anti-α-fodrin inhibits secretion from permeablized chromaffin cells. Nature 326:498-501.

Rizzoli SO, Betz WJ (2005) Synaptic vesicle pools. Nature Reviews Neuroscience 6:57-69.

Schroeder TJ, Jankowski JA, Senyshyn J, Holz RW, Wightman RM (1994) Zones of exocytotic release on bovine adrenal medullary cells in culture. Journal of Biological Chemistry 269:17215-17220.

Schulte A, Chow RH (1996) A simple method for insulating carbon-fiber microelectrodes using anodic electrophoretic deposition of paint. Analytical Chemistry 68:3054-3058.

Schulte A, Chow RH (1998) Cylindrically etched carbon-fiber microelectrodes for low-noise amperometric recording of cellular secretion. Analytical Chemistry 70:985-990.

Senda T, Nishii Y, Fujita H (1991) Immunocytochemical localization of synapsin I in the adrenal medulla of rats. Histochemistry 96:25-30.

Ungar A, Phillips JH (1983) Regulation of the adrenal medulla. Physiological Reviews 63:787-843.

Venton BJ, Seipel AT, Phillips PEM, Westel WC, Gitler D, Greengard P, Augustine GJ, Wightman RM (2006) Cocaine increases dopamine release by mobilization of a synapsin-dependent reserve pool. Journal of Neuroscience 26:3206-3209.

Vitale ML, Rodriguez del Castillo A, Tchakarov L, Trifaro J-M (1991) Cortical filamentous actin disassembly and scinderin redistribution during chromaffin cell stimulation precede exocytosis, a phenomenon not exhibited by gelsolin. Journal of Cell Biology 113:1057-1067.

Voets T, Neher E, Moser T (1999) Mechanisms underlying phasic and sustained secretion in chromaffin cells from mouse adrenal slices. Neuron 23:607-615.

Wiegand UK, Duncan RR, Greaves J, Chow RH, Shipston MJ, Apps DK (2003) Red, yellow, green go! -- A novel tool for microscopic segregation of secretory vesicle pools according to their age. Biochemical Society Transactions 31:851-856.

Wightman RM, Schroeder TJ, Finnegan JM, Ciolkowski EL, Pihel K (1995) Time course of release of catecholamines from individual vesicles during exocytosis at adrenal medullary cells. Biophysical Journal 68:383-390.

Zhang L, Marcu MG, Nau-Staudt K, Trifaro J-M (1996) Recombinant scinderin enhances exocytosis, an effect blocked by two scinderin-derived actin-binding peptides and PIP_2. Neuron 17:287-296.

CHAPTER TWO

CHARACTERIZATION OF FACILITATION OF QUANTAL RELEASE INDUCED BY A D1-LIKE RECEPTOR ON BOVINE CHROMAFFIN CELLS

INTRODUCTION

Exocytotic release of chemical messengers is a common mechanism for communication between biological cells. This process is tightly regulated and several controlling mechanisms have been identified including the influx of Ca^{2+} from the extracellular space, the normal trigger for exocytosis, and the regulation of the number of vesicles in the readily releasable pool. At many cells that undergo exocytosis, autoreceptors play an important regulatory role. For example, most neurons, including those that release dopamine, norepinephrine, and serotonin, autoreceptor activation inhibits further release. Activation of serotonin somatodendritic autoreceptors inhibit subsequent synthesis and release (Blier et al., 1998). Autoreceptors on dopaminergic neurons are D2-like (the D2 receptor class is comprised of the D_2, D_3, and D_4 dopaminergic receptors), and their actions are absent in mice with a genetic deletion of the D_2 receptor (Benoit-Marand et al., 2001). Similar autoreceptor control has been shown for norepinephrine (Starke, 2001). An exception to the general inhibitory nature of neuronal autoreceptors appears to be glutamatergic synapses in the entorhinal cortex of juvenile rats that contain NMDA autoreceptors that enhance release (Yang et al., 2006).

Nonneuronal cells that secrete by exocytosis also have autoreceptors. Aspinwall et al. demonstrated that insulin-stimulated pancreatic β-cells secrete insulin (Aspinwall et al., 1999). Additionally, pancreatic β-cells have recently been shown to have insulin receptors on their surface that, when deleted, result in a dramatically lowered level of insulin secretion (Ueki et al., 2006). Thus, in contrast to neurons, these autoreceptors appear to promote

increased release. Inhibitory autoreceptor regulation has been reported at bovine chromaffin cells from the adrenal gland. Early investigations, prompted by the phylogenetic relationship between chromaffin cells and sympathetic neurons that are well established to have autoreceptors, determined that autoreceptors on bovine chromaffin cells had properties that pharmacologically resemble dopaminergic receptors (Artalejo et al., 1985; Gonzalez et al., 1986), and their activation inhibited release. Subsequent research showed that D2 dopamine receptors are located on bovine chromaffin cells and their activation inhibited release (Bigornia et al., 1990). A D1-like receptor (the D1 receptor class is comprised of the D_1 and D_5 dopaminergic receptors) has also been identified on bovine chromaffin cells (Artalejo et al., 1990). Activation of this receptor facilitates an inward Ca^{2+} current that could promote exocytosis (Artalejo et al., 1990). Surprisingly, it was experimentally shown that D1 receptor activation was found to inhibit catecholamine secretion (Dahmer and Senogles, 1996a).

In this work we describe a reinvestigation of the action of the D1 receptor on exocytosis from bovine chromaffin cells. All of the prior secretion experiments that investigated autoreceptors on bovine chromaffin cells exposed them to secretagogues for multiple minutes. In contrast, the D1 mediated facilitation Ca^{2+} currents were measured on a subsecond time scale. In this work we evaluated release from bovine chromaffin cells using similar subsecond stimuli. This was accomplished by first optimizing the temperature and timing for K^+-based depolarization of individual chromaffin cells, while monitoring in real time release via amperometry and internal Ca^{2+} with fura-2. With release evoked by brief stimuli at 37ºC we found clear evidence for facilitation of exocytotic release mediated by a D1-like receptor on the surface of bovine chromaffin cells.

EXPERIMENTAL PROCEDURES

Cultured Chromaffin Cells

Bovine chromaffin cells were prepared from adrenal glands obtained from a local abattoir as previously described (Leszczyszyn et al., 1990). Chromaffin cells were obtained from the adrenal medulla via digestion with collagenase (Worthington Biochemical Corporation, Lakewood, NJ). Density gradient centrifugation using Renografin was used to obtain a culture solution epinephrine-enriched fraction of cells. Cells were plated at a density of 3 x 10^5 cells/35-mm diameter plate (Becton Dickinson, Franklin Lakes, NJ) containing a 25-mm glass coverslip (Carolina Biological, Burlington, NC). Cell culture plates were kept at 37ºC in a 5% CO_2-supplemented incubator (Fisher Scientific, Hampton, NH). Cells were used days 3-7 postplating.

Electrodes and Electrochemistry

Carbon-fiber disk microelectrodes were prepared from T-650 fibers as previously described (Kawagoe et al., 1993). Carbon fibers were aspirated into glass capillaries. A pipette puller (Narishige, Long Island, NY) was used to seal the glass around the carbon fiber. The carbon fibers were cut at the glass seal, and the seal was reinforced with epoxy (15% m-phenylenediamine mixed with Epon 828 resin (Miller-Stephenson, Danbury, CT)) heated to 80^{o}C. The electrodes were cooled at room temperature for 12 h, cured at 100^{o}C for 12 h, followed by curing at 150^{o}C for 12 h. Before use, electrodes were beveled at 45º on a diamond polishing wheel (Sutter Instruments, Novato, CA) using impedance monitoring and soaked in isopropyl alcohol for a minimum of 20 min (Bath et al., 2000). Constant potential amperometry was used to monitor exocytotic events and was measured using an Axopatch

200B (Axon Instruments, Molecular Devices, Union City, CA). The microelectrode was held at 0.650 V vs. an Ag/AgCl reference (Bioanalytical Systems, West Lafayette, IN); individual release events were detected as current spikes. The resulting signal was filtered at 5 kHz with a low-pass Bessel filter and collected at 10 kHz. Amperometric recordings were then filtered at 400 Hz using a Gaussian filter.

Release Measurements

Culture plates containing cells in buffer (in mM) 145 NaCl, 5 KCl, 1 $MgCl_2$, 11.2 glucose, 10 HEPES, and 2 $CaCl_2$) were placed on the stage of a Zeiss 35 inverted microscope (Zeiss, Thornwood, NY). The position of the carbon-fiber microelectrode and stimulating pipette was controlled with piezoelectric micromanipulators (Burleigh Instruments, Exfo, Plano, TX). Exocytosis was evoked with 60 mM K^+ delivered by pressure ejection from the stimulating pipettes that were constructed with a horizontal puller (Sutter Instruments, Novato, CA). The diameter of the pipette tip was adjusted to 10 μm using a microforge (Narishige, Long Island, NY). Ejection of the high K^+ solution was accomplished with a Picospritzer set at 7 psi (General Valve Corporation, Parker Hannifin, Fairfield, NJ) using either a 0.5 or 2-s bolus. The stage holding the cell plate was either kept at room temperature, 25ºC, or heated with a water bath (Fisher Scientific, Hampton, NH) to 37ºC.

Ca^{2+} Measurements

Ca^{2+}-imaging employed the fluorescent dye, fura-2, and an imaging system (Empix, Inc., Mississauga, ON, Canada) attached to a microscope (Nikon, Lewisville, TX). An initial fura-2 solution was diluted with 40 μL DMSO and 10 μL of 10% pluronic. This fura-2

solution was diluted to 1 μM in experimental buffer containing 0.10 % BSA (Molecular Probes, Invitrogen, Carlsbad, CA). Cells were incubated in this solution for 20 min at 25ºC, followed by a rinse for 20 min at 25ºC in the experimental buffer. Ca^{2+}-imaging experiments were conducted either simultaneously with amperometry or alone. Intracellular fura-2 bound to Ca^{2+} was excited at 340 nm while free fura-2 was excited at 380 nm. Emission was monitored at 510 nm using a digital CCD camera and software (Empix Imaging, Inc, Mississauga, ON, Canada). The ratio of the emission with 340 nm excitation and 380 nm excitation was determined. The ratiometric measurements were then converted to $[Ca^{2+}]_i$ as previously described (Grynkiewicz et al., 1985; Finnegan and Wightman, 1995).

Autoreceptor experiments

Experiments were conducted at 37ºC using an S2/S1 protocol. The number of exocytotic events following an initial delivery (S1) of 60 mM K^+ for 0.5-s was compared to a second delivery 60 mM K^+ (S2) 10 or 30 s later. To evaluate D1 receptors, the D1 antagonist, SCH-23390 (1 μM, 10 μM, 100 μM Sigma-Aldrich, St. Louis, MO), was present in the buffer. To evaluate D2 receptors, the D2 antagonist, raclopride (1 μM, 10 μM, 100 μM Sigma-Aldrich, St. Louis, MO), was present in the buffer. To evaluate D1 receptors via a D1 agonist, SKF-38393 was introduced to the buffer. Paired 0.5-s boluses spaced 30 s apart were used to deliver the 60 mM K^+ secretagogue to cells. At 10 s after the initial stimulus, 100 uM SKF-38393 (Sigma-Aldrich, St. Louis, MO), a D1 agonist, was delivered to the buffer and remained present during the second stimulus.

To evaluate the endogenous ligand, a 3-s bolus of 50 μM epinephrine was applied to the cell 22 s after S1 and S2 was applied 5 s later. As a control, the experiment was repeated at separate cells with ejection of experimental buffer substituted for epinephrine.

Data analysis and statistics

Spike analysis was performed using MiniAnalysis (Synaptosoft, Decatur, GA). For selection as spikes, the amplitude had to exceed the root-mean-square current noise by a factor of 5. Student's t-test and one-way ANOVA were used to determine significance among data sets. A value of $p < 0.05$ was taken to indicate a significant difference.

RESULTS

Vesicular release and Ca^{2+} dynamics evoked by 0.5-s and 2-s stimuli at 25ºC

At 25ºC, 0.5-s pressure ejection of 60 mM K^+ onto a chromaffin cell was sufficient to cause Ca^{2+} influx into the cell, measured by fura-2 fluorescence, and this was accompanied by exocytotic spikes measured by amperometry (example traces in left panel of Figure 2.1). Intracellular $[Ca^{2+}]$ reached a maximum after the 60 mM K^+ ejection was terminated and then slowly returned to baseline. The decay of the $[Ca^{2+}]_i$ was sufficiently slow that it failed to reach the original level within 10 s of the initial K^+ exposure. A second, 0.5-s pressure ejection of 60 mM K^+, 10 s after the first, caused a smaller increase in $[Ca^{2+}]_i$ that returned to baseline. Again, exocytosis was observed during the time $[Ca^{2+}]_i$ was elevated.

To quantify the effects of consecutive 0.5-s stimuli on the occurrence of exocytotic events at 25ºC, we examined the ratio of the number of spikes evoked on a second K^+

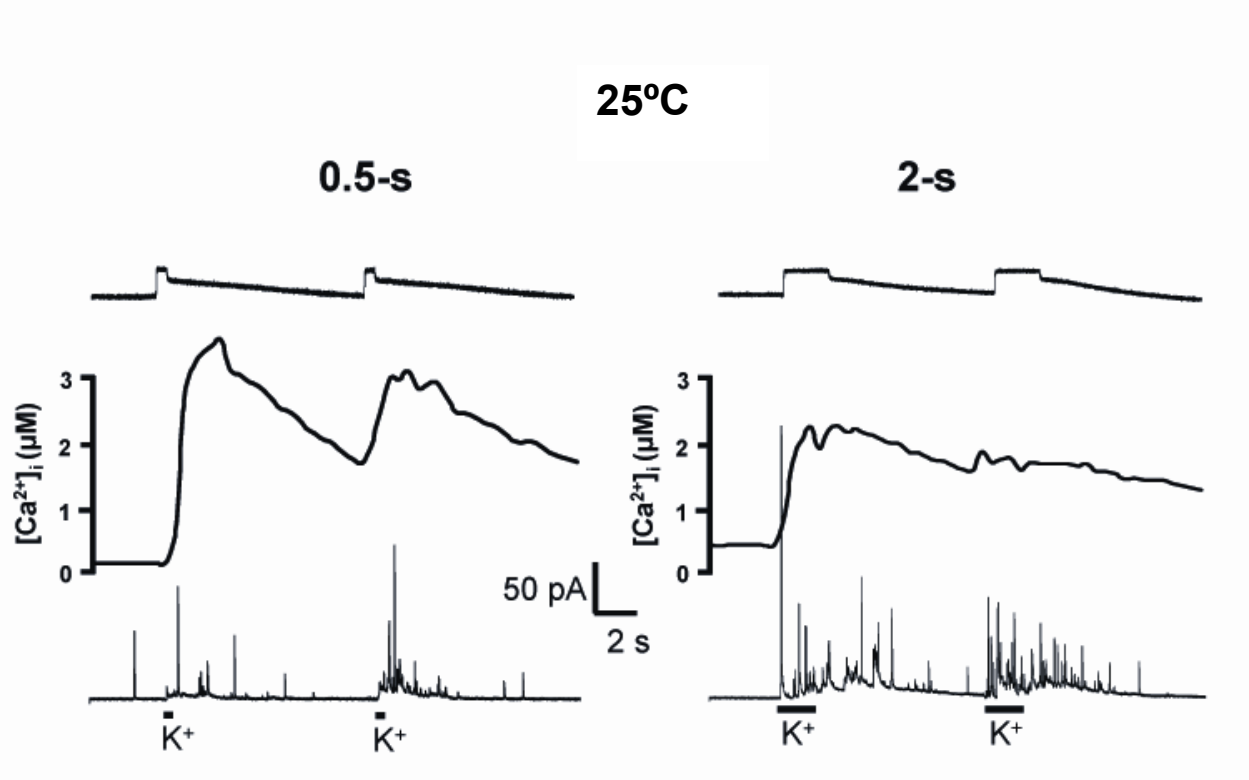

Figure 2.1. Comparison of 0.5-s and 2-s exposures to 60 mM K^+ at 25ºC. Stimulations were paired with a 10-s interstimulus interval. Uppermost traces show bolus of 10 µM dopamine applied to electrode to show ejection profile. Middle traces show $[Ca^{2+}]_i$ collected with fura-2; bottom traces show amperometric traces of release. Right and left panels show 0.5-s and 2-s stimulations, respectively.

exposure (S2) to those evoked on the first (S1). If preceding stimuli do not affect subsequent exocytotic events, this spike number ratio should be unity. The ratios were examined with different intervals between the stimuli to allow increasing recovery times (Table 2.1). With a 10-s or 20-s interval between 0.5-s, 60 mM K^+ exposures, the spike number ratios were approximately unity, but they exceeded unity with 30 or 40 s between stimuli. The ratio of the areas under the $[Ca^{2+}]_i$ curves was also calculated as an S2/S1 ratio. With a 10-s interval between stimuli, the S2/S1 $[Ca^{2+}]_i$ area ratio was 0.45 ± 0.06, but increased to a value between 0.7 and 0.8 with longer intervals between stimuli (Table 2.2). The average $[Ca^{2+}]_i$ area ratio measured across the four intervals was 0.71 ± 0.04 and was significantly depressed from unity ($p < 0.05$).

Similar experiments were done at 25ºC with 2-s pressure ejections of 60 mM K^+. With the longer stimulus, the $[Ca^{2+}]_i$ reached a maximum during the stimulus, evoking exocytosis, but again was slow to return to prestimulus values (see right panel of Figure 2.1). A second exposure 10 s later did not evoke much of a change in $[Ca^{2+}]_i$, but did evoke further exocytosis. Surprisingly, the number of spikes evoked on the first exposure with 2-s exposure to 60 mM K^+ (21.5 ± 1.8) was not significantly different from that evoked with a 0.5-s pulse (15.1 ± 2.5; $p \geq 0.05$; Figure 2.2A). However, the $[Ca^{2+}]_i$ area with the 2-s pressure ejection (44.95 ± 6.29 arbitrary units) was significantly greater than with a 0.5-s exposure (25.08 ± 1.54 arbitrary units; $p < 0.05$; Figure 2.2B).

The spike number ratios for consecutive stimuli using the 2-s stimulus were also found to be variable and near unity, but no consistent trend with interval between the stimuli was seen (Table 2.1). The $[Ca^{2+}]_i$ area ratio was very low with a 10-s interval between 2-s exposures to 60 mM K^+, and it increased for longer intervals (Table 2.2). The average

Table 2.1. Spike number ratios, S2/S1. Values are shown at 25ºC for 0.5-s at 10-, 20-, 30-, and 40-s intervals (n = 5, 7, 13, 12, respectively) and 2-s stimuli for 10-, 20-, 30-, and 40-s intervals (n = 5, 22, 23, 13, respectively). Spike number ratios are also shown at 37ºC for 0.5-s at 10-, 20-, 30-, and 40-s intervals (n = 10, 9, 16, 10, respectively) and 2-s stimuli for 10-, 20-, 30-, and 40-s intervals (n = 13, 11, 17, 10, respectively).

Interstimulus interval (s)	**25ºC**		**37ºC**	
	0.5-s stimulus	**2-s stimulus**	**0.5-s stimulus**	**2-s stimulus**
10	1.1 ± 0.3	1.0 ± 0.1	2.0 ± 0.1	1.2 ± 0.2
20	1.0 ± 0.2	0.69 ± 0.10	1.6 ± 0.4	1.7 ± 0.2
30	1.8 ± 0.3	1.2 ± 0.1	1.6 ± 0.1	1.3 ± 0.2
40	1.3 ± 0.2	0.76 ± 0.10	1.7 ± 0.4	1.5 ± 0.2

Table 2.2. $[Ca^{2+}]_i$ area ratios, S2/S1. Values are shown at 25ºC for 0.5-s at 10-, 20-, 30-, and 40-s intervals (n = 5, 7, 9, 12, respectively) and 2-s stimuli for 10-, 20-, 30-, and 40-s intervals (n = 5, 13, 17, 14, respectively). $[Ca^{2+}]_i$ area ratios are also shown at 37ºC for 0.5-s at 10-, 20-, 30-, and 40-s intervals (n = 6, 6, 6, 7, respectively) and 2-s stimuli for 10-, 20-, 30-, and 40-s intervals (n = 5 for all intervals).

Interstimulus interval (s)	**25ºC**		**37ºC**	
	0.5-s stimulus	**2-s stimulus**	**0.5-s stimulus**	**2-s stimulus**
10	0.45 ± 0.06	0.18 ± 0.05	1.2 ± 0.1	0.82 ± 0.04
20	0.88 ± 0.03	0.57 ± 0.10	1.2 ± 0.1	0.65 ± 0.06
30	0.79 ± 0.07	0.51 ± 0.05	1.1 ± 0.1	0.61 ± 0.04
40	0.71 ± 0.08	0.47 ± 0.05	0.87 ± 0.05	0.52 ± 0.06

measured over the four intervals being 0.43 ± 0.05, which was significantly lower than unity ($p < 0.05$), again indicating insufficient time for recovery on the second stimulus. Clearly, the 2-s stimulus at 25ºC sufficiently perturbs the mechanisms that regulate $[Ca^{2+}]_i$ such that the responses on the second exposure differ considerably from those on the first exposure.

Vesicular release and Ca^{2+} dynamics evoked by 0.5-s and 2-s stimuli at 37ºC

Identical experiments were repeated at 37ºC. At this temperature, the Ca^{2+} responses were more rapid (Figure 2.3). With a 0.5-s delivery of 60 mM K^+, $[Ca^{2+}]_i$ was maximal soon after the stimulus, and returned to near baseline within 10 s, and multiple exocytotic spikes were observed. With a 10-s interval between stimuli, the spike number ratio approached 2, and it was above 1.5 with longer intervals between stimuli (Table 2.1). These S2/S1 spike number ratios evoked during 0.5 s exposures were significantly higher than unity ($p < 0.05$) indicating facilitation of release at 37ºC. The $[Ca^{2+}]_i$ area ratios were above unity with a 10-s interval between stimuli, and remained high until the stimuli were separated by 40 s (Table 2.2).

At physiological temperature, a 2-s stimulus of 60 mM K^+ caused Ca^{2+} influx that was maximal during the ejection, and which decayed to base line within 10 s. At 37ºC, there were significantly more spikes evoked with a 2-s bolus (25.5 ± 2.5) than with a 0.5-s pulse (14.2 ± 1.7; $p < 0.05$, Figure 2.2).

The spike number ratio was 1.2 with 10 s between 2-s ejections of 60 mM K^+ at 37ºC (Table 2.1). With longer intervals between stimuli, the spike number ratio hovered between 1.3 and 1.7; these spike number ratios were significantly higher than unity, also indicating

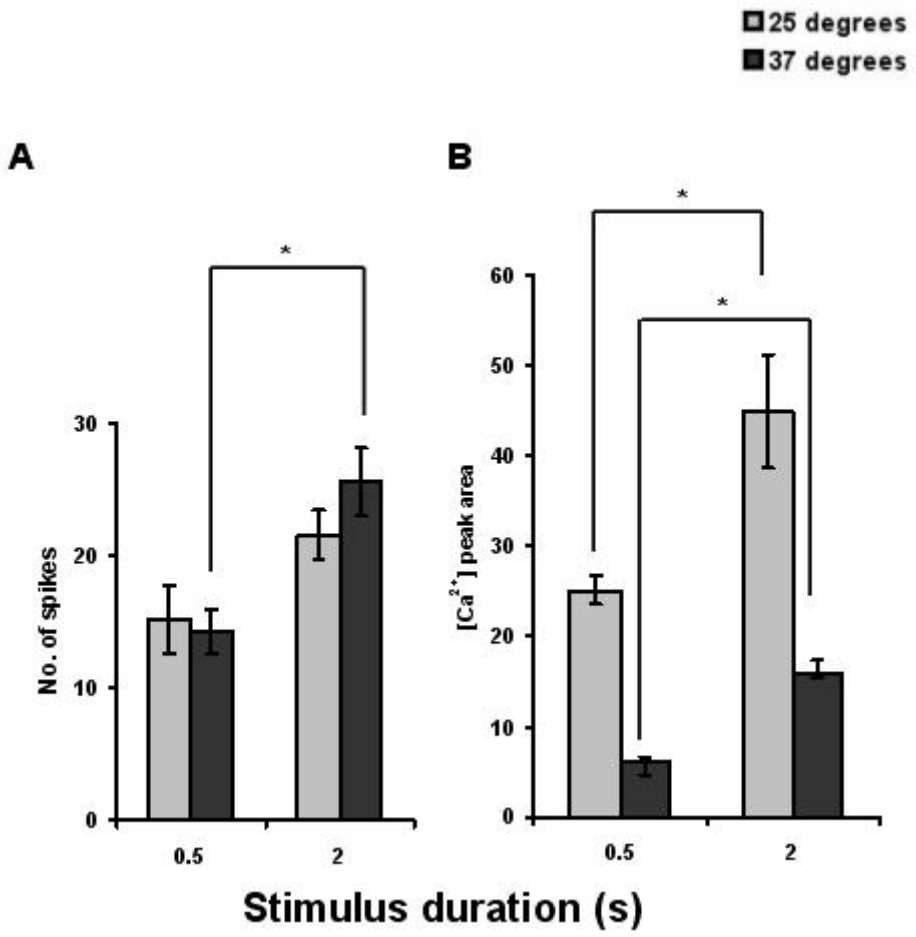

Figure 2.2. Effects of stimulus time and temperature on vesicular release and Ca^{2+} influx. *A,* Number of spikes elicited using 0.5-s (n = 53) and 2-s stimuli (n = 42) at 25ºC were not statistically significant. There was a significant difference between the number of spikes elicited at the two stimuli at 37ºC ($p < 0.05$). Temperature did not show an effect on number of evoked spikes at a particular stimulus duration. *B*, Ca^{2+} dynamics in response to temperature and stimulus conditions. Ca^{2+} area during evoked Ca^{2+} influx using 0.5-s (n = 5) and 2-s stims (n = 7) at 25ºC was statistically significant ($p < 0.05$); 0.5-s stimuli (n = 25) and 2-s stimuli (n = 20) at 37ºC also evoked average Ca^{2+} areas that were significantly different ($p < 0.05$) Ca^{2+} dynamics are more sensitive to temperature and stimulus duration.

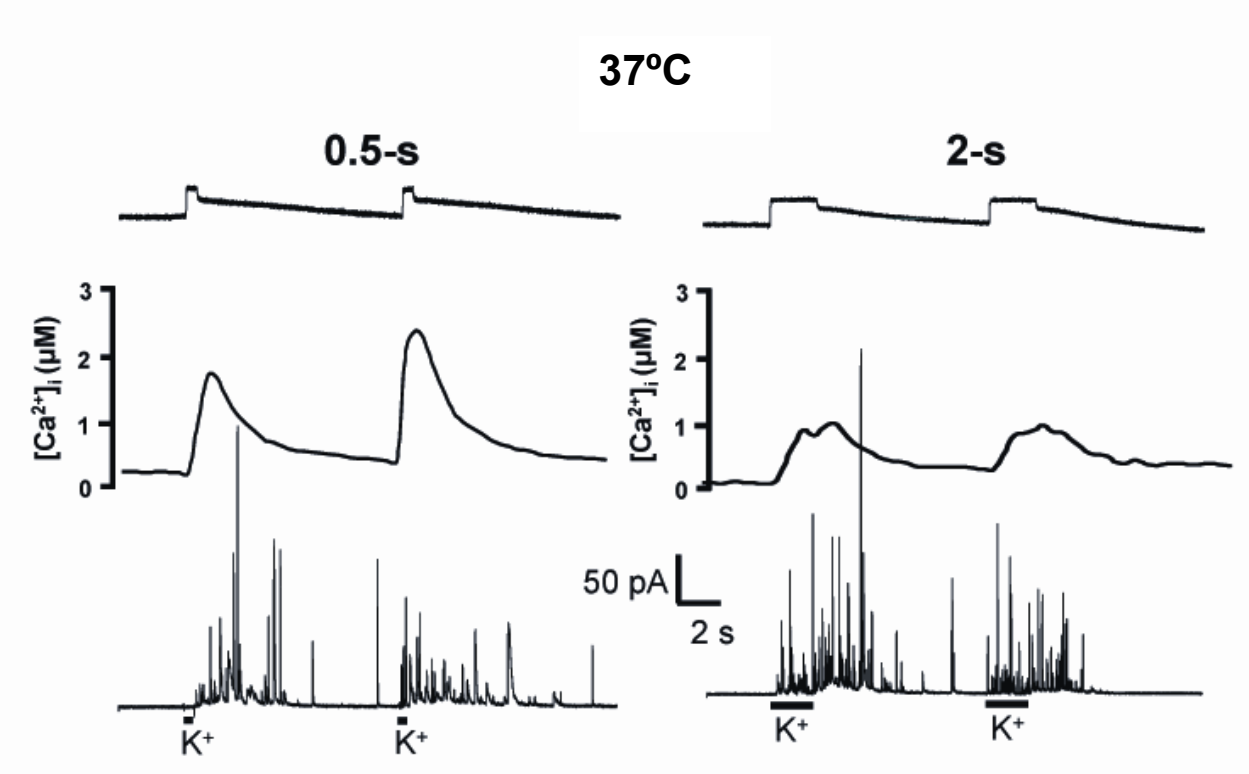

Figure 2.3. Comparison of 0.5-s and 2-s exposures to 60 mM K^+ at 37°C. Stimulations were paired with a 10-s interstimulus interval. Uppermost traces show bolus of 10 µM dopamine applied to electrode to show ejection profile. Middle traces show $[Ca^{2+}]_i$ collected with fura-2; bottom traces show amperometric traces of release. Right and left panels show 0.5-s and 2-s stimulations, respectively.

the presence of facilitation ($p < 0.05$). With all time intervals, the average $[Ca^{2+}]_i$ area ratio with 2-s pressure ejections was less than unity (Table 2.2). The average ratio over the 10-, 20-, 30-, and 40-s intervals was 0.65 ± 0.01, which is significantly different from unity ($p < 0.05$). Thus, even at 37ºC, 2-s exposures to 60 mM K^+ perturbed the cell sufficiently that $[Ca^{2+}]_i$ could not achieve the initial evoked value on subsequent stimuli, at least with the inter-stimulus times investigated. Note that while there was little change in the number of spikes evoked at the two different temperatures, the $[Ca^{2+}]_i$ area ratios were significantly smaller at 37ºC with both ejection durations (Figure 2.2). This is because $[Ca^{2+}]_i$ is more rapidly restored to low levels at the higher temperature.

Facilitation and depression of vesicular release via the D1 receptor

To investigate whether the elevated number of spikes seen following a second exposure to 0.5-s exposure to 60 mM K^+ at 37ºC was due to specific receptor interactions, we examined the effects of selective pharmacological agents. In the first experiment, the effect of different concentrations of the D1-receptor antagonist, SCH-23390, on spike number ratio was examined with 0.5 s K^+ pressure ejections that were 10 s apart. The average control S2/S1 spike number ratio (without drug) for the 10-s interval yielded a mean of 2.2 ± 0.2. The amount of facilitation decreased with increasing concentrations of SCH-23390 (Figure 2.4). Only treatment with 10 and 100 μM SCH-23390 showed a significant depression as compared to control ($p < 0.05$).

To test if D2 receptors were participating in this effect on release, the D2 antagonist, raclopride, was used in an analogous study. The average control spike number ratio, S2/S1,

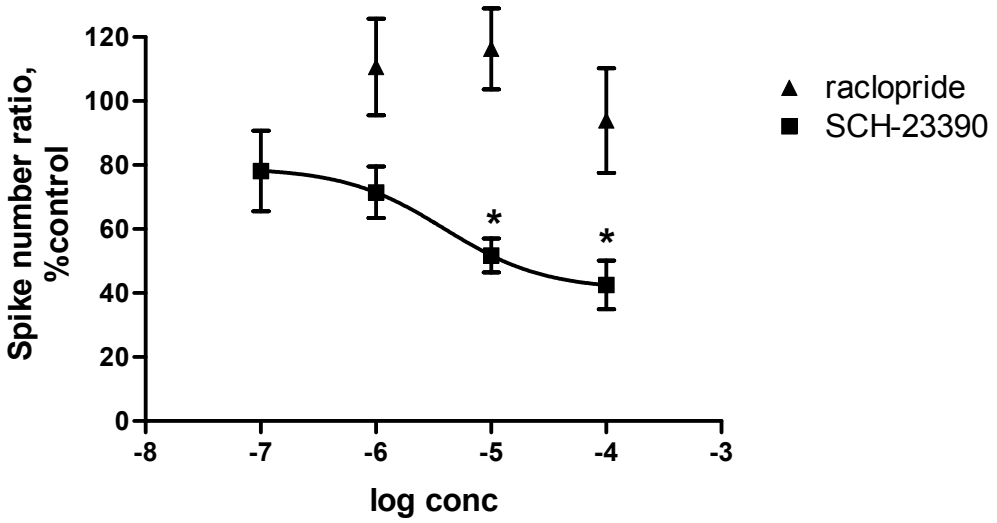

Figure 2.4. Dose response curve of D1 and D2 antagonists. Data was obtained using 0.5-s K^+ stimuli at 37ºC with 10-s intervals. To investigate the presence of a D2-receptor mediated effect on facilitation, raclopride, a D2 antagonist, was incubated with cells at 1, 10, and 100 μM (n = 5, 10, 7, respectively). The S2/S1 responses were compared to control values measured at the same cell. Various concentrations of SCH-23390 (0.1, 1, 10, 100 μM; n = 8, 7, 7, 8, respectively) were also used to examine its effect on facilitation. Spike number ratios obtained at 10 and 100 μM SCH-23390 were significantly different from control values ($p < 0.05$).

(without drug) across the three concentrations used was 2.2 ± 0.3 with 0.5-s exposures 10 s apart. Three concentrations of raclopride were used: 1 μM, 10 μM, and 100 μM (Figure 2.4). No changes in spike number ratios were observed.

Next, the effect of a D1-receptor agonist was evaluated. In these experiments, the K^+ stimuli were 30 s apart because, under control conditions (Table 2.1), facilitation was not as pronounced as with the shorter intervals. SKF-38393 (100 μM), a D1-receptor agonist, was introduced into the buffer 10 s after the first 0.5 s K^+ pressure ejection. The spike number ratio was 2.5 ± 0.4 following the agonist compared to 1.2 ± 0.2 ($p < 0.05$) in the absence of the agonist (Figure 2.5). The facilitation caused by SKF-38393 was blocked when 10 μM of the D1-receptor antagonist, SCH-23390, was included in the buffer ($p < 0.05$; Figure 2.5).

Epinephrine-induced facilitation

To test whether the physiological ligand that is secreted by chromaffin cells would elicit facilitation, the experiment was repeated with a transient application of 50 μM epinephrine. Epinephrine was applied as a 3-s bolus 22 s after the first 0.5-s bolus of K^+; 5 s after completion of the epinephrine application, the second 0.5-s bolus of K^+ was applied to the cell. Epinephrine evoked facilitation in release as was seen with the D1 agonist, SKF-38393 (Figure 2.6). Transient application of 50 μM epinephrine to chromaffin cells yielded a spike number ratio of 2.7 ± 0.4 (Figure 2.6, inset) which was 265.4 ± 43.9% of the control ratio, which was obtained by pressure ejecting experimental buffer instead of epinephrine (1.1 ± 0.1; $p < 0.05$; Figure 2.6).

To test whether the effect of epinephrine was D1 receptor-mediated, two consecutive S2/S1 protocols were used. In the first, epinephrine was introduced 5 s before S2. Then, the

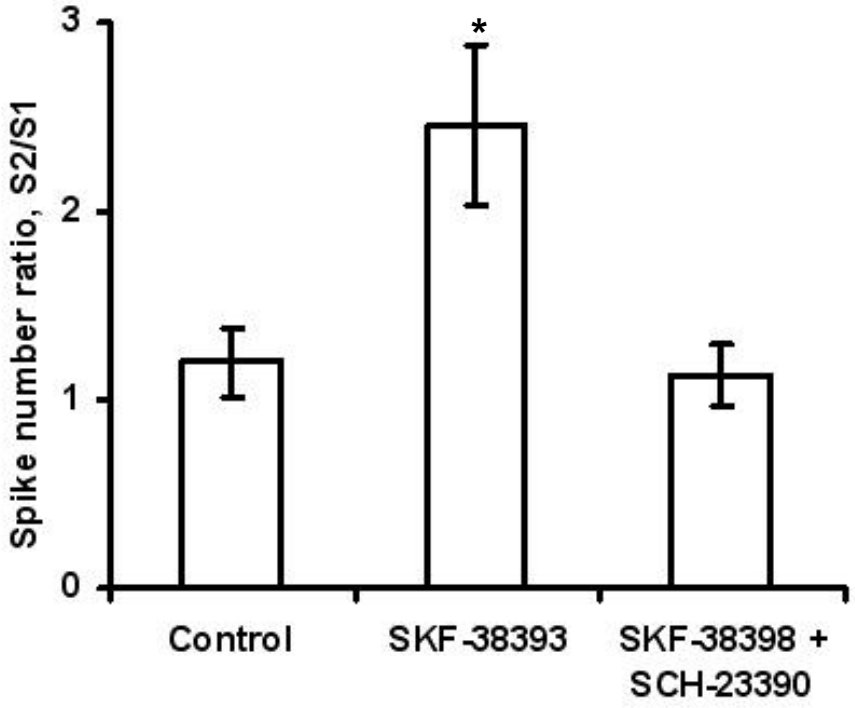

Figure 2.5. D1 receptor-mediated facilitation. Experiments were conducted with a 30-s interstimulus interval. Spike number ratios showed recovery in control cells (n = 9) and facilitation in cells incubated with 100 μM SKF-38393, a D1 agonist (n = 9). Co-incubation of 100 μM SKF-38393 and 10 μM SCH-23390 showed inhibition of the facilitation effect (n = 5). Incubation with SKF-38393 alone was significantly different from control value and co-incubation of SKF-38393 and SCH-23390 ($p < 0.05$).

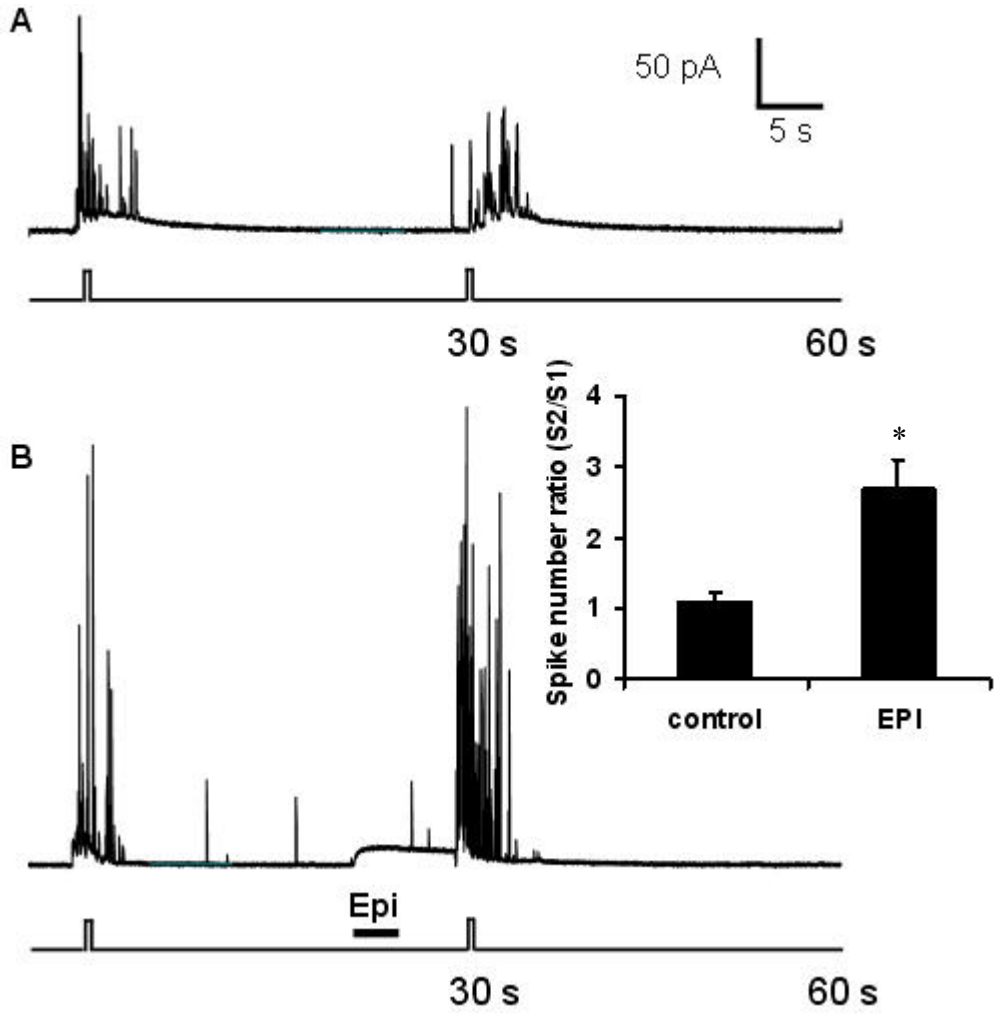

Figure 2.6. **Epinephrine-induced facilitation.** Experiments were conducted with a 30-s interstimulus interval. *A,* Control trace where experimental buffer was applied to the cell for 3-s records recovery of release upon the second stimulus, S2. *B,* Release was recorded with 3-s application of 50 μM epinephrine. S2 in these cells showed a greater number of elicited spikes. Note the baseline change due to detection of the pressure ejection of epinephrine. Inset shows average S2/S1 values for control cells and cells that received brief applications of epinephrine (n = 12). The values were shown to be significantly different ($p < 0.05$).

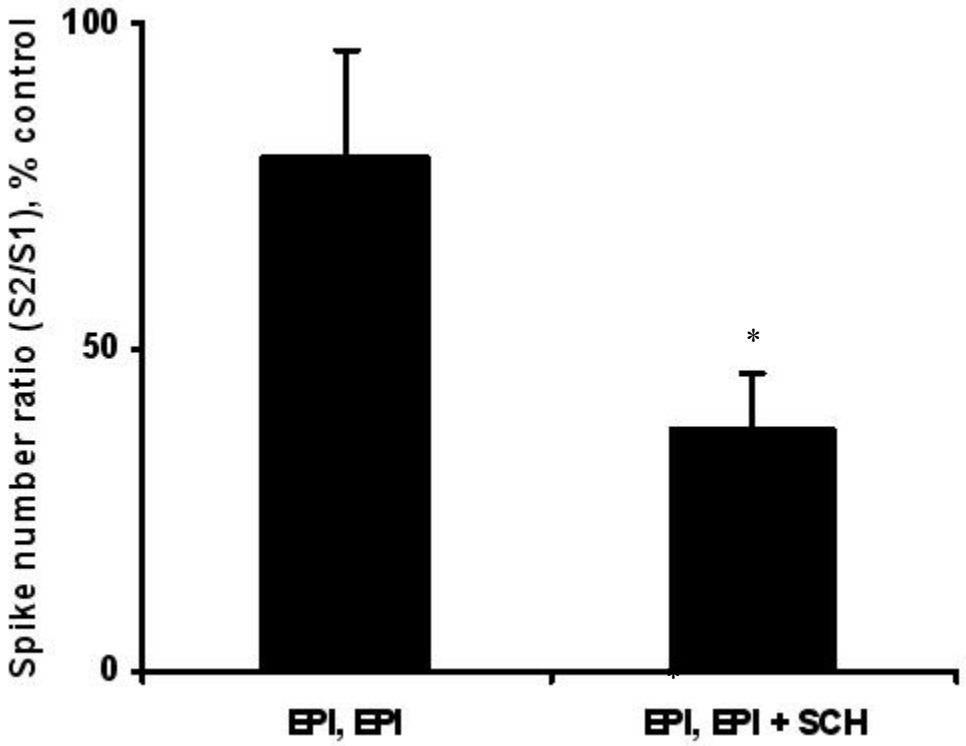

Figure 2.7. Epinephrine-induced facilitation is D1-modulated. Experiments were conducted with 30-s interstimulus interval. To investigate if the epinephrine-induced facilitation was mediated by a D1-like receptor, SCH-23390 was used to attempt to block the effect. A pair of S2/S1 stimuli were evaluated at each cell with 50 μM epinephrine applied during S2; after 5 min, a second set of identical paired stimuli was used with transient application with (n = 5) or without 10 μM SCH-23390 (n = 7). Values are shown as the percent of the initial S2/S1 spike number ratios.

experiment was repeated 5 min later, with or without a D1-receptor antagonist. The second epinephrine application in the absence of drug showed facilitation, but its S2/S1 spike number ratio was 79.2 ± 16.5% of the first (Figure 2.7). This may indicate desensitization that is occurring at the receptor. However, in the presence of SCH-23390 (10 μM) the facilitation effect was blocked. The ratio of S2/S1 spike number ratios was 37.4 ± 8.7%, which was significantly different than the response in the absence of drug ($p < 0.05$; Figure 2.7).

DISCUSSION

The results described here demonstrate that there is an autoreceptor on bovine chromaffin cells that facilitates release of epinephrine. Previous work has demonstrated the presence of dopaminergic D1 (Artalejo et al., 1985; Artalejo et al., 1990) and D2 (Bigornia et al., 1990) receptors on bovine chromaffin cells. Consistent with those findings, chromaffin cells have been shown to express RNA for the D_4 and D_5 dopaminergic receptors (Dahmer and Senogles, 1996a). Additionally, it has been shown that D1 receptor activation (presumably through activation of the D_5 receptor) causes facilitation of Ca^{2+} currents (Artalejo et al., 1990). Since it was postulated that the Ca^{2+} influx linked to the D1 receptor was sufficient to evoke further release (Artalejo et al., 1991), we tested for this effect. Clear evidence for facilitation of release was found at physiological temperature and with subsecond exposure to small amounts of K^+. This facilitation was blocked by a D1 receptor antagonist in a dose-dependent manner. The facilitation could be mimicked by a D1 agonist as well as the endogenous secreted species, epinephrine. Thus, we have established a functional role for the previously identified D1 receptor on bovine chromaffin cells.

Crucial to our observation of facilitated autoreceptor-dependent release was the optimization of the stimulus conditions. Rapid application of secretagogues was enabled by the fabrication of ejection pipettes that permit delivery of a relatively sharp concentration profile even on a 0.5-s timescale (Hochstetler et al., 2000). The pipette tips have a diameter of 10 μm or less, which minimizes leakage of the secretagogue from the tip. The paired stimuli approach that employed a 0.5-s or 2-s exposure to 60 mM K^+ was sufficient to promote release of multiple vesicles with each exposure. Since the electrode samples approximately 6% of the cellular surface, each 0.5-s exposure can be estimated from the data in Figure 2.2 to release approximately 250 vesicles. Because one estimate of the readily releasable pool is approximately 175 (Voets et al., 1999) of the total 10,000 vesicles in the cell (Ungar and Phillips, 1983), the majority of our release is believed to come from this compartment.

The spike number ratio was always unity or greater with the 0.5-s stimuli. In contrast, with 2-s stimuli, the spike number ratio was often lower than unity at 25ºC suggesting that the cell (or the vesicle pools and their associated release mechanisms) on the second stimulus is still recovering from the first stimulus (Dinkelacker et al., 2000). Consistent with prior work, the number of spikes initially evoked by the same stimulus duration was similar at both temperatures (Pihel et al., 1996; Walker et al., 1996). The strongest evidence that the cell is dramatically perturbed with the 2-s stimuli comes from the $[Ca^{2+}]_i$ area ratios. Only with 0.5-s stimuli at 37ºC were $[Ca^{2+}]$ area ratios near unity achieved consistently. Indeed, with short times between pulses, the $[Ca^{2+}]$ area ratios exceeded unity. This finding is entirely consistent with the facilitated Ca^{2+} currents measured by Artalejo and coworkers (Artalejo et al., 1992). The cells were able to recover

more effectively at 37ºC as the $[Ca^{2+}]_i$ relaxed back to near resting levels within even a 10-s interstimulus interval. Ca^{2+} uptake, primarily into mitochondria, reestablishes $[Ca^{2+}]$ resting levels in chromaffin cells (Yang and Kao, 2001; Haynes et al., 2006) and the return to resting $[Ca^{2+}]$ levels was more rapid at physiological temperature. Thus, we elected to use a 0.5-s stimulus and a 10-s interval to investigate receptor-mediated facilitation.

To test the hypothesis that facilitation of exocytosis is mediated by interaction of a released substance with a D1 dopamine receptor (Artalejo et al., 1991), the conditions that showed facilitation were repeated in the presence of SCH-23390, a D1 antagonist. While this agent blocked facilitated release in a dose-dependent manner, facilitated release was unaffected by the D2 antagonist, raclopride. The doses of SCH-23390 needed to inhibit facilitation are quite high. Two possibilities may contribute to this finding. First, the binding of SCH-23390 to sites on chromaffin cell is considerably weaker than to other tissues that have D1 receptor sites (Dahmer and Senogles, 2000). Because of this, we are probably more correct to refer to this receptor as a "D1-like receptor." Second, the assay used involves the competition between released epinephrine and the antagonist. Further evidence that a D1-like receptor is involved in facilitation was obtained with the D1 agonist, SKF-38393. This agent induced exocytotic facilitation in a 30-s paired pulse interval, a paradigm that normally shows limited facilitation.

Consistent with the concept that the facilitation is an autoreceptor effect, epinephrine induced robust facilitation of the number of vesicular release events at a modest concentration compared to the surface concentration upon its release (Finnegan et al., 1996). Desensitization appears to occur because the epinephrine-induced facilitation was somewhat diminished upon repeating the application (Figure 2.7). However, the facilitation induced by

epinephrine appears receptor mediated because it was inhibited by the D1-receptor antagonist, SCH-23390. Previously, it was proposed that intracellular or plasma dopamine was the primary species responsible for activating dopaminergic receptors on bovine chromaffin cells (Artalejo et al., 1990; Bigornia et al., 1990). This work shows that released epinephrine could be the catecholamine activating the D1-like receptor. Indeed, epinephrine is well known to have a high affinity for the D1 receptor (IC_{50} = 68 nM) (Seeman, 1980). Epinephrine is in abundance in this preparation since the majority of chromaffin cells package and release epinephrine; the ratio of epinephrine- to norepinephrine-containing cells is approximately 70%:30% (Moro et al., 1990). Moreover, the experiments performed in this work were conducted on the epinephrine-enriched fraction of cells obtained from the cell culture preparation. Therefore, the observed facilitation originates by binding of epinephrine to a functional D1-like autoreceptor.

Several earlier studies demonstrated a D2 receptor-mediated inhibition of catecholamine release (Artalejo et al., 1985; Gonzalez et al., 1986; Bigornia et al., 1990). Furthermore, a previous reports of D1 receptor-mediated secretion at chromaffin cells suggested a decrease in release (Dahmer and Senogles, 1996a). However, many of these were done at room temperature, a condition not explored here. Both D1 and D2 mediated-effects were attributed to inhibition of sodium uptake that would cause an attenuated membrane depolarization (Dahmer and Senogles, 1996b). We attribute the difference in responses obtained here to differences in the time scale of secretagogue application. Prior studies of catecholamine release from bovine chromaffin cells used incubation times of minutes. In this work each secretagogue exposure was transient and attempted to mimic physiological conditions of a brief burst of action potentials. D1 receptor activation may

have predominantly short-term effects, as indicated by our results, while the effect of D2 receptor activation may become predominant over longer time periods.

The D1 receptor-mediated facilitation that occurs in chromaffin cells points to a positive feedback cycle that operates with paired stimuli that are spaced closely together. Previously, using a paired stimuli approach, an overfilling of the releasable pool of vesicles was noted at relatively short interstimulus intervals (approximately 2-10 s) in bovine chromaffin cells (Dinkelacker et al., 2000). The autoreceptor that we have functionally characterized in this work may be the origin of this apparent overfilling. By activating facilitating Ca^{2+} currents, more Ca^{2+} is available to stimulate greater release. Autoreceptor-mediated positive feedback occurs in other systems as well. In addition to the positive feedback observed with application of insulin to β-pancreatic cells (Aspinwall et al., 1999), another positive feedback regulator is gonadotropin-releasing hormone (GnRH). GnRH potentiates the pulsatile secretion of GnRH neurons *in vitro* (Khadra and Li, 2006). GnRH agonists were also shown to potentiate the pulsatile neuronal response while GnRH antagonists had an inhibitory effect. Moreover, oxytocin (OT) and its agonist enhance bursting activity in OT neurons while the OT antagonist inhibits this same response (Jourdain et al., 1998). In the chromaffin cell, which is part of the "fight-or-flight" mechanism, a positive feedback system is desirable. In this way, the body is flooded with adrenaline in order to be prepared for high stress situations. Closely spaced stimuli would signal to these cells the urgent need for the rapid release of large amounts of catecholamine into the bloodstream and initiate the positive feedback cycle necessary for an immediate response to the presented threat or stress.

REFERENCES

Artalejo AR, Garcia AG, Montiel C, Sanchez-Garcia P (1985) A dopaminergic receptor modulates catecholamine release from the cat adrenal gland. Journal of Physiology 362:359-368.

Artalejo CR, Ariano MA, Perlman RL, Fox AP (1990) Activation of facilitation calcium channels in chromaffin cells by D_1 dopamine receptors through a cAMP/protein kinase A-dependent mechanism. Nature 348:239-242.

Artalejo CR, Dahmer MK, Perlman RL, Fox AP (1991) Two types of Ca2+ currents are found in bovine chromaffin cells: facilitation is due to the recruitment of one type. J Physiol 432:681-707.

Artalejo CR, Rossie S, Perlman RL, Fox AP (1992) Voltage-dependent phosphorylation may recruit Ca2+ current facilitation in chromaffin cells. Nature 358:63-66.

Aspinwall CA, Lakey JRT, Kennedy RT (1999) Insulin-stimulated insulin secretion in single pancreatic beta cells. Journal of Biological Chemistry 274:6360-6365.

Bath BD, Michael DJ, Trafton BJ, Joseph JD, Runnels PL, Wightman RM (2000) Subsecond adsorption and desorption of dopamine at carbon-fiber microelectrodes. Analytical Chemistry 72:5994-6002.

Benoit-Marand M, Borrelli E, Gonon F (2001) Inhibition of dopamine release via presynaptic D2 receptors: time course and functional characteristics in vivo. J Neurosci 21:9134-9141.

Bigornia L, Allen CN, Chung-Ren J, Lyon RA, Titeler M, Schneider AS (1990) D2 dopamine receptors modulate calcium channel currents and catecholamine secretion in bovine adrenal chromaffin cells. Journal of Pharmacology and Experimental Therapeutics 252:586-592.

Blier P, Pineyro G, el Mansari M, Bergeron R, de Montigny C (1998) Role of somatodendritic 5-HT autoreceptors in modulating 5-HT neurotransmission. Annals of the New York Academy of Sciences 861:204-216.

Dahmer MK, Senogles SE (1996a) Dopaminergic inhibition of catecholamine secretion from chromaffin cells: evidence that inhibition is mediated by D4 and D5 receptors. Journal of Neurochemistry 66:222-232.

Dahmer MK, Senogles SE (1996b) Differential inhibition of secretagogue-stimulated sodium uptake in adrenal chromaffin cells by activation of D4 and D5 dopamine receptors. Journal of Neurochemistry 67:1960-1964.

Dahmer MK, Senogles SE (2000) Atypical SCH23390 binding sites are present on bovine adrenal medullary membranes. Neurochem Res 25:321-326.

Dinkelacker V, Voets T, Neher E, Moser T (2000) The readily releasable pool of vesicles in chromaffin cells is replenished in a temperature-dependent manner and transiently overfills at 37 degrees C. J Neurosci 20:8377-8383.

Finnegan JM, Wightman RM (1995) Correlation of real-time catecholamine release and cytosolic Ca^{2+} at single bovine chromaffin cells. Journal of Biological Chemistry 270:5353-5359.

Finnegan JM, Pihel K, Cahill PS, Huang L, Zerby SE, Ewing AG, Kennedy RT, Wightman RM (1996) Vesicular quantal size measured by amperometry at chromaffin, mast, pheochromocytoma, and pancreatic β-cells. Journal of Neurochemistry 66:1914-1923.

Gonzalez MC, Artalejo AR, Montiel C, Hervas PP, Garcia AG (1986) Characterization of a dopaminergic receptor that modulates adrenomedullary catecholamine release. Journal of Neurochemistry 47:382-388.

Grynkiewicz G, Poenie M, Tsien RY (1985) A new generation of Ca^{2+} indicators with greatly improved fluorescence properties. Journal of Biological Chemistry 260:3440-3450.

Haynes CL, Buhler LA, Wightman RM (2006) Vesicular Ca^{2+}-induced secretion promoted by intracellular pH-gradient disruption. Biophysical Chemistry 123:20-24.

Hochstetler SE, Puopolo M, Gustincich S, Raviola E, Wightman RM (2000) Real-time amperometric measurements of zeptomole quantities of dopamine released from neurons. AnalChem 72:489-496.

Jourdain P, Israel J-M, Dupouy B, Oliet SHR, Allard M, Vitiello S, Theodosis DT, Poulain DA (1998) Evidence for a hypothalamic oxytocin-sensitive pattern-generating network governing oxytocin neurons *in vitro*. Journal of Neuroscience 18:6641-6649.

Kawagoe KT, Zimmerman JB, Wightman RM (1993) Principles of voltammetry and microelectrode surface states. Journal of Neuroscience Methods 48:225-240.

Khadra A, Li Y-X (2006) A model for the pulsatile secretion of gonadotropin-releasing hormone from synchronized hypothalamic neurons. In: Biophysical Journal.

Leszczyszyn DJ, Jankowski JA, Viveros OH, Diliberto J, E. J., Near JA, Wightman RM (1990) Nicotinic receptor-mediated catecholamine secretion from individual chromaffin cells. Journal of Biological Chemistry 265:14736-14737.

Moro MA, Lopez MG, Gandia L, Michelena P, Garcia AG (1990) Separation and culture of living adrenaline- and noradrenaline-containing cells from bovine adrenal medullae. Analytical Biochemistry 185:243-248.

Pihel K, Travis ER, Borges R, Wightman RM (1996) Exocytotic Release from Individual Granules Exhibits Similar Properties at Mast and Chromaffin Cells. Biophysical Journal 71:1633-1640.

Seeman P (1980) Brain dopamine receptors. Pharmacological Reviews 32:229-313.

Starke K (2001) Presynaptic autoreceptors in the third decade: focus on alpha2-adrenoceptors. J Neurochem 78:685-693.

Ueki K, Okada T, Hu J, Liew CW, Assmann A, Dahlgren GM, Peters JL, Shackman JG, Zhang M, Artner I, Satin LS, Stein R, Holzenberger M, Kennedy RT, Kahn CR, Kulkarni RN (2006) Total insulin and IGF-I resistance in pancreatic beta cells causes overt diabetes. Nat Genet 38:583-588.

Ungar A, Phillips JH (1983) Regulation of the adrenal medulla. Physiological Reviews 63:787-843.

Voets T, Neher E, Moser T (1999) Mechanisms underlying phasic and sustained secretion in chromaffin cells from mouse adrenal slices. Neuron 23:607-615.

Walker A, Glavinovic MI, Trifaro J (1996) Temperature dependence of release of vesicular content in bovine chromaffin cells. Pflugers Arch 432:885-892.

Yang D-M, Kao L-S (2001) Relative contribution of the Na^{+}/Ca^{2+} exchanger, mitochondria and endoplasmic reticulum in the regulation of cytosolic Ca^{2+} and catecholamine secretion of bovine adrenal chromaffin cells. Journal of Neurochemistry 76:210-216.

Yang J, Woodhall GL, Jones RS (2006) Tonic facilitation of glutamate release by presynaptic NR2B-containing NMDA receptors is increased in the entorhinal cortex of chronically epileptic rats. J Neurosci 26:406-410.

CHAPTER THREE

ALTERED VESICULAR RELEASE CHARACTERISTICS IN THE HUNTINGTON'S R6/2 MOUSE MODEL

INTRODUCTION

Huntington's disease (HD) is a neurodegenerative disorder that is caused by an unstable CAG expansion on the gene encoding the protein huntingtin. This expansion results in the formation of excessive polyglutamine repeats (>40) at the N-terminus (The Huntington's Disease Collaborative Research Group 1993). R6/2 transgenic mice are a model for HD and express exon 1 of the mutated human HD gene with a CAG repeat length of 141-157 (Mangiarini et al., 1996). These mice display progressive neuronal abnormalities and develop evident symptoms at 9-11 weeks of age.

One of the neuronal systems that becomes dysfunctional in Huntington's disease is the dopaminergic system (Reynolds et al., 1999; Jakel and Maragos, 2000). Hickey et al. (2002) showed that R6/2 mice were behaviorally less responsive to cocaine and methamphetamine (METH) than wild-type (WT) littermates. In previous work from this laboratory, the blunted responses to the psychostimulants were replicated and the processes of dopamine uptake and release were evaluated in brain slices from R6/2 mice of different ages (Johnson et al., 2006). The dopamine uptake system in the striatum in the mutant mice was identical to that in WT mice, and cocaine and methamphetamine inhibited dopamine uptake to a similar extent in both types of mice. In contrast, the concentration of dopamine released by local electrical stimulation was found to be impaired in animals as young as six weeks of age, and this deficit progressed with age. The diminished dopamine release in these studies corresponds with the decreased basal dopamine levels measured with microdialysis in

the R6/1 model (Petersen et al., 2002), which exhibits a less severe phenotype than the R6/2 model. These findings correlate with resultsfrom microdialysis studies in which basal extracellular levels of dopamine were found to be lower in R6/2 mice than in age-matched WT mice (Abercrombie and Russo, 2002).

The lowered release could have several origins. Release would be reduced if mechanisms associated with exocytosis were impaired. Then release observed at the single vesicle level would occur at a lower frequency than with tissue from WT mice. Another origin could be a diminished amount of catecholamine packaged into vesicles. In this case, release observed at the single vesicle level would occur with the same frequency as from tissue from WT mice but the amount released per exocytotic release would be diminished. To investigate these alternatives we examined release from adrenal chromaffin cells isolated from R6/2 mice and compared the results with both types of cells isolated from WT mice. In chromaffin cells, the frequency of evoked release was the same from both types of mice. However, both the amount released per vesicle and the time for extrusion of the vesicle contents was diminished in R6/2 mice, suggesting reduced vesicular packaging, an ATP dependent process, in the mutant mice. Because diminished ATP production has been implicated in Huntington's disease (Brennan et al., 1985), we investigated whether the diminished release was due to a compromised state of ATP-dependent packaging mechanisms. Indeed, following overnight incubations with 3-nitroproprionic acid, a respiratory chain uncoupler, the amounts released per exocytotic event and the accompanying extrusion times were diminished in chromaffin cells from WT mice but not in R6/2 mice. Thus, impaired exocytosis through reduced vesicular storage can be found in secretory cells from mutant mice expressing huntingtin.

EXPERIMENTAL PROCEDURE

Animals

Mice were handled in accordance with protocols approved by the Institutional Animal Care and Use Committee. The R6/2 line of transgenic mice and wild-type (WT) littermates were obtained from the Jackson Laboratory (Bar Harbor, Maine). Twelve- to fourteen-week-old mice were deeply anesthetized by ether inhalation and decapitated.

Adrenal medullary chromaffin cells

The adrenal glands were immediately removed and the medullae were decapsulated from the cortex and placed in Ca^{2+}- and Mg^{2+}-free Locke's buffer, which consisted of (in mM): NaCl, 154; KCl, 3.6; $NaHCO_3$, 5.6; D-glucose, 5.6; and HEPES, 10. The pH was adjusted to 7.2 using NaOH. Following dissection, the medullae were placed in 400 µL of papain (Sigma-Aldrich, St. Louis, MO) solution (25 U/mL) and incubated at 37ºC for 30 min. The papain solution was then removed, and the medullae were rinsed twice with 200-µL aliquots of Ca^{2+}- and Mg^{2+}-free Locke's buffer. The medullae were transferred to 500 µL of D-MEM/F-12 containing penicillin/streptomycin, nystatin, and gentamicin along with 10% fetal bovine serum and 2% horse serum. The tissue was triturated and the resulting solution was plated onto plastic cell culture plates (Falcon 3001, Becton Dickinson, Lincoln Park, NJ) containing 25 mm glass coverslips (size 0, Carolina Biological, Burlington, NC). Plates were stored at 37ºC in a 5% CO_2-supplemented incubator. Experiments were performed postplating days 0-2.

Electrodes and electrochemistry

Carbon-fiber disk microelectrodes were prepared as previously described using T-650 carbon fibers (Amoco, Greenville, SC) (Kawagoe et al., 1991a). Carbon fibers were aspirated into glass capillaries (A-M Systems, Inc, Carlsborg, WA) and the capillaries were subsequently heated and pulled (Narishige, Long Island, NY). The extending carbon fiber was cut flush with the end of the glass tip, and the carbon fiber was sealed in place with epoxy (EPON resin 828, Miller-Stephenson, Danbury, CT; m-phenylenediamine, DuPont, Wilmington, DE). Electrodes were cured at 100^{o}C for 12 h followed by 12 h at 150^{o}C. Before use, electrodes were polished on a diamond polishing wheel at 45º (Sutter Instruments, Novato, CA) and soaked for 10 min. in 2-propanol purified with activated carbon (Bath et al., 2000).

Release measurements

Chromaffin cells were placed in buffer containing (in mM): NaCl, 145; KCl, 5; $MgCl_2$, 1; $CaCl_2$, 2; D-glucose, 11.2; and HEPES, 10. The pH was adjusted to 7.4 using NaOH. The culture plates were placed on the stage of an inverted microscope (Zeiss, Thornwood, NY). Cells were maintained at 37ºC with a heated stage connected to a constant temperature, circulating, water bath (Fisher Scientific, Hampton, NH). Glass-pressure ejection pipettes used to introduce secretagogues onto cells had a tip diameter of ~10 μm and were connected to a gas valve (Picospritzer, General Valve Corporation, Parker Hannifin, Fairfield, NJ) operated at 7 psi . The pipettes were prepared with a micropipette puller (Sutter Instruments, Novato, CA) and fire-polished in a microforge (Narishige, Long Island,

NY). The tips of ejection pipettes were placed ~20 µm from the cell to evoke release. A carbon-fiber electrode was placed in firm contact with the cell surface.

Amperometric currents were recorded with an Axopatch 200B (Axon Instruments, Molecular Devices, Union City, CA). The electrodes were held at +0.65 V vs. a Ag/AgCl reference electrode for measurements at chromaffin cells. The current was filtered at 5 kHz with a low-pass Bessel filter and digitized at 10 kHz.

Release from chromaffin cells was evoked by pressure ejection of a 60-mM KCl solution with the NaCl concentration adjusted to maintain isoosmolarity with the buffer.

3-nitropropionic acid (3-NP)

In some experiments with chromaffin cells, the effects of incubation with 3-NP was examined. A stock solution of 1.68 M 3-NP (Sigma-Aldrich, St. Louis, MO) was prepared in ethanol. Two hours after plating, 1 mM 3-NP or vehicle (0.06% v/v) was added to the plates. Cells were then incubated for approximately 20 h in these solutions. Subsequently, amperometric measurements during release evoked by 60 mM K^+ were made as described above.

Data analysis

Spike analysis was performed using MiniAnalysis (Synaptosoft, Decatur, GA). For inclusion in the analysis, spikes had to be at least five times larger than the root-mean-square current noise. The average spike area (Q), average spike width at half height ($t_{1/2}$) and average spike frequency were recorded for each amperometric trace (Colliver et al., 2000). The spike area, obtained by integrating the measured current with respect to time, reveals the

total charge for each exocytotic event. By Faraday's law, Q = nFm where Q is the charge, n is the number of electrons lost during the oxidation of each molecule, and F is Faraday's constant, the number of oxidized molecules released, m, can be calculated. For these data, a two-electron process was assumed. The distribution of spike areas does not follow a Gaussian shape; however, the cube roots of spike area fall into a Gaussian distribution (Wightman et al., 1995b). Therefore, for each cell, a mean of the cubed root of the spike area, $Q^{1/3}$, was calculated. From this value, a mean Q value was calculated for each cell and included in the cumulative mean for a particular experimental group. The $t_{1/2}$ value is a measure of the time for extrusion of the vesicle contents. The $t_{1/2}$ values also do not follow a Gaussian distribution; for each cell, a mean of the cubed root of the $t_{1/2}$ was also calculated. The cumulative mean for a particular experimental group was also determined using the mean $t_{1/2}$ value calculated for each cell. Spike frequency (f) in chromaffin cells was determined by dividing the number spikes counted by the time period over which they occurred. Spikes with an interspike interval greater than 1 s were excluded.

To analyze for pre-spike features, which are also termed feet, all the spikes in each trace that were preceded by a pre-spike feature were selected manually. Foot analysis was performed in a MiniAnalysis sub-routine by marking the apex of the spike, the baseline of the spike, and the inflection point between the foot and the full fusion spike. The integrated area was divided into foot area and full fusion spike area based on the inflection point.

Statistics

Statistical analyses in comparisons of spike frequency, average Q, and average $t_{1/2}$ were performed using a Student's t-test. For foot analysis, an average ratio of the foot and

the spike was recorded for each trace. Linear regression or *t*-test analysis was performed on these trace-averaged characteristics to test statistical significance ($p < 0.05$). Statistical tests conducted in studies involving 3-NP were done using single factor ANOVA. Values are shown as mean ± SEM.

RESULTS

Amperometric spike characteristics at adrenal medullary chromaffin cells

Chromaffin cells isolated from the medulla of adrenal glands release epinephrine and norepinephrine. Release evoked in cells with 3-s applications of 60 mM K^+ revealed differences in amperometric spike characteristics between cells from WT (n = 30 cells) and R6/2 (n = 21 cells) mice (representative traces shown in Figures 3.1A and 3.1B). When spike Q values were averaged, a significant difference ($p < 0.05$) was observed between WT (Q = 0.42 ± 0.02 pC) and R6/2 (Q = 0.24 ± 0.02 pC) cells (Figure 3.1C). On average, 5.6×10^5 more molecules were released from vesicles from WT mice than from R6/2 mice. A significant difference in $t_{1/2}$ ($p < 0.05$) was also measured between WT (7.39 ± 0.41 msec) and R6/2 (5.84 ± 0.48 msec) cells (Figure 3.1D). The smaller average $t_{1/2}$ from the R6/2 cells indicates the time course of extrusion of epinephrine and norepinephrine is faster than in WT cells. The spike frequency of WT (7.36 ± 0.51 Hz) and R6/2 (6.63 ± 0.74 Hz) cells were not significantly different ($p > 0.05$) (Figure 3.1E).

To compare the process of vesicle mobilization in adrenal medullary chromaffin cells, dual-pulse experiments were performed. Cells were stimulated twice with 1-s applications of 60 mM K^+ at 10-s intervals; data were analyzed as a ratio (S2/S1) of the number of spikes in the second stimulation, S2, versus the number of spikes in the first stimulation, S1. No

significant difference in spike number ratios was calculated ($p > 0.05$) between wild-type (0.65 ± 0.10) and R6/2 (0.83 ± 0.10) cells (Figure 3.2A). The number of spikes evoked on the first stimulus, S1, was also compared between WT and R6/2 mice. There was no significant difference between the number of evoked spikes from naïve cells ($p > 0.05$); WT mice showed an average of 25.7 ± 3.5 spikes ($N = 19$ cells) while R6/2 mice showed an average of 34.2 ± 4.1 elicited spikes ($N = 19$ cells).

In approximately 10% of amperometric spikes, a pre-spike feature occurs that indicates the presence of a nanometer-scale fusion pore. These pre-spike features, also known as feet, were analyzed to contrast fusion efficiency in the two mouse models. In chromaffin cells, there was no significant difference in the average number of feet per trace (4.27 ± 0.55 WT; 3.72 ± 0.54 R6/2), the average foot-to-spike area ratio (0.21 ± 0.03 WT; 0.19 ± 0.04 R6/2), or the percentage of cells that exhibit feet (90% WT; 96% R6/2).

Application of 3-nitropropionic acid (3-NP)

To test the hypothesis that ATP depletion may be a contributing cause of the diminished efficiency of vesicle packaging, chromaffin cells from WT and R6/2 mice were treated with the mitochondrial toxin, 3-nitropropionic acid (3-NP). Vehicle-treated WT chromaffin cells showed a mean spike area of 0.50 ± 0.07 pC while 3-NP-treated WT chromaffin cells had a mean area of 0.26 ± 0.04 pC. Vehicle-treated R6/2 chromaffin cells had an average spike area of 0.23 ± 0.02 pC, and whereas for 3-NP-treated R6/2 chromaffin

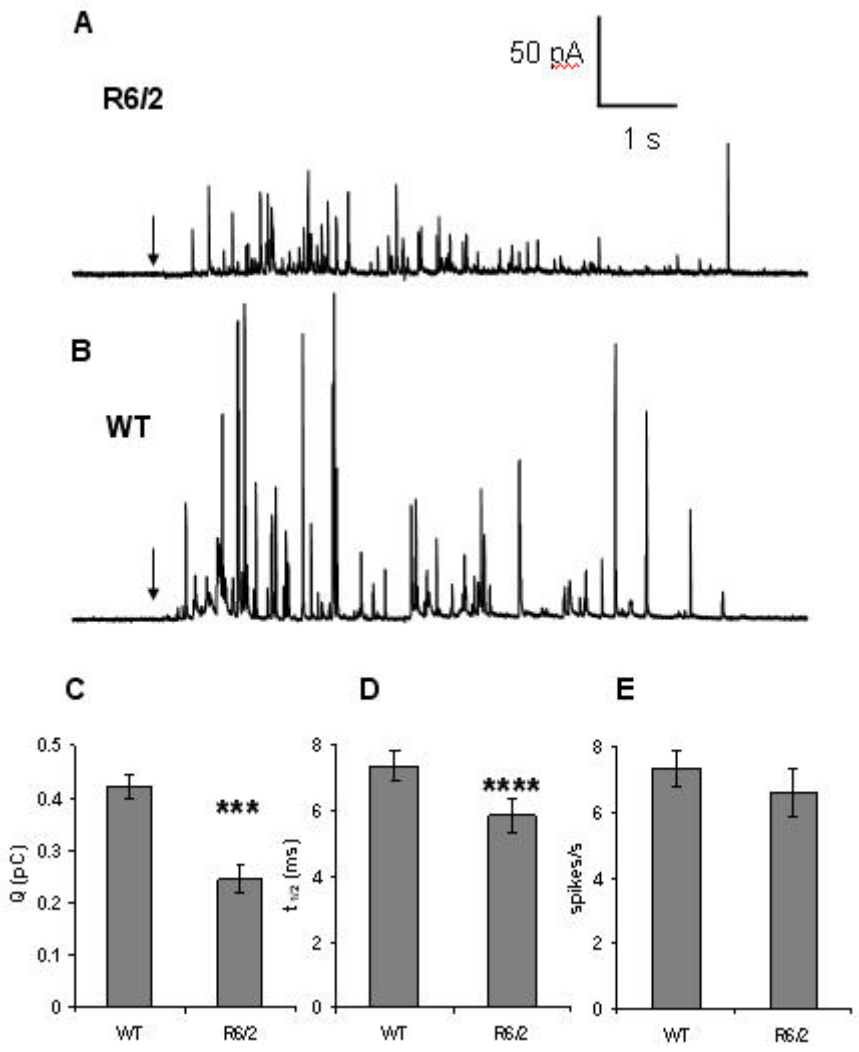

Figure 3.1. Vesicular release characteristics are different in adrenal chromaffin cells from R6/2 mice than from WT mice. (A) Amperometric trace (E_{app} = +0.650 V) of individual exocytotic events evoked by 60 mM K^+ from a chromaffin cell isolated from an R6/2 mouse. (B) Release events measured under identical conditions from a chromaffin cell isolated from a WT mouse. The bar graphs compare (C) average spike area, (D) average spike half-width, and (E) average spike frequency for release events at WT and R6/2 mice. Values are the mean ± SEM obtained at 30 WT cells and 21 R6/2 cells (*** and **** signify $p < 0.05$).

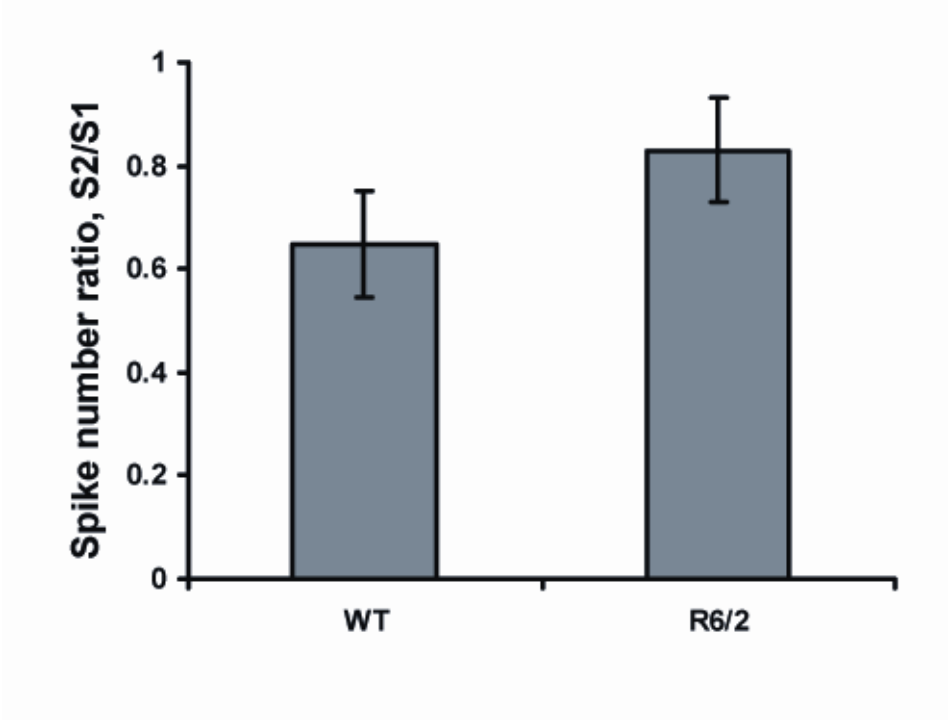

Figure 3.2. Vesicular mobilization monitored at WT and R6/2 chromaffin cells. Cells were stimulated in an S2/S1 protocol in which paired stimuli were applied to the cells with a 10-s interstimulus interval. The number of spikes in the second stimulus, S2, were compared to those from the first stimulus, S1. Cells were stimulated with 1-s applications of 60 mM K^+. Both groups show slight depression in release (N = 19 WT cells; N = 19 R6/2 cells). There was no significant difference between WT and R6/2 cells ($p > 0.05$).

cells the average spike area was 0.18 ± 0.03 pC. The average of vehicle-treated WT chromaffin cells is significantly different from those of the 3-NP-treated WT cells, vehicle-treated R6/2 cells, and 3-NP-treated R6/2 cells (Figure 3.3A; $p<0.05$, ANOVA). On average, there was a difference of 7.3×10^7 molecules released per vesicle between the vehicle-treated and 3-NP-treated WT cells.

Because vesicle priming is also an ATP-dependent process, the frequency of an amperometric spike burst was also evaluated. The average spike frequency for vehicle-treated WT cells was 4.79 ± 0.56 Hz ; 3-NP-treated WT cells yielded a mean spike frequency of 3.63 ± 0.50 Hz. For vehicle-treated R6/2 cells, the mean frequency was 3.43 ± 0.35 Hz. The average frequency for 3-NP-treated R6/2 cells was 4.63 ± 0.91 Hz. There was no significant difference among the experimental groups (Figure 3.3B; $p > 0.05$).

DISCUSSION

Prior work established that release of dopamine from striatal neurons in mice expressing human huntingtin is impaired (Johnson et al., 2006). Consistent with this, exocytosis from adrenal chromaffin cells isolated from R6/2 mice is impaired when examined at the single vesicle level. Chromaffin cells, which are phylogenetically related to neurons of the central nervous system (Anderson and Axel, 1986; Anderson, 1989, 1993) exhibit responses pointing to compromised vesicular stores in R6/2 mice compared to WT controls. While the frequency of exocytotic events evoked by transient depolarization is not statistically different at cells from the two types of mice, the amounts released are lower and the extrusion time is diminished in chromaffin cells from R6/2 mice. The results following overnight incubation with the mitochondrial toxin, 3-NP, suggest that the diminished storage

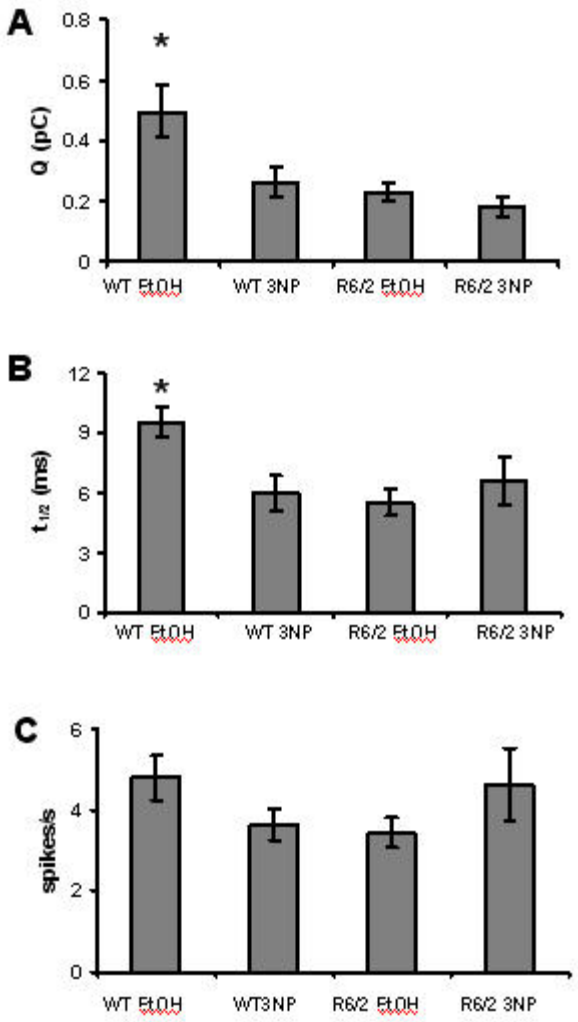

Figure 3.3. Vesicular release characteristics are altered by the mitochondrial toxin, 3-nitropropionic acid (3-NP). (A) Comparison of Q across the four experimental groups. WT adrenal chromaffin cells treated with vehicle (N = 13) show significant difference in Q from WT adrenal chromaffin cells treated with 3-NP (N = 8), R6/2 adrenal chromaffin cells treated with vehicle (N = 12), and R6/2 adrenal chromaffin cells treated with 3-NP (N = 6) (* signifies $p < 0.05$). (B) Comparison of $t_{1/2}$ across the four experimental groups. WT adrenal chromaffin cells treated with vehicle show significant difference in vesicle extrusion time as indicated by $t_{1/2}$ from WT adrenal chromaffin cells treated with 3-NP, R6/2 adrenal chromaffin cells treated with vehicle, and R6/2 adrenal chromaffin cells treated with 3-NP (* signifies $p < 0.05$). (C) WT adrenal chromaffin cells treated with vehicle show no significant difference in spike frequency ($p > 0.05$) across the four experimental groups.

is a consequence of an ATP-dependent process. The average Q, which indicates the average catecholamine amount extruded by the vesicles, is lower in WT mice than in previously published results. Finnegan et al. demonstrated that the average Q observed at bovine chromaffin cells was approximately twice the amount that was observed in the present studies (Finnegan et al., 1996). Grabner et al. also showed that murine chromaffin cells exhibit a lower Q than bovine chromaffin cells (Grabner et al., 2005). The value obtained in the studies conducted by Grabner et al. show closer agreement to our data than that of the bovine chromaffin cells indicating a difference in quantal size between the two species.

Because the huntingtin protein is expressed in adrenal medullary chromaffin cells (Mangiarini et al., 1996), we searched for a similar decrease in exocytotic release that had been seen previously in striatal neurons (Johnson et al., 2006). While exocytotic release frequency and number of evoked spikes were unchanged in the chromaffin cells of R6/2 mice, the vesicular amounts released and the durations of vesicle content extrusion were diminished, suggesting that reduced amounts of catecholamines were packaged in the vesicles. This may be one mechanism that accounts for the reduced dopamine release Johnson et al. (2006) demonstrated in striatal neurons.

Impaired ATP production may be responsible for this reduction in exocytotic release. It has been shown that subacute treatment of 3-NP is another viable model for Huntington's disease (Brouillet et al., 2005). 3-NP is an inhibitor of mitochondrial function and lowers production of ATP. Indeed, ATP production has been demonstrated to be aberrant in the brains of Huntington's disease patients (Brennan et al., 1985). ATP plays two important roles in packaging of catecholamines into vesicles within chromaffin cells. First, the electrochemical gradient created by the ATP-driven H^+ pump drives vesicle loading by the

monoamine-proton antiporter, VMAT1 found on chromaffin cell vesicles (Henry et al., 1994; Eiden et al., 2004) Second, ATP is packaged within chromaffin cell vesicles with a 1:4 stoichiometry with catecholamines (Kopell and Westhead, 1982). Association of negatively charged ATP with the protonated amine side chain of catecholamines is thought to promote storage of the vesicle contents (Kopell and Westhead, 1982). Impairment of either or both of these mechanisms could compromise vesicular catecholamine storage: catecholamine molecules would either be unable to enter the vesicles effectively or would not remain packaged at normal levels within the vesicles.

To test whether impaired ATP production affects vesicle secretion from chromaffin cells, cells from R6/2 and WT mice were incubated overnight with 3-NP. While release characteristics were unchanged in cells from R6/2 mice, release from treated chromaffin cells from WT mice showed characteristics similar to release from untreated R6/2 chromaffin cells: amounts released per vesicular event were reduced and extrusion times were diminished. These data indicate that secretory stores in cells from WT mice are sensitive to diminished production of ATP, whereas they are not in R6/2 mice. The lack of an effect of 3-NP in R6/2 mice may indicate that a compromised ATP-dependent mechanism is a major cause of deleterious effects in vesicular release. ATP is also important in priming vesicles for exocytosis (Holz et al., 1989). Our experiments did not reveal deficits in that aspect of exocytosis in either mouse type as spike frequency was not significantly different. Although there is no evidence for costorage of ATP and dopamine in dopaminergic neurons, the neuronal-vesicular transporter, VMAT2, is similarly dependent on the ATP-dependent H^+ pump for loading of dopamine. Thus, this may be an underlying mechanism for the diminished release seen in striatal slices.

Expression of mutant huntingtin in PC12 cells causes a depletion of complexin II, a protein that binds to the SNARE complex that is central to the membrane fusion apparatus. This is accompanied by an inhibition of the frequency of evoked exocytotic events that can be rescued by overexpression of complexin II (Edwardson et al., 2003). However, it has been shown that overexpression of complexin II in bovine chromaffin cells decreases the time course of vesicle extrusion while also diminishing amperometric area (Archer et al., 2002). This discrepancy in the results obtained from chromaffin cells and PC12 cells may indicate an optimal cytosolic concentration above which inhibition of exocytosis occurs as overexpression of complexin II in chromaffin cells abolished function and overexpression of complexin II in PC12 cells rescued function (Archer et al., 2002). Our results show that the decrease in quantal size does not appear to be directly related to complexin II as we were able to replicate the results seen in R6/2 cells in cells of WT mice following overnight incubation of 3-NP. Use of 3-NP to reproduce the R6/2 phenotype of vesicular release indicates that our observations may be linked to an ATP-dependent mechanism instead of complexin II.

REFERENCES

Abercrombie ED, Russo ML (2002) Neurochemistry in the R6/2 transgenic mouse model of Huntington's disease. Society for Neuroscience, Orlando, FL Program no. 195.12.

Anderson DJ (1989) The neural crest cell lineage problem: neuropoiesis? Neuron 3:1-12.

Anderson DJ (1993) Molecular control of cell fate in the neural crest: The sympathoadrenal lineage. Annual Reviews in Neuroscience 16:129-158.

Anderson DJ, Axel R (1986) A bipotential neuroendocrine precursor whose choice of cell fate is determined by NGF and glucocorticoids. Cell 47:1079-1090.

Archer DA, Graham ME, Burgoyne RD (2002) Complexin regulates the closure of the fusion pore during regulated vesicle exocytosis. Journal of Biological Chemistry 277:18249-18252.

Bath BD, Michael DJ, Trafton BJ, Joseph JD, Runnels PL, Wightman RM (2000) Subsecond adsorption and desorption of dopamine at carbon-fiber microelectrodes. Analytical Chemistry 72:5994-6002.

Brennan WJ, Bird E, Aprille J (1985) Regional mitochondrial respiratory activity in Huntington's disease brain. Journal of Neurochemistry 44:1948-1950.

Brouillet E, Jacquard C, Bizat N, Blum D (2005) 3-Nitropropionic acid: a mitochondrial toxin to uncover physiopathological mechanisms underlying striatal degeneration in Huntington's disease. Journal of Neurochemistry 95:1521-1540.

Eiden LE, Schafer MK-H, Weihe E, Schutz B (2004) The vesicular amine transporter family (SLC18) amine/proton antiporters required for vesicular accumulation and regulated exocytotic secretion of monoamines and acetylcholine. Pflugers Archiv European Journal of Physiology 447:636-640.

Finnegan JM, Pihel K, Cahill PS, Huang L, Zerby SE, Ewing AG, Kennedy RT, Wightman RM (1996) Vesicular quantal size measured by amperometry at chromaffin, mast, pheochromocytoma, and pancreatic β-cells. Journal of Neurochemistry 66:1914-1923.

Grabner CP, Price SD, Lysakowski A, Fox AP (2005) Mouse chromaffin cells have two populations of dense core vesicles. Journal of Neurophysiology 94:2093-2104.

Henry JP, Botton D, Sagne C, Isambert MF, Desnos C, Blanchard V, Raisman-Vozari R, Krejci E, Massoulie J, Gasnier B (1994) Biochemistry and molecular biology of the vesicular monoamine transporter from chromaffin granules. Journal of Experimental Biology 196:251-262.

Holz RW, Bittner MA, Peppers SC, Senter RA, Eberhard DA (1989) MgATP-independent and MgATP-dependent exocytosis. Journal of Biological Chemistry 264:5412-5419.

Jakel RJ, Maragos WF (2000) Neuronal cell death in Huntington's disease: a potential role for dopamine. Trends in Neuroscience 23:239-245.

Johnson MA, Rajan V, Miller CE, Wightman RM (2006) Dopamine release is severely compromised in the R6/2 mouse model of Huntington's disease. Journal of Neurochemistry.

Kawagoe K, Jankowski J, Wightman RM (1991) Etched carbon-fiber electrodes as amperometric detectors of catecholamine secretion from isolated biological cells. Analytical Chemistry 63:1589-1594.

Kopell WN, Westhead EW (1982) Osmotic pressures of solutions of ATP and catecholamines relating to storage in chromaffin granules. Journal of Biological Chemistry 257:5707-5710.

Mangiarini L, Sathasivam K, Seller M, Cozens B, Harper A, Hetherington C, Lawton M, Trottier Y, Lehrach H, Davies SW, Bates GP (1996) Exon 1 of the HD Gene with an Expanded CAG Repeat Is Sufficient to Cause a Progressive Neurological Phenotype in Transgenic Mice. Cell 87:493-506.

Petersen A, Puschban Z, Lotharius J, NicNiocaill B, Wiekop P, O'Connor WT, Brundin P (2002) Evidence for dysfunction of the nigrostriatal pathway in the R6/1 line of transgenic Huntington's disease mice.

Reynolds GP, Dalton CF, Tillery CL, Mangiarini L, Davies SW, Bates GP (1999) Brain neurotransmitter deficits in mice transgenic for the Huntington's disease mutation. Journal of Neurochemistry 72:1773-1776.

Wightman RM, Schroeder TJ, Finnegan JM, Ciolkowski EL, Pihel K (1995) Time course of release of catecholamines from individual vesicles during exocytosis at adrenal medullary cells. Biophysical Journal 68:383-390.

CHAPTER FOUR

AMPEROMETRIC CHARACTERIZATION OF EXOCYTOSIS IN CHROMAFFIN CELLS LACKING SYNAPSIN II

INTRODUCTION

Exocytosis is a highly efficient process that is tightly regulated. One form of regulation is achieved through vesicle mobilization from different vesicle pools. Three vesicle pools have been defined: the readily releasable pool, the recycling pool, and the reserve pool (Voets et al., 1999; Rizzoli and Betz, 2005). The readily releasable pool contains vesicles that are docked and/or primed at the cell membrane and prepared for release upon stimulation. The recycling pool contains vesicles that have been newly retrieved from the plasma membrane after fusion and which are ready to replenish the readily releasable pool. The reserve pool contains the majority of the vesicles within the cell, is located away from the plasma membrane, and is believed to be regulated by association to the actin cytoskeleton. Because the reserve pool contains the vast majority of vesicles, regulation of vesicle mobilization may rely heavily upon availability of vesicles from this pool.

Synapsin is an intracellular phosphoprotein that has been implicated in maintaining vesicles in the reserve pool. Synapsin is believed to serve as a link between vesicles and the actin cytoskeleton, and upon phosphorylation, dissociates from the actin cytoskeleton to mobilize vesicles (Hilfiker et al., 1998). There are three isoforms of synapsin that have been discovered: I, II, and III. Synapsins I, II, and III are found in neurons where they associate with synaptic vesicles; however, synapsin II is the only isoform to have been located in chromaffin cells of the adrenal medulla (Browning et al., 1987).

Previous work has shown that depolarizing secretagogues such as acetylcholine (Ach), potassium, veratridine, and barium induced an increase in the phosphorylation of

synapsin II in bovine chromafffin cells (Haycock et al., 1988). Further studies indicate that nicotinic and K^+ stimulation, but not muscarinic stimulation, augment catecholamine release and synapsin II phosphorylation (Firestone and Browning, 1992). Since disruption of synapsin I function in synapses has been shown to increase total vesicular release by promoting dissociation of vesicle-bound synapsin from the actin cytoskeleton (Hilfiker et al., 1998), prior studies where synapsin II phosphorylation also increased exocytotic release appear to point to a similar role in vesicle mobilization.

This work aims to characterize catecholaminergic vesicular release in chromaffin cells lacking synapsin II using amperometry and to characterize the accompanying Ca^{2+} dynamics using the fluorescent complexing agent, fura-2. We have found that amperometric spike characteristics between WT mice and mice lacking synapsin II (TKO) show no significant differences in spike area or halfwidth, indicating that quantal size is unaffected. Consistent with a role in vesicle mobilization, we have observed an enhanced number of vesicles released from TKO cells upon depolarizing stimulation with K^+

EXPERIMENTAL PROCEDURE

Acutely dissociated chromaffin cell culture

Animals were handled in accordance with protocols approved by the Institutional Animal Care and Use Committee. The line of transgenic mice lacking the three isoforms of synapsin (I, II, and III), mixed from C57/BL6 and s129 strains, and wild-type littermates were obtained from the Augustine laboratory at Duke University. Two- to four-month old mice were anesthetized deeply by ether inhalation and subsequently decapitated. The adrenal glands were separated and the medullae were isolated from the cortical tissue. The dissection

was performed using Ca^{2+}- and Mg^{2+}-free Locke's buffer, which contained (in mM): NaCl, 154; KCl, 3.6; $NaHCO_3$, 5.6; D-glucose, 5.6; and HEPES, 10. The pH was adjusted to 7.2 using NaOH. Following dissection, the medullae were placed in 400 µL of papain solution (25 U/mL) and incubated at 37ºC for 30 min. The papain solution was then decanted, and the medullae were rinsed twice with 200-µL aliquots of Ca^{++}- and Mg^{++}-free Locke's buffer. The medullae were then placed in 500 µL of DMEM/F-12 containing penicillin/streptomycin, nystatin, and gentamicin along with 10% fetal bovine serum and 2% horse serum. The tissue was triturated and the resulting solution was plated. Experiments were performed 0-2 days postplating.

Ca^{2+} measurements using fura-2

Fluorescent monitoring of Ca^{2+} dynamics was accomplished using the fluorescent tag, fura-2, as described previously (Finnegan and Wightman, 1995). An imaging system (Empix) with excitation filters alternated between 340 and 380 nm while emission was measured at 510 nm. An initial fura-2 solution was diluted with 40 µL DMSO and 10 µL of 10% pluronic. This fura-2 solution was diluted to 1 µM in experimental buffer containing 0.10 % BSA (Molecular Probes, Invitrogen, Carlsbad, CA). Cells were incubated in this final solution for 20 min at 25ºC, followed by a rinse for 20 min at 25ºC in the experimental buffer. Ca^{2+}-imaging experiments were conducted after the incubation period. Cells were visualized using an inverted microscope (Nikon, Lewisville, TX) and imaging software (Empix Imaging, Inc, Mississauga, ON, CANADA. The ratiometric measurements were then converted to $[Ca^{2+}]_i$ as previously described (Grynkiewicz et al., 1985; Finnegan and Wightman, 1995).

Electrodes and electrochemistry

Carbon-fiber disk microelectrodes were prepared as previously described using T-650 carbon fibers (Amoco, Greenville, SC) (Kawagoe et al., 1991b). Carbon fibers were aspirated into glass capillaries (A-M Systems, Inc, Carlsborg, WA) and the capillaries were subsequently heated and pulled to create a glass seal (Narishige, Long Island, NY). The extending carbon fiber was cut level with the glass seal; the seal was insulated further with epoxy (EPON resin 828, Miller-Stephenson, Danbury, CT; m-phenylenediamine, DuPont, Wilmington, DE). Electrodes were cured at 100°C for 12h and then cured at 150°C for 12 h. Before use, electrodes were polished on diamond polishing wheels at 45º (Sutter Instruments, Novato, CA) and soaked for at least 10 min in 2-propanol purified with activated carbon (Bath et al., 2000). During experiments, electrodes were held at a constant potential of +650 mV vs. a Ag/AgCl reference electrode.

Release experiments

The experimental buffer consisted of (in mM): NaCl, 145; KCl, 5; $MgCl_2$, 1; $CaCl_2$, 2; D-glucose, 11.2; and HEPES, 10. The pH was adjusted to 7.4 using NaOH. The high potassium solution used to stimulate cells contained 60 mM KCl and was adjusted to maintain isoosmolarity with the experimental buffer. Cells were maintained at 37ºC with a heated stage on the microscope and circulating water bath (Fisher Scientific, Pittsburgh, PA). Exocytosis was elicited from cells by delivering a 0.5-s or 1-s bolus of 60 mM K^+ from a glass pipette with a tip diameter of ~10 μm via pressure ejection (Picospritzer, General Valve Corporation, Parker Hannifin, Fairfield, NJ). The pipettes were manufactured using a

horizontal micropipette puller (Sutter Instruments, Novato, CA) and fire-polished in a microforge to attain an opening diameter of 6-10 μm (Narishige, Long Island, NY). The stimulating pipette was then placed ~20 μm from the cell during experiments. Amperometric measurements were recorded using an Axopatch 200B (Axon Instruments, Union City, CA); vesicular release events were detected as current spikes. The resulting signal was filtered at 5 Hz with a low-pass Bessel filter and collected at 10 kHz.

Transfection of synapsin IIa and EGFP-only vector.

In some experiments, chromaffin cells were transfected with plasmid containing synapsin IIa and EGFP plasmid or the EGFP-only plasmid via lipid delivery. EGFP was present in both plasmids to verify expression in cells. After allowing plates to incubate at 37ºC in 5% CO_2 overnight, the original plating media was replaced with Opti-MEM media with reduced serum (Invitrogen, Carlsbad, CA). Next, 0.4 μg of plasmid along with 0.2 μL of the lipid complexing agent Lipofectamine (Invitrogen, Carlsbad, CA) was added to each plate that was to be transfected. Plates were allowed to incubate for 4-6 h after which time, the media was replaced with the DMEM/F-12 (Gibco/Invitrogen, Carlsbad, CA) and the plates were incubated for approximately 24 h. Exocytosis was examined after the 24-h incubation period using 0.5-s applications of high K^+ solution at 37ºC.

Data analysis

Amperometric traces were filtered at 400 Hz using a digital Gaussian filter. Spike analysis was then performed using MiniAnalysis (Synaptosoft, Decatur, GA). Spikes

analyzed were at least five times the root-mean-square current noise. Average spike area (Q), average spike width ($t_{1/2}$) and average spike frequency were recorded for each amperometric trace (Colliver et al., 2000). The distribution of spike areas does not follow a Gaussian shape; however, the cube roots of the spike areas fall into a Gaussian distribution (Wightman et al., 1995b). For each cell, a mean of the cubed root of the spike area, $Q^{1/3}$, was calculated. From this value, the mean Q was calculated for each cell and included in the cumulative mean for a particular experimental group. The $t_{1/2}$ value is a measure of the time for extrusion of the vesicle contents. The $t_{1/2}$ values also do not follow a Gaussian distribution; for each cell, a mean of the cubed root of the $t_{1/2}$ was also calculated. The cumulative mean for a particular experimental group was also determined using the mean $t_{1/2}$ value calculated for each cell.

Statistics

Statistical analyses in comparisons of spike frequency, average Q, which was derived from the mean value of $Q^{1/3}$, and average $t_{1/2}$, which was also derived from the mean value of the cube root of $t_{1/2}$, were performed using a Student's t-test.

RESULTS

Vesicular release evoked by K^+ and Ba^{2+}

Release from chromaffin cells obtained from triple knockout mice (TKO) showed enhanced release compared to that evoked from cells obtained from wild-type littermates (WT) using identical stimuli (for example traces, see Figure 4.1). The increase in release observed in TKO cells was quantified by counting the number of spikes elicited by the K^+

stimulus. Using a 0.5-s 60 mM K^+ stimulus, the average number of spikes elicited in 10 s from naïve WT cells was 19 ± 3 while the average from naïve TKO cells was 36 ± 5 ($p < 0.05$). A 1-s stimulus evoked a mean number of spikes from WT cells of 30 ± 5; the mean number of spikes from TKO cells was 57 ± 7 ($p < 0.05$; Figure 4.2).

Vesicular release characteristics and Ca^{2+} dynamics

Comparison of the amperometric spike characteristics of the adrenal cells from TKO mice and the WT mice showed no significant difference between the amount released per vesicle (Q) or the average time for each extrusion event ($t_{1/2}$) ($p > 0.05$) (Figure 4.3A, B). The average $t_{1/2}$ value for the WT cells was 10.7 ± 1.9 ms; the average $t_{1/2}$ value for the TKO cells was 12.2 ± 1.4 ms. The WT cells yielded a mean Q value of 0.45 ± 0.03 pC while the TKO cells yielded a mean Q value of 0.47 ± 0.04 pC. The distribution of Q for WT and TKO cells is shown in Figure 4.2C and E while the distribution of $Q^{1/3}$ is shown in Figure 4.3 D and F.

The intracellular Ca^{2+} influx during high potassium application between cells from the two mouse types exhibited no significant difference (Figure 4.2B). The average area under the $[Ca^{2+}]$ peak in WT cells was 3.4 ± 0.9 arbitrary units compared to 3.6 ± 1.0 in TKO cells indicating that the difference seen in vesicular release is not linked to differences in Ca^{2+} influx.

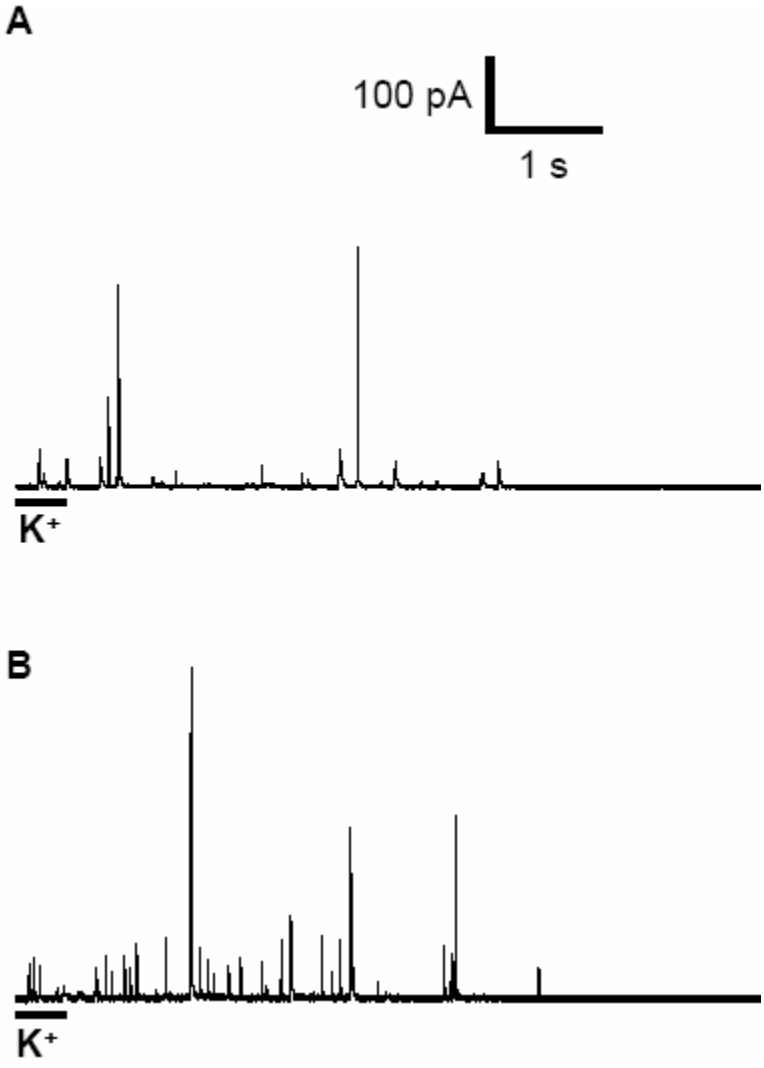

Figure 4.1. Comparison of K^+-stimulated release at 37ºC between WT and TKO cells. (A) Representative amperometric trace recorded from a (A) WT cell and a (B) TKO cell using a 0.5-s stimulus.

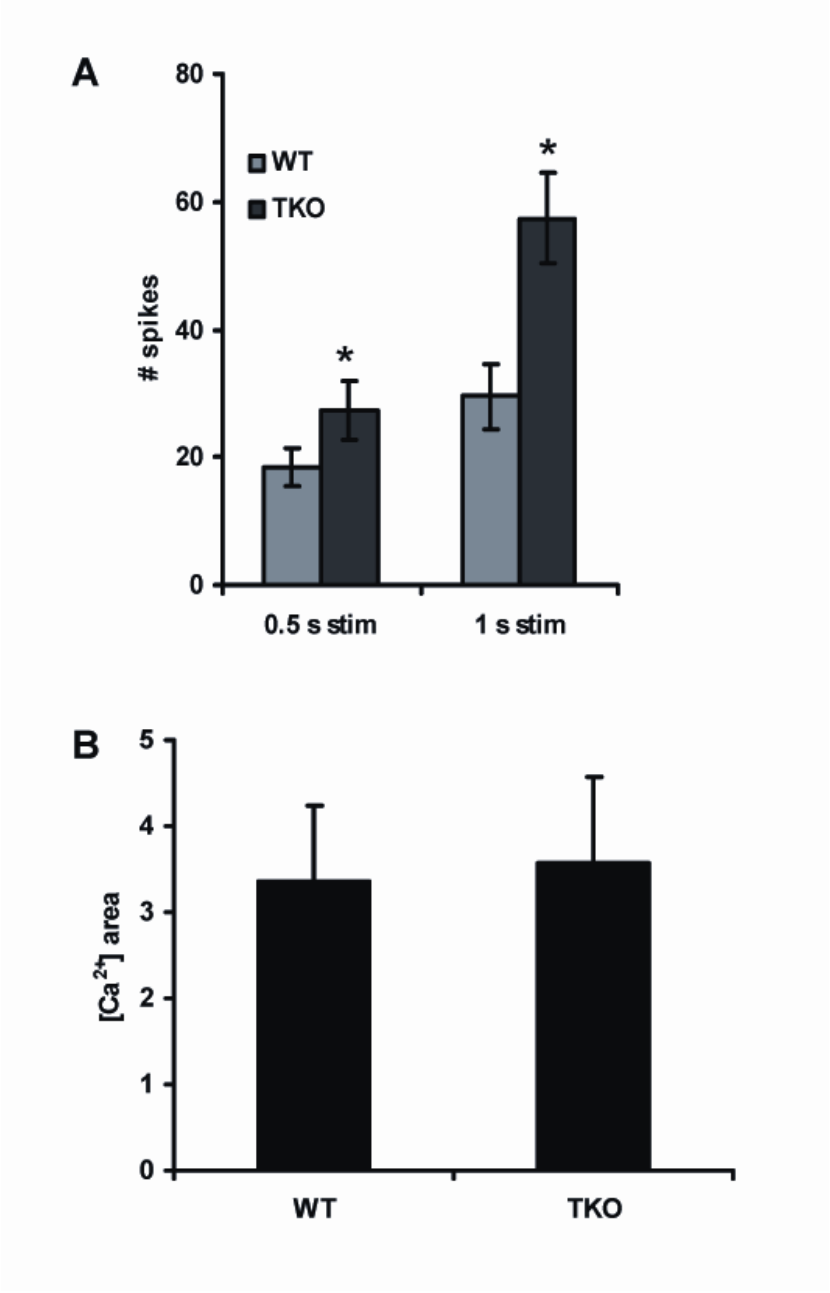

Figure 4.2. Comparison of the number of evoked spikes and Ca^{2+} dynamics between WT and TKO cells. (A) Exocytosis was evoked high K^+. The 0.5-s stimulus ($p < 0.05$) and the 1-s stimulus ($p < 0.05$) elicited an increased number in spikes from the TKO cells . (B) Comparison of Ca^{2+}dynamicsbetween WT and TKO cells. Ca^{2+} area shows no significant difference between WT cells ($n = 7$) and TKO cells ($n = 5$) ($p > 0.05$) indicating that the difference in K^+-stimulated release is not due to differences in Ca^{2+} influx.

Rescue experiments via transfection of synapsin IIa

Experiments were conducted in which cells of both types were transfected with synapsin IIa and EGFP to verify expression via lipid delivery (for example traces, see Figure 4.4). Three different conditions were imposed on WT cells and TKO cells. In the first condition, termed control, the cells were not transfected but were kept in the same media as the transfected cells. In the second condition, WT and TKO cells were exposed to EGFP-only plasmid as a control for the transfection process. In the third condition, WT and TKO cells were incubated with plasmid containing synapsin IIa and EGFP. The mean number of spikes elicited in 10 s from naïve cells was compared across groups (Figure 4.5). TKO control released significantly more vesicles than WT control upon a 0.5- s K^+ stimulus as seen in previous experiments; on average the TKO control group released 24 ± 3 vesicles while the WT control released 12 ± 2 vesicles ($p < 0.05$). TKO cells transfected with EGFP-only plasmid yielded 26 ± 2 spikes while corresponding transfected WT cells exhibited 13 ± 2 spikes ($p < 0.05$). These values demonstrate that the transfection process is not interfering with the amount of release seen from both WT and TKO cells. Introduction of synapsin IIa to TKO cells appeared to recover the function of the protein as the number of vesicles released by the TKO plasmid cells (13 ± 2) was very similar to that of the WT control group. The number of spikes evoked in the TKO control cells and TKO plasmid cells is also significantly different ($p < 0.05$). Additionally, introduction of synapsin IIa to WT cells revealed reduced release in that these cells only exhibited a mean of 5.9 ± 1.6 spikes over a 10-s period.

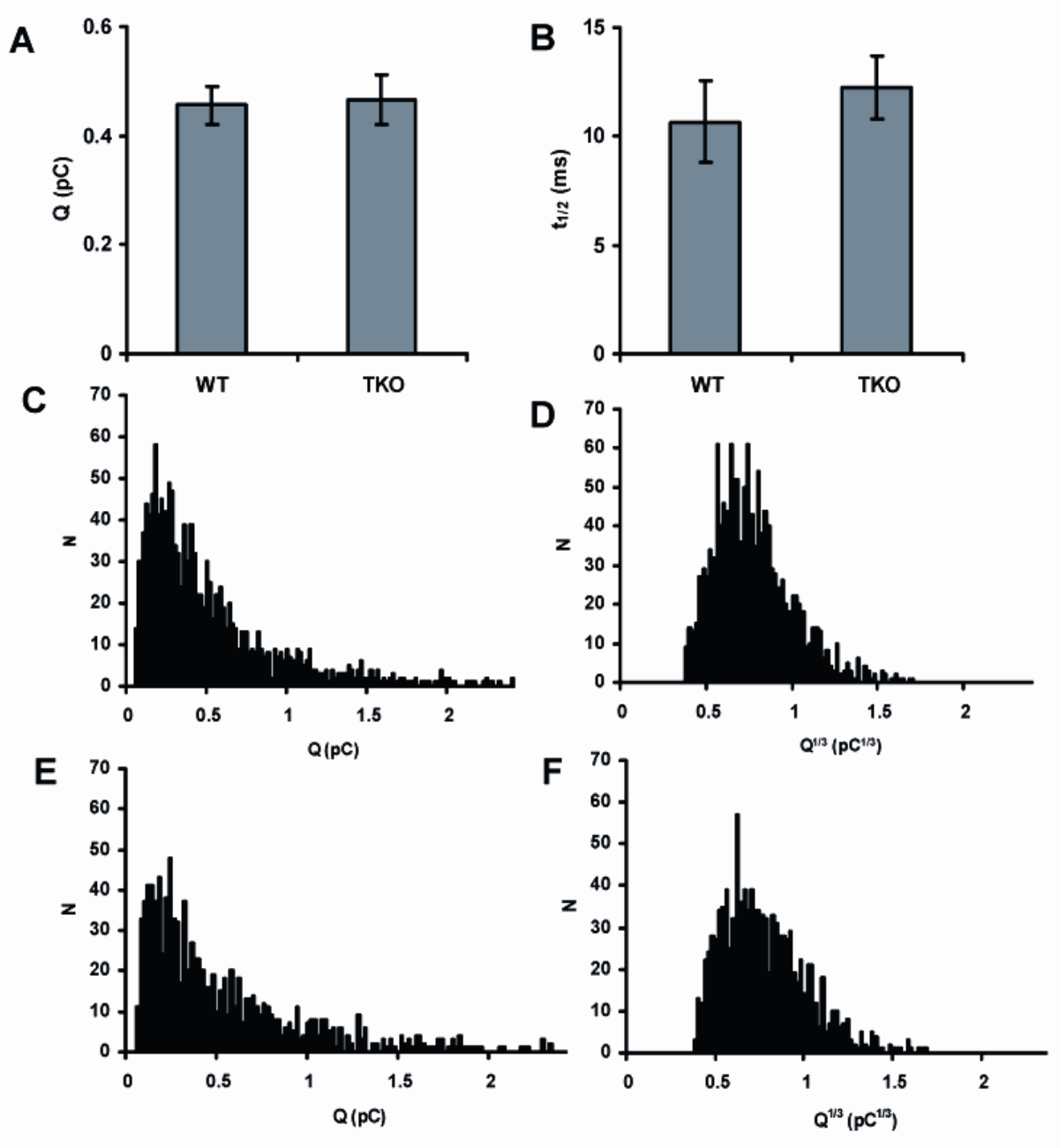

Figure 4.3. Comparison of amperometric spike characteristics between WT and TKO cells. Measurements were made in 7 WT cells and 6 TKO cells. (A) Mean Q observed in WT and TKO cells (NSD, $p > 0.05$). (B) Mean $t_{1/2}$ measured in WT and TKO cells (NSD, $p > 0.05$). Distribution of Q is shown for (C) WT cells and (E) TKO cells. Distribution of $Q^{1/3}$ is shown for (D) WT cells and (E) TKO cells

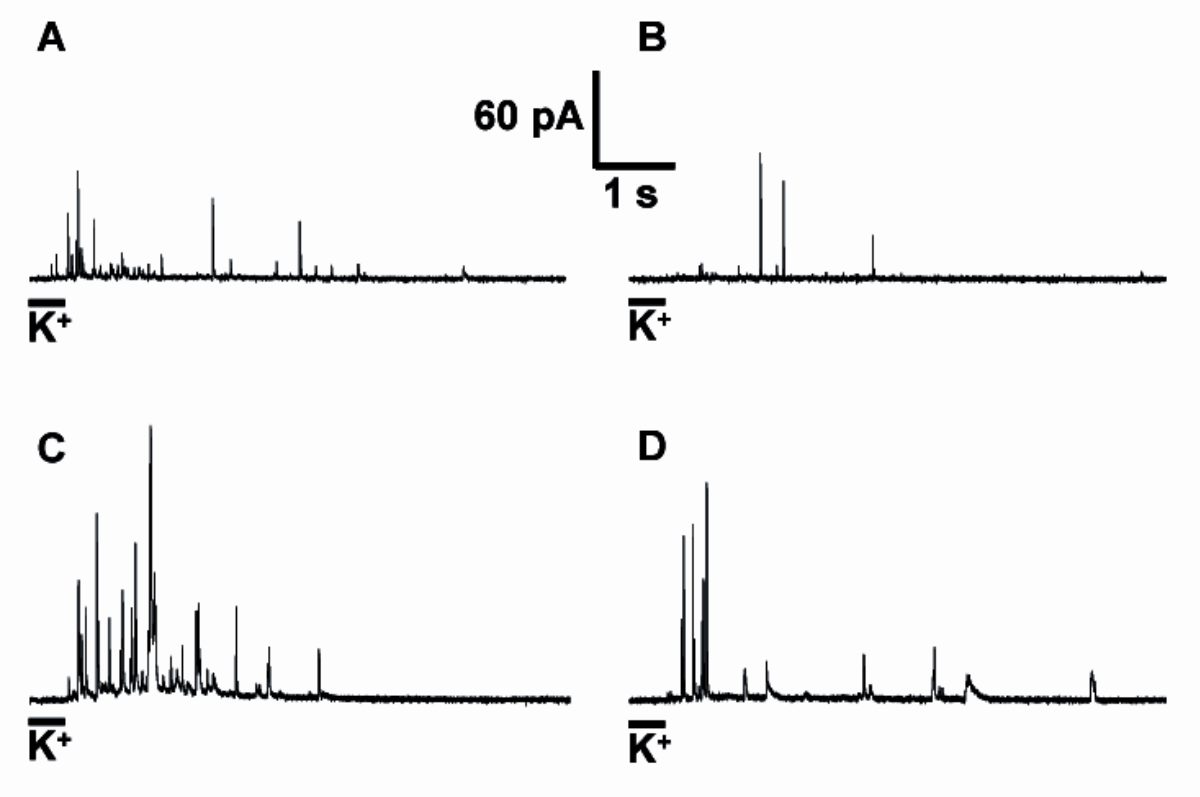

Figure 4.4. Release from control cells and cells transfected with synapsin IIa. Representative traces show release evoked with 60 mM K^+ from a (A) WT control cell (B) WT cell transfected with synapsin IIa (C) TKO control cell (E) and TKO cell transfected with synapsin IIa.

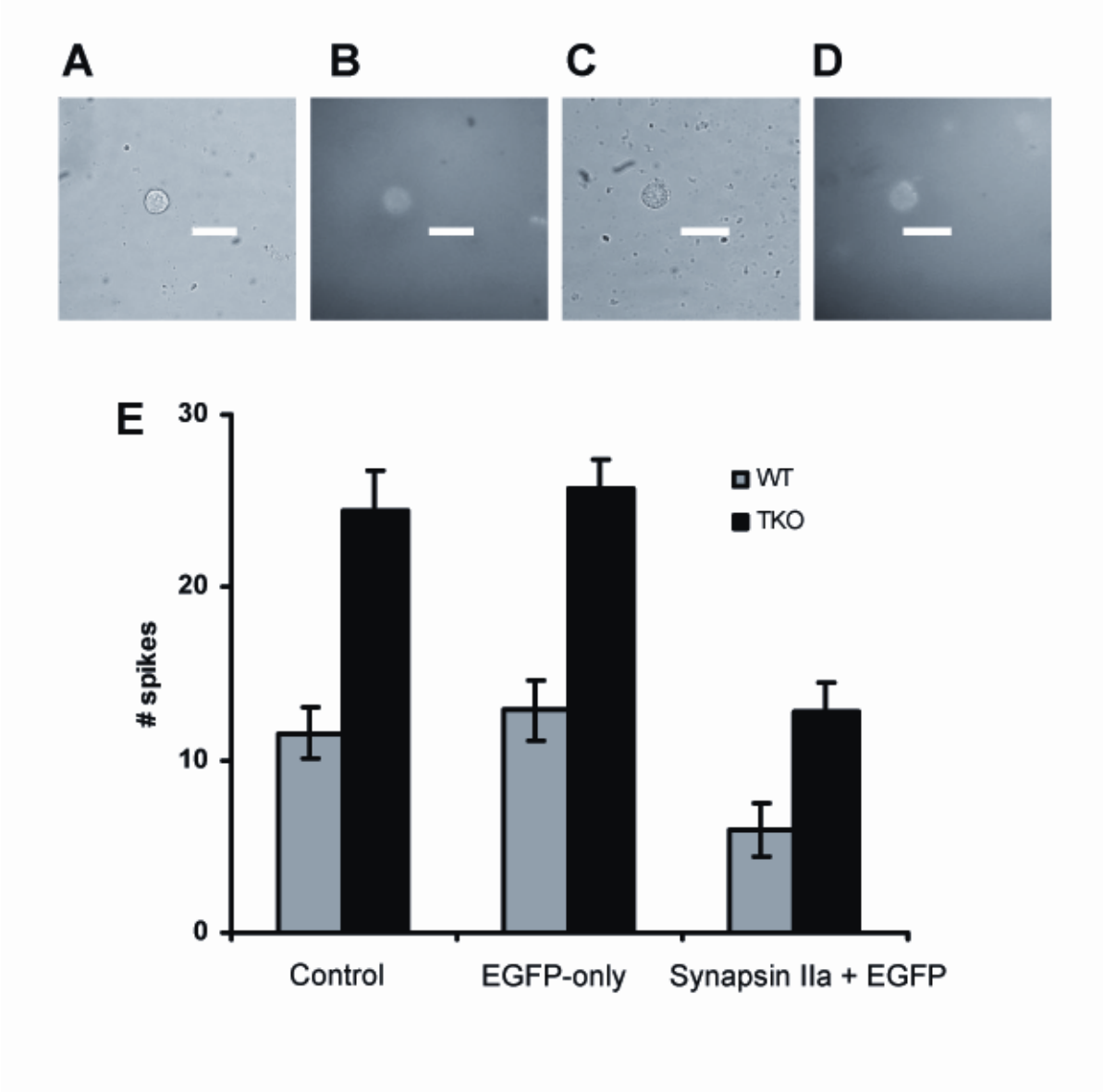

Figure 4.5. Rescue experiments with synapsin IIa in chromaffin cells. (A) Brightfield image of TKO cell transfected with synapsin IIa-EGFP. Fluorescence image is shown in (B). (C) Brightfield image of TKO cell transfected with EGFP-only plasmid. Fluorescence image is shown in (D). Scale bars indicate 25 μm. (E)Control results show release measurements taken in plates incubated only in experimental media (n = 13 WT cells; n = 19 TKO cells). EGFP-only plasmid data show measurements that were taken in plates incubated for ~ 6 h with plasmid containing only EGFP (n = 8 WT cells; n = 14 TKO cells). The last set of data show measurements taken at cells incubated for ~ 6 h with plasmid containing synapsin IIa (n = 11 WT cells; n = 15 TKO cells). Release from WT cells transfected with synaspin IIa is significantly diminished from control and EGFP-only plasmid ($p < 0.05$). Similarly, release from TKO cells transfected with synapsin IIa is decreased significantly from control and EGFP-only plasmid as well ($p < 0.05$). As seen previously, release from TKO cells is always significantly higher than release from WT cells in the same experimental group.

DISCUSSION

The data presented here demonstrate that the only known synapsin isoform found in chromaffin cells, synapsin II, has an important function in vesicle mobilization. Amperometric detection of exocytosis revealed a greater amount of vesicular release in TKO cells than in WT cells at both 0.5- and 1-s high K^+ stimuli. Additionally, transfection of synapsin IIa into both TKO and WT cells diminished release indicating that the presence of synapsin restricts the number of available vesicles and increases the vesicles in the reserve pool. The Ca^{2+} data from the two mouse models was not statistically different suggesting that the difference in release is not due to impaired Ca^{2+} influx. Though synapsin appears to affect vesicle mobilization, there were no significant differences in the amount of release per vesicle or the rate of extrusion of their contents between TKO and WT mice. The use of amperometry allows examination of individual release events, which permits the study of vesicular event characteristics. Thus, the absence of synapsin permits more vesicles to available for release through vesicle mobilization, but does not affect vesicle packaging.

Early work provided evidence of synapsin II activity during exocytosis in bovine chromaffin cells (Haycock et al., 1988; Firestone and Browning, 1992). Synapsin II phosphorylation increased in response to depolarizing stimuli such as high K^+, barium, veratridine, and acetylcholine. Firestone and Browning also showed that histaminergic stimulation, which releases Ca^{2+} from internal stores via the inositol triphosphate (IP_3)-mediated pathway, increased synapsin II phosphorylation (Firestone and Browning, 1992). Additionally, they demonstrated that although both subforms of synapsin II, IIa and IIb, displayed increased levels of phosphorylation upon stimulation, synapsin IIa exhibited a significantly higher level of phosphorylation than that of IIb.

Since synapsin IIa was phosphorylated to a greater extent than IIb, we introduced a plasmid containing synapsin IIa into both WT and TKO cells to examine how subsequent release would be affected. We postulated that the TKO cells transfected with synapsin IIa would recover the phenotype expressed by the WT cells; that is, the TKO cells with rescued synapsin IIa function would release a similar number of vesicles to the WT cells as compared to the excessive release seen previously in TKO cells. Indeed, transfection of the synapsin IIa isoform into TKO cells replicated the phenotype displayed in WT cells. Furthermore, transfection of synapsin IIa into WT cells evidently produced overexpression of synapsin IIa and reduced release to a greater extent. The ability to rescue the function of synapsin IIa further confirmed the importance of synapsin in sequestering vesicles in the reserve pool in chromaffin cells.

These data complement the data obtained by Firestone et al., which showed that synapsin IIa phosphorylation increased in conjunction with catecholamine release in bovine chromaffin cells (Firestone and Browning, 1992). Inhibiting phosphorylation of synapsin II subsequently blocked catecholamine release. Our data show that in mice lacking the gene for synapsin II, vesicular release is enhanced, presumably because the absence of synapsin II permits the free movement of a greater number of vesicles. Thus, the reserve pool may not be as tightly regulated in knockout mice as in their WT counterparts. Moreover, the data obtained from the transfection experiments underline the role that synapsin II may play in reserve pool sequestration. In "recovering" the function of synapsin II, TKO mice showed diminished release that was comparable to the amount of vesicular release observed in WT mice. This points to a possible role that synapsin II may play as a vesicular tether in chromaffin cells.

To gain a better understanding of total release in these WT and TKO cells, we used Ba^{2+} stimuli. Stimulation with Ba^{2+} not only recruits vesicles from the readily releasable and recycling pools but presumably recruits vesicles from the reserve pool as well (Duncan et al., 2003). Ba^{2+} stimuli induce slower and prolonged release compared to K^+ (Heldman et al., 1989; von Ruden et al., 1993). Application of Ba^{2+} to the chromaffin cells of TKO and WT mice showed similar amounts of total release. Contrasted with high K^+ stimuli evoking significantly more release in TKO mice, Ba^{2+} stimuli appeared to equalize the amount of release observed between the two groups. Stimulating with Ba^{2+} may recruit vesicles indiscriminately from the readily releasable and recycling pools and the reserve pool, thus showing similar amounts of release between TKO and WT chromaffin cells. Because the high K^+ stimulus recruits vesicles mainly from the readily releasable and recycling pools (Duncan et al., 2003), the larger amount released from the TKO chromaffin cells indicate an increased amount of vesicles located in the readily releasable pool that may otherwise be sequestered in the reserve pool. Stimulation with Ba^{2+} appears to suggest that the total number of vesicles in the TKO cells is not necessarily affected; rather, the fraction available in the reserve pool is altered.

The results shown in this manuscript demonstrate a function of synapsin in chromaffin cells analogous to its demonstrated role in neurons. Synapsin is thought to be associated with vesicles in its dephosphorylated form; when phosphorylated, it is believed that synapsin is able to dissociate from the actin cytoskeleton and allow vesicles greater mobility in the cytosol. All isoforms of synapsin contain a phosphorylation site that serves as a substrate for cyclic AMP-dependent protein kinase (PKA) and calcium calmodulin dependent kinase I (CaMKI). Studies involving neurons have shown greater release when

the function of synapsin I has been inhibited. Llinas et al. demonstrated that introduction of dephosphorylated synapsin I into the squid giant axon reduced exocytotic release (Llinas et al., 1991). Another study provided evidence of synapsin as a vesicular tether as introduction of synapsin I antibodies into lamprey reticulospinal axons seemingly eliminated the synapsin-dependent pool that was located distally from the plasma membrane (Pieribone et al., 1995).

The three isoforms of synapsin may have subtly different and complementary roles in vesicle mobilization. Previous work studied CA1 pyramidal cells in hippocampal slices from synapsin I/II knockouts as well as mice that had synapsin I or II knocked out individually. This work showed that synapsin I and II may have subtly different functions in vesicle mobilization, but that each isoform is important in vesicle mobilization during repetitive stimuli (Rosahl et al., 1995). The synapsin I knockout exhibited increased paired-pulse facilitation (PPF) and normal post tetanic potentiation (PTP) while the synapsin II knockout showed normal PPF and decreased PTP. The double knockout mouse model, however, showed a more pronounced depression in PTP with an inconsistent change in PPF; this data shows that synapsin I and II may play a role in the ability of vesicle mobilization to sustain with responses to repetitive stimuli. Synapsin III knockout mice also exhibited an increase in the number of vesicles available in the recycling pool providing further evidence for the role of synapsin in vesicle mobilization (Feng et al., 2002). However, in studies conducted on mice lacking all three synapsins (TKO), inhibitory postsynaptic potentials were diminished in neurons from TKO mice, indicating a differing role of the synapsins at inhibitory synapses (Gitler et al., 2004). Additionally, recent work has shown that cocaine augments release presumably by mobilizing the synapsin-dependent reserve pool (Venton et al., 2006). This

ability of cocaine to enhance release is observed in WT mice but is greatly reduced in TKO mice.

Because chromaffin cells and neurons derive from similar embryonic precursors (Anderson, 1993), a similar function of synapsin in both cell types may be expected. Synapsin appears to operate as a tether between vesicles and the actin cytoskeleton and sequester a subpopulation of vesicles in the reserve pool. Regulation of vesicle mobilization by limiting the vesicles which are immediately available for release may provide a means for the cell to respond effectively to rapid and repetitive stimuli.

REFERENCES

Anderson DJ (1993) Molecular control of cell fate in the neural crest: The sympathoadrenal lineage. Annual Reviews in Neuroscience 16:129-158.

Bath BD, Michael DJ, Trafton BJ, Joseph JD, Runnels PL, Wightman RM (2000) Subsecond adsorption and desorption of dopamine at carbon-fiber microelectrodes. Analytical Chemistry 72:5994-6002.

Browning MD, Huang C-K, Greengard P (1987) Similarities between Protein IIIa and Protein IIIb, two prominent synaptic vesicle-associated phosphoproteins. Journal of Neuroscience 7:847-856.

Duncan RR, Greaves J, Wiegand UK, Matskevich I, Bodammer G, Apps DK, Shipston MJ, Chow RH (2003) Functional and spatial segregation of secretory vesicle pools according to vesicle age. Nature 422:176-180.

Feng J, Chi P, Blanpied TA, Xu Y, Magarinos AM, Ferreira A, Takahashi RH, Kao H-T, McEwen BS, Ryan TA, Augustine GJ, Greengard P (2002) Regulation of neurotransmitter release by synapsin III. Journal of Neuroscience 22:4372-4380.

Finnegan JM, Wightman RM (1995) Correlation of real-time catecholamine release and cytosolic Ca^{2+} at single bovine chromaffin cells. Journal of Biological Chemistry 270:5353-5359.

Firestone J, Browning M (1992) Synapsin II phosphorylation and catecholamine release in bovine adrenal chromaffin cells: additive effects of histamine and nicotine. Journal of Neurochemistry 58:441-447.

Gitler D, Xu Y, Kao H-T, Lin D, Lim S, Feng J, Greengard P, Augustine GJ (2004a) Molecular determinants of synapsin targeting to presynaptic terminals. Journal of Neuroscience 24:3711-3720.

Gitler D, Takagishi Y, Feng J, Ren Y, Rodriguiz RM, Wetsel WC, Greengard P, Augustine GJ (2004b) Different presynaptic roles of synapsins at excitatory and inhibitory synapses. Journal of Neuroscience 24:11368-11380.

Grynkiewicz G, Poenie M, Tsien RY (1985) A new generation of Ca^{2+} indicators with greatly improved fluorescence properties. Journal of Biological Chemistry 260:3440-3450.

Haycock JW, Greengard P, Browning MD (1988) Cholinergic regulation of protein III phosphorylation in bovine adrenal chromaffin cells. Journal of Neuroscience 8:3233-3239.

Heldman E, Levine M, Raveh L, Pollard HB (1989) Barium ions enter chromaffin cells via voltage-dependent calcium channels and induce secretion by a mechanism independent of calcium. Journal of Biological Chemistry 264:7914-7920.

Hilfiker S, Schweizer FE, Kao H-T, Czernik AJ, Greengard P, Augustine GJ (1998) Two sites of action for synapsin domain E in regulating neurotransmitter release. Nature Neuroscience 1:29-35.

Kawagoe KT, Jankowski JA, Wightman RM (1991) Etched carbon-fiber electrodes as amperometric detectors of catecholamine secretion from isolated biological cells. Analytical Chemistry 63:1589-1594.

Llinas R, Gruner JA, Sugimori M, McGuinness TL, Greengard P (1991) Regulation by synapsin I and Ca^{2+}-calmodulin-dependent protein kinase II of transmitter release in squid giant synapse. Journal of Physiology 436:257-282.

Pieribone VA, Shupliakov O, Brodin L, Hilfiker-Rothenfluh S, Czernik AJ, Greengard P (1995) Distinct pools of synaptic vesicles in neurotransmitter release. Nature 375:493-497.

Rizzoli SO, Betz WJ (2005) Synaptic vesicle pools. Nature Reviews Neuroscience 6:57-69.

Rosahl TW, Spillane D, Missler M, Herz J, Selig DK, Wolff JR, Hammer RE, Malenka RC, Sudhof TC (1995) Essential functions of synapsins I and II in synaptic vesicle regulation. Nature 375:488-493.

Venton BJ, Seipel AT, Phillips PEM, Westel WC, Gitler D, Greengard P, Augustine GJ, Wightman RM (2006) Cocaine increases dopamine release by mobilization of a synapsin-dependent reserve pool. Journal of Neuroscience 26:3206-3209.

Voets T, Neher E, Moser T (1999) Mechanisms underlying phasic and sustained secretion in chromaffin cells from mouse adrenal slices. Neuron 23:607-615.

von Ruden L, Garcia AG, Lopez MG (1993) The mechanism of Ba^{2+}-induced exocytosis from single chromaffin cells. Federation of European Biochemical Societies Letters 336:48-52.

Wightman RM, Schroeder TJ, Finnegan JM, Ciolkowski EL, Pihel K (1995) Time course of release of catecholamines from individual vesicles during exocytosis at adrenal medullary cells. Biophysical Journal 68:383-390.

APPENDIX I

ELECTRODE FABRICATION TOWARD SMALLER SENSORS

INTRODUCTION

During exocytosis from chromaffin cells, different species such as peptides, catecholamines, ATP, and Ca^{2+} are released from individual vesicles (Holz, 1986). This release is triggered by depolarization of the cell membrane and the resulting influx of calcium through voltage-gated calcium channels. The increase in intracellular calcium causes docked vesicles to fuse with the plasma membrane and extrude their contents into the extracellular space (Figure AI.1A). Partial release can be seen during the formation of a fusion pore or complete release of vesicular contents can result from full fusion with the plasma membrane. Catecholamines are oxidizable molecules that permit electrochemical detection of vesicular release.

Electrochemical techniques have proven valuable in the detection of vesicular release via oxidation of catecholamines. In chromaffin cells, the secreted catecholamines are primarily epinephrine, and to a lesser extent, norepinephrine (Holz, 1986; Moro et al., 1990). Vesicular release can be identified as individual current spikes in amperometry or fast-scan cyclic voltammetry (FSCV). FSCV can provide an identifier for electroactive molecules; voltammograms may provide characteristic features that can be helpful in identifying the analyte of interest. Constant potential amperometry provides superior temporal resolution for studying vesicular release; the electrode instantaneously electrolyzes the analyte molecules in the immediate vicinity due to the steep concentration gradient thus resulting in very sharp current spikes. The positioning of the electrode directly on the cell surface also precludes radial diffusion of exocytosed contents from other regions of the cell to the electrode

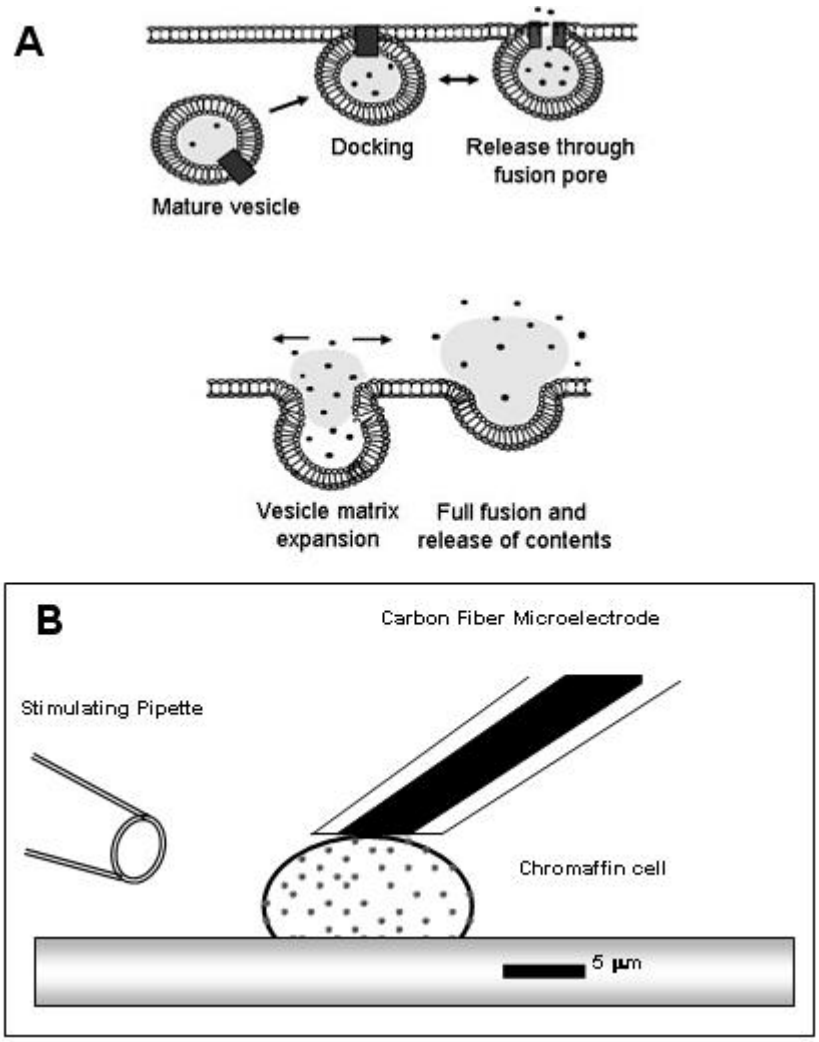

Figure AI.1. Vesicle fusion and experimental setup. (A) Vesicle fusion to the plasma membrane can extrude into the extracellular space electroactive molecules that can be oxidized and detected by constant potential amperometry. (B) Diagram of experimental setup used to detect vesicular release via amperometry. The carbon-fiber microelectrode apposes the cell surface; a stimulating pipette placed adjacent to the cell contains secretagogue that is delivered via pressure ejection.

diffusion of exocytosed contents from other regions of the cell to the electrode (Figure AI.1B). Both FSCV and amperometry have been used in conjunction with carbon-fiber microelectrodes to detect neurotransmitter release in intact tissue and isolated biological cells. For the subsequent discussion, amperometry will be the central technique to provide information on quantized release from chromaffin cells and will also be used in the characterization of electrodes being developed for the analysis of exocytosis at single neurons.

Moreover, carbon-fiber microelectrodes have proven valuable in monitoring release from single cells. These sensors provide the ability to probe physically small places and permit detection of the exocytotic response of an individual cell. Instead of obtaining the response of an entire population, these electrodes allow the analysis of individual cells and provide the capability to observe variability within a population.

MICROELECTRODE CONSTRUCTION FOR IN VITRO CELL STUDIES

The traditional disk microelectrodes that are used to probe individual cells are glass-encased and typically have an electroactive area with a diameter of 5-7 μm (Figure AI.2). An electrode with a smaller electroactive area will be required to analyze murine neurons due to their smaller dimensions. In order to achieve such a size, it will be necessary to flame-etch the electrode in order to create a tip of smaller diameter and to use a thinner insulating material that would introduce minimal noise.

To develop a protocol to produce these electrodes, electrodes must be characterized at each step of the construction process in order to optimize conditions. By using a carbon fiber that has a smaller inherent diameter, it will be easier to work toward electrodes of smaller

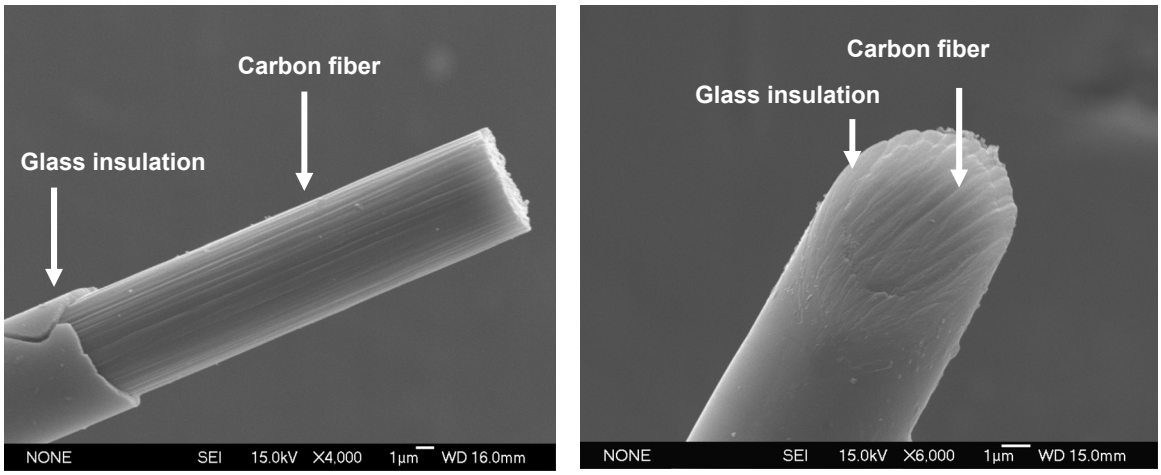

Figure AI.2. Scanning electron micrographs (EMs) of T-650 carbon-fiber microelectrodes. Left: a cylinder electrode approximately 25 µm in length. Right: a disk electrode approximately 6 µm in diameter.

electroactive area. T-650 carbon fibers are used preferentially to P-55 carbon fibers because T-650 fibers are typically 6 μm in diameter while P-55 fibers are approximately 10 μm. Carbon-fiber disk microelectrodes were prepared as previously described using T-650 carbon fibers (Amoco, Greenville, SC) (Kawagoe et al., 1991b; Kawagoe et al., 1993). Carbon fibers were aspirated into glass capillaries. A pipette puller (Narishige, Long Island, NY) was used to seal the glass around the carbon fiber. The carbon fibers were cut at the glass seal, and the seal was reinforced with epoxy (15% m-phenylenediamine mixed with Epon 828 resin (Miller-Stephenson, Danbury, CT)) heated to 80°C. Electrodes were cured at 100°C for 12h and then cured at 150°C for 12 h. Before use, electrodes were polished on diamond polishing wheels at 45º (Sutter Instruments, Novato, CA) and soaked for at least 10 min in 2-propanol purified with activated carbon (Bath et al., 2000). During experiments, electrodes were held at a constant potential of +650 mV vs. a Ag/AgCl reference electrode. A cylinder electrode was constructed similarly to a disk electrode; the carbon fiber was cut approximately 50-100 μm from the glass seal for EP electrodes and 500 μm for FEEP electrodes to avoid destroying the glass seal during flame-etching (Figure AI.2, left). A suitable seal was reinforced with epoxy, and acetone was applied briefly to remove epoxy from the electroactive area of the cylinder while avoiding disintegration of the seal. Electrodes were cured at 100°C for 4h and then cured at 150°C for 12 h.

An insulating material, electropaint (polyacrylamide), was then deposited on the exposed carbon fiber by immersing the electrode in 10 mL of a 1:1 solution of electropaint (BASF, Germany) to double distilled water while +2 V was applied to the electrode for 2 min. Polyacrylamide is stored in excess base to maintain it in its soluble, deprotonated form,

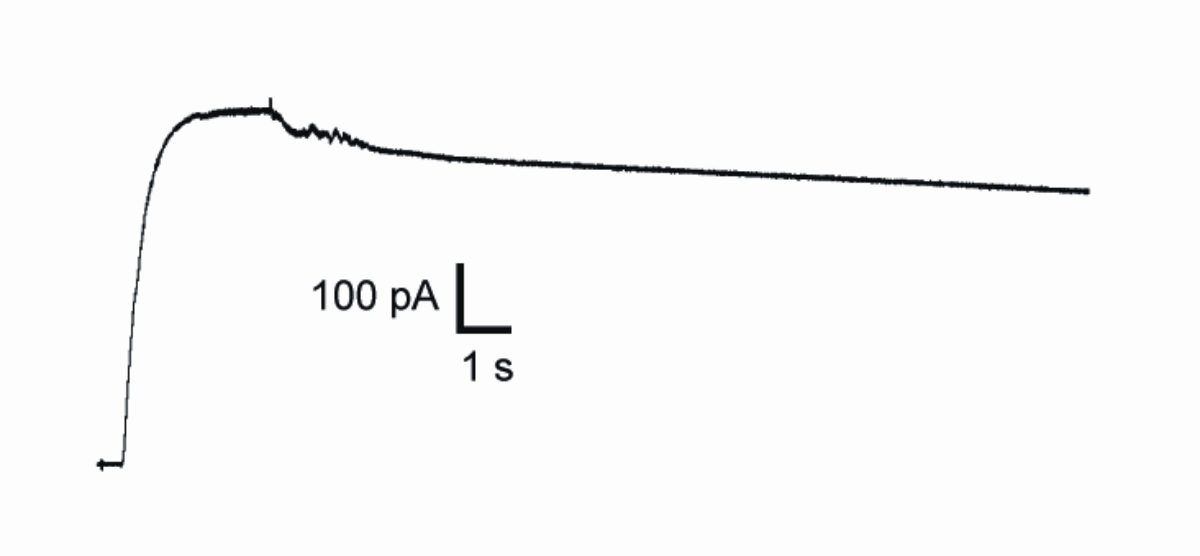

Figure AI.3. Quasi-steady state current obtained from bare cylinder electrode using stop-flow method.

PAA^-. Applying a positive DC potential to the electrode oxidizes water in the immediate vicinity of the electrode, and shifts polyacrylamide to its insoluble form, PAAH, which can then adsorb to the electrode surface (Schulte and Chow, 1996; Conyers and White, 2000). Afterwards, the electrode was cured at 200˚C for 5 min. Heating the polymer renders it chemically inert and capable of insulating the carbon-fiber (Schulte and Chow, 1996). Finally, the electrode was polished briefly at a 45˚ angle using impedance monitoring. Electrodes at each step of construction (exposed cylinder, electropainted cylinder, flame-etched electropainted cylinder), along with disk electrodes, were characterized using amperometry.

Electrode characterization using amperometry and stop-flow

Experiments were carried out in buffer containing in (mM): 150 NaCl, 5 KCl, 1.2 $MgCl_2$, 10 TRIS, and 2 $CaCl_2$. Electrodes were characterized using a brief delivery of 10 µM dopamine as a bolus in flow injection analysis analyzed with amperometry. Using a flow cell, the analyte was introduced to the electrode. After a steady current value was obtained, the flow of buffer was halted in order to record the current that resulted from the diffusion of analyte molecules to the electrode. This current is said to be under diffusion control (Figure AI.3). Additionally, because there was no flow of buffer, the bulk concentration would be the concentration of analyte introduced into the flow cell. The stop-flow method permits the determination of the electroactive area of the electrode. During the delivery of analyte, the dopamine is consumed at the electrode such that the surface concentration of dopamine at the electrode becomes zero. This is described by the Cottrell equation and holds true when the diffusion layer ($\sqrt{Dt}$) is smaller than the electrode radius. The kinetics of charge transfer are

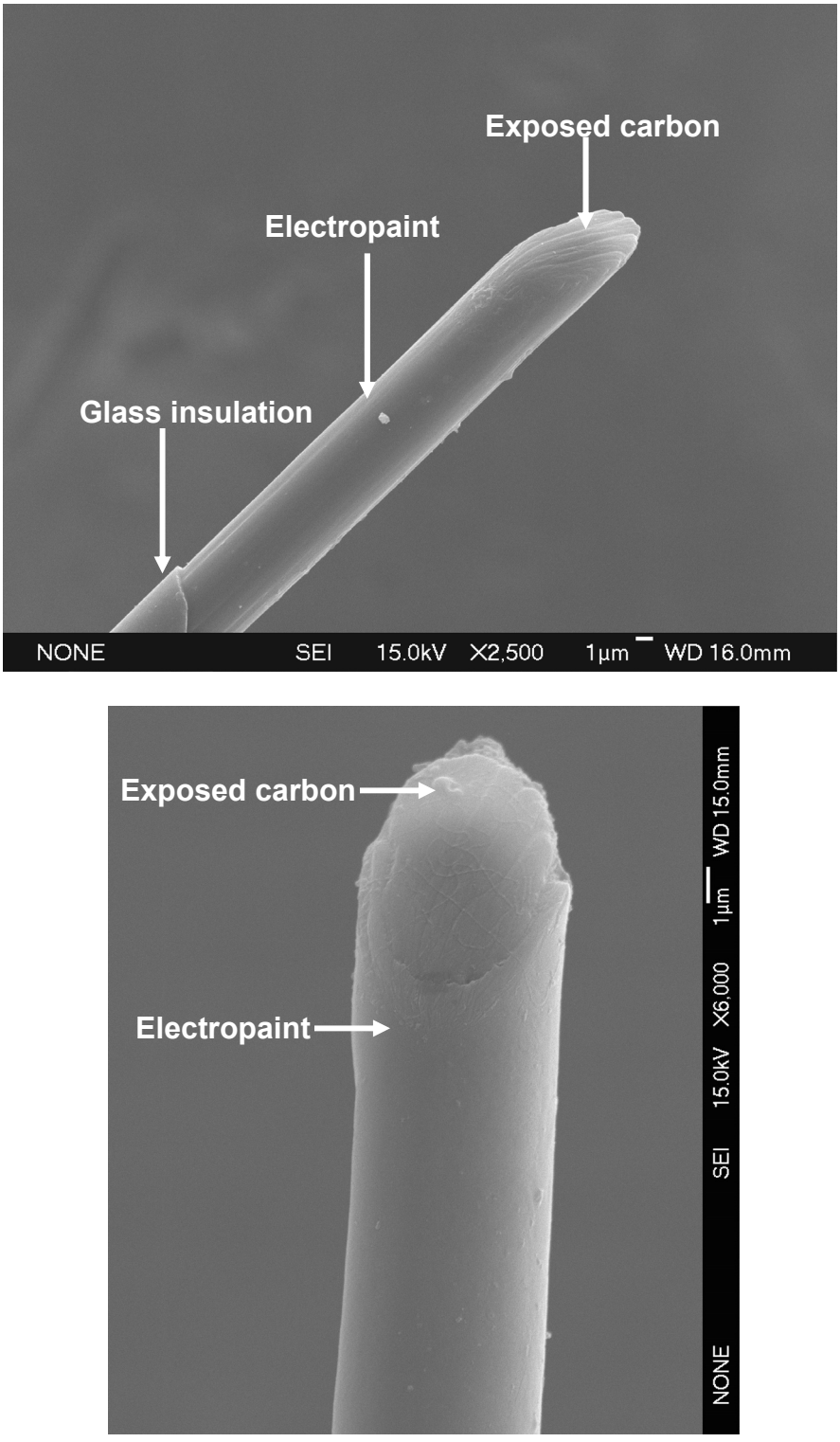

Figure AI.4. EP electrodes. EMs of two carbon-fiber microelectrodes insulated with electropaint and beveled at 45º.

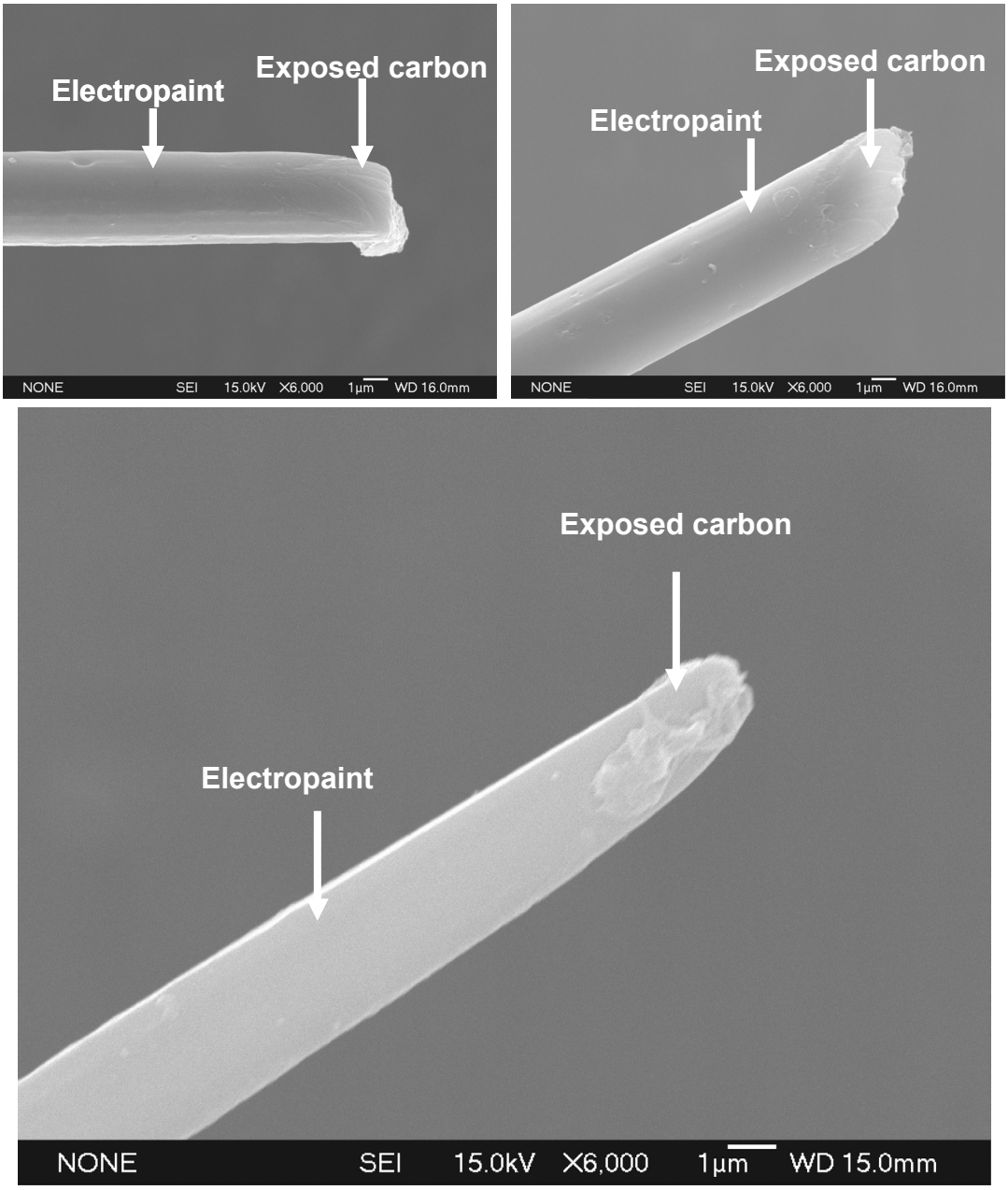

Figure AI.5. **FEEP electrodes**. EMs of three flame-etched carbon-fiber microelectrodes insulated with electropaint and beveled briefly on a diamond polishing wheel.

so rapid that the reaction is limited only by the rate at which the molecules diffuse to the electrode. At longer times, when the diffusion layer ($\sqrt{Dt}$) is much greater than the electrode radius, the current decays to the bulk concentration, C^*_o. This illustrates the corrosion of the sharp concentration gradient that was present during the pulse. This long-term phenomenon can be described by the following equations:

Equations for cylinder and disk:

$$i_{qss} = \frac{2nFAD_O C_O^*}{r_0 \ln \tau} \qquad \text{quasi-steady state at cylinder} \quad \textbf{Eqn. AI.1.}$$

$$\text{where } \tau = \frac{4D_o t}{r_0^2}$$

$$i_{ss} = 4nFD_O C_O^* r_0 \qquad \text{steady state at disk} \qquad \textbf{Eqn. AI.2.}$$

The current obtained after the pulse is the steady-state current, due to the fact that the diffusion layer at this point is relatively large compared to the electrode radius, which can be used to calculate the electroactive area of the corresponding electrode. For the exposed cylinders, Equation AI.1 was used; for polished electropainted cylinders and polished flame-etched electropainted cylinders, Equation AI.2 was employed.

Bare cylinders and polished electropainted cylinders were characterized and results were in reasonable agreement with theoretical values (Table A1.1). Assuming that the bare cylinder is 100 μm in length with a radius of 2.55 μm, the calculated surface area would be 1622 μm^2. The electrodes characterized in this set of experiments showed an exposed surface area that was reasonably close to the theoretical value. Analysis of unpolished electropainted electrodes exhibited no current when dopamine was present in the flow cell indicating that the insulating material was effective. For a typical glass-encased electrode, the radius is

Table A1.1. Calculated electrode parameters. Summary of results from electrode characterization. Error shown is S.E.M.

ELECTRODE TYPE	Mean calculated electroactive area (μm^2)	Mean calculated radius (µm)	N
Bare cylinder	1605 ± 44	N/A	6
100 µm length cylinder (theoretical)	1622	2.55	N/A
Polished EP disk	39 ± 14	3.05 ± 0.63	9
Polished flame-etched EP disk	3.01 ± 1.35	0.86 ± 0.28	4
Disk	35 ± 14	3.05 ± 0.79	4
Disk (theoretical)	27	major radius = 3.5 µm minor radius = 2.5 µm	N/A

assumed to be that of the carbon fiber, 2.55 μm. The radii of the glass-encased and electropainted electrodes are also in reasonable agreement with the theoretical value. It is also important to note that although beveled electrodes have an elliptical area, the approximation of a circular area is a reasonable one. An ellipse has major and minor radii, the average radius of the ellipse may be somewhat larger than the actual radius of the fiber; however, in this characterization, the difference between the elliptical and circular areas appears negligible.

Imaging electrodes

Electrode images were obtained using scanning electron microscopy. The images or micrographs (EMs) of bare cylinder and glass-encased disk, EP disk, and FEEP disk electrodes are shown in Figures AI.2, AI.4, and AI.5, respectively. The bare cylinder illustrates the initial configuration of the electropaint-insulated electrodes. The EM of the glass-encased disk displays the traditional disk electrode used in isolated cell studies and illustrates the beveled surface of exposed carbon fiber flush with the glass seal. EP electrodes are shown in Figure AI.4; the smooth layer of electropaint is evident as well as the beveled surface that exposes the carbon fiber. FEEP electrodes do not show a bevel as polishing was done by briefly touching the electrode to the polishing wheel to remove minimal amounts of electropaint (Figure AI.5). Because of this polishing method, the electropaint can be seen to accumulate on the surface as the time of polishing was not sufficient to remove the excess electropaint. It may be necessary to implement a technique that can detach excess electropaint such using a sonicating solution.

Use of glass-insulated and electropaint-insulated disks in detecting exocytosis

Glass-encased disks have been used extensively in electrochemical studies of isolated cells. The cell surface area sampled depends on the size of the electroactive area of the electrode sensor. A glass-encased T-650 carbon-fiber disk electrode can typically sample 6% of the surface area of a chromaffin cell approximately 15 μm in diameter. For greater spatial resolution, insulated flame-etched disks have been used to probe exocytotic hotspots (Schroeder et al., 1994). However, decreasing the electroactive area compromises sensitivity; the signal-to-noise ratio may be diminished because the signal is decreased, the noise is increased, or a combination of both.

It is possible to measure vesicular release from chromaffin cells using electropaint-insulated (EP) disks and flame-etched electropaint-insulated (FEEP) disks. EP disks also provide slightly greater spatial resolution than glass-encased disks, presumably because beveling does not require as much pressure to polish down the insulating layer. The mean radius of the electroactive area of glass-encased disks was measured as 3.05 ± 0.79 μm; EP disks had a mean radius of 3.05 ± 0.63 μm, which is identical to the measured mean radius of glass-encased disks. FEEP disks exhibited a mean radius of 0.86 ± 0.28 μm. Figure AI.6 displays images taken of the experimental setup as visualized with an inverted microscope (Nikon, Lewisville, TX).

FEEP disks may also be used to detect release in intact tissue, e.g. perfused brain slices. FEEP disks may allow for measurement of release from dopamine terminals in the brain with the aid of fluorescent labeling. For this purpose, mice genetically engineered to express human placental alkaline phosphatase (hPLAP) in cells that express tyrosine hydroxylase (TH) may provide specific labeling to aid in identification of catecholaminergic

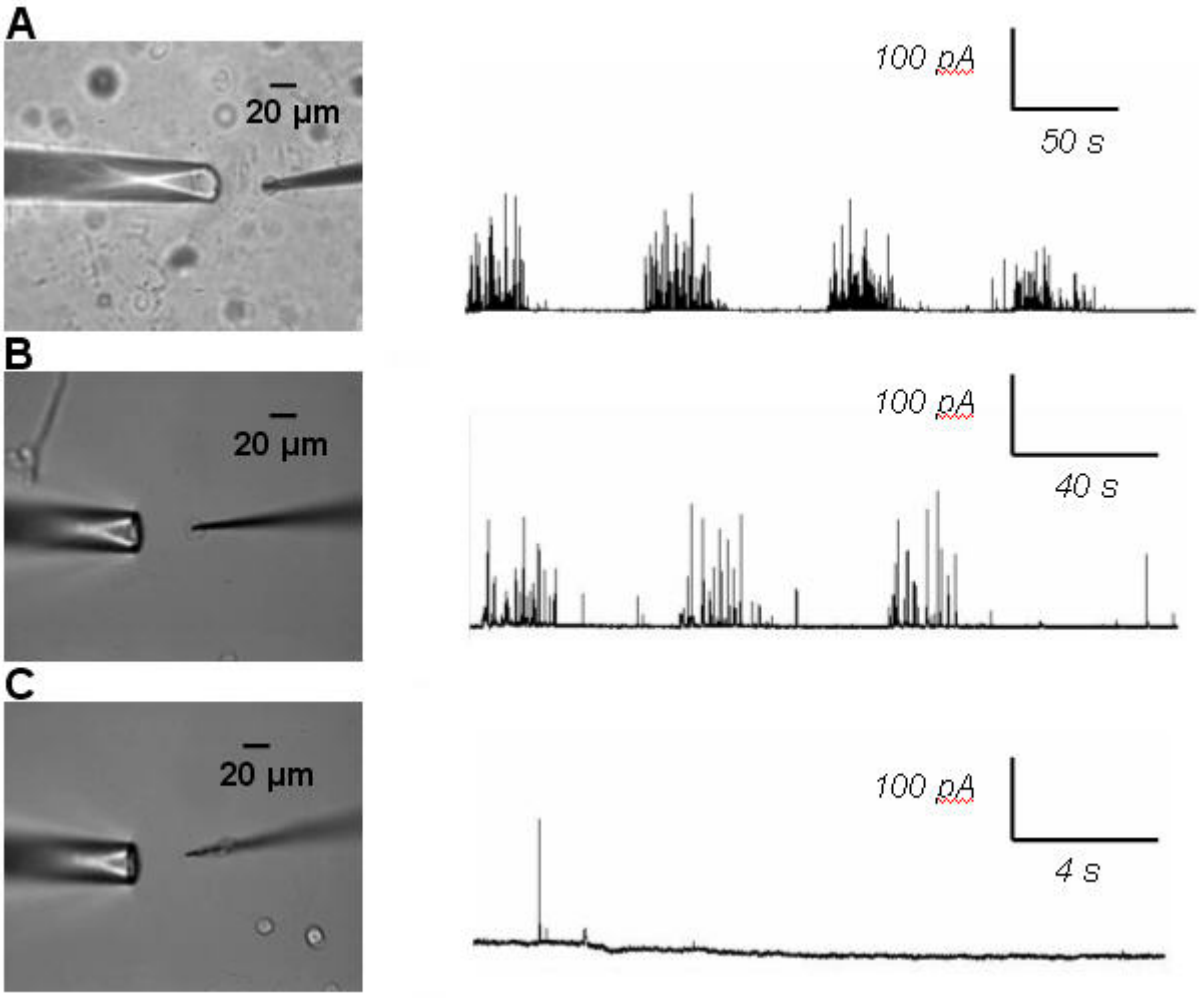

Figure AI.6. Vesicular release detected at a single bovine chromaffin cell with glass-encased, EP, and FEEP electrodes.. Release was measured using a (A) glass-encased disk, (B) EP disk, (C) FEEP disk. The decrease in release corresponds with the decrease in electroactive area. Right panel shows experimental setup with glass pipette delivering 60 mM K^+ for 3-s via pressure ejection on the left and the carbon-fiber microelectrode on the right placed on a single bovine chromaffin cell. Release was monitored at 25ºC.

cells (Puopolo et al., 2001). Additionally, EP disks may be useful in monitoring release from individual cells in perfused adrenal slices. Chromaffin cells are clustered in groups approximately 80 μm in diameter (Iijima et al., 1992). With perfused tissue, another difficulty that may arise is more rapid fouling of the electrode surface. This may be remedied by treating the electrode with a perfluorinated ion exchange resin, Nafion, (Kawagoe et al., 1993) which could protect the surface from fouling, but also provides increased selectivity against negatively charged species, such as ascorbate, that may be present at significant concentrations in intact tissue but does not appear to interfere in isolated cell culture.

REFERENCES

Bath BD, Michael DJ, Trafton BJ, Joseph JD, Runnels PL, Wightman RM (2000) Subsecond adsorption and desorption of dopamine at carbon-fiber microelectrodes. Analytical Chemistry 72:5994-6002.

Conyers JL, White HS (2000) Electrochemical characterization of electrodes with submicrometer dimensions. Analytical Chemistry 72:4441-4446.

Holz RW (1986) The role of osmotic forces in exocytosis from adrenal chromaffin cells. Annual Reviews in Physiology 48:175-189.

Iijima T, Matsumoto G, Kidokoro Y (1992) Synaptic activation of rat adrenal medulla examined with a large photodiode array in combination with a voltage-sensitive dye. Neuroscience 51:211-219.

Kawagoe KT, Jankowski JA, Wightman RM (1991) Etched carbon-fiber electrodes as amperometric detectors of catecholamine secretion from isolated biological cells. Analytical Chemistry 63:1589-1594.

Kawagoe KT, Zimmerman JB, Wightman RM (1993) Principles of voltammetry and microelectrode surface states. Journal of Neuroscience Methods 48:225-240.

Moro MA, Lopez MG, Gandia L, Michelena P, Garcia AG (1990) Separation and culture of living adrenaline- and noradrenaline-containing cells from bovine adrenal medullae. Analytical Biochemistry 185:243-248.

Puopolo M, Hochstetler SE, Gustincich S, Wightman RM, Raviola E (2001) Extrasynaptic release of dopamine in a retinal neuron: Activity dependence and transmitter modulation. Neuron 30:211-225.

Schroeder TJ, Jankowski JA, Senyshyn J, Holz RW, Wightman RM (1994) Zones of exocytotic release on bovine adrenal medullary cells in culture. Journal of Biological Chemistry 269:17215-17220.

Schulte A, Chow RH (1996) A simple method for insulating carbon-fiber microelectrodes using anodic electrophoretic deposition of paint. Analytical Chemistry 68:3054-3058.

APPENDIX II

PROBING EXOCYTOSIS IN MURINE ADRENAL SLICES

INTRODUCTION

Isolated cell culture has been useful in studying exocytosis and its associated processes. This type of cell preparation permits measurements to be made at individual cells and monitor the variability that can occur in a population of cells. Perfused tissue is also a valuable *in vitro* preparation because it allows for study of an individual cell in an environment that mimics the *in vivo* conditions more closely than dissociated cell culture. Pharmacological studies can be performed on intact slices; however, cellular mechanisms are more easily investigated on individual cells. Though isolated cell culture can provide information about cell mechanisms while minimizing other possible interferences, perfused tissue or slice preparations permit observations of cellular response in close proximity to other cells. Neighboring cells will undoubtedly have an effect on the cell of study that is otherwise unseen in isolated cell culture. The harsh conditions of digestion in cell culture preparations may also destroy or impair other proteins that may otherwise be functional in intact tissue.

The tissue of interest is that of adrenal medulla in slice preparations of murine adrenal glands. Chromaffin cells compose much of the adrenal medulla and are organized in clusters approximately 80 μm in diameter that contain an estimated 100 chromaffin cells (Iijima et al., 1992). These clusters may function as units as they are innervated with approximately four nerve fibers assuming that each cell is innervated with one to four nerve terminals (Iijima et al., 1992; Kajiwara et al., 1997). Studying chromaffin cells in adrenal slices may

also allow for the presence of the native stimulus: cholinergic stimulation from partially intact splanchic nerve terminals.

Studies of exocytosis have been performed with whole-cell capacitance measurements in adrenal slices. Voets et al. studied vesicle pools in murine adrenal slices with photolytic uncaging of Ca^{2+} (Voets et al., 1999). Quantal release was also studied by investigating EPSCs in rat adrenal glands (Barbara and Takeda, 1996). The presence of a Ca^{2+} channel subtype, the R-type, was also discovered in adrenal slices that does not appear to be present in dissociated cells in culture (Albillos et al., 2000). This Ca^{2+} channel may not be present in isolated cells because it does not survive intact during the digestion process. Furthermore, because cells are closely apposed in adrenal slices, intercellular communication occurs. Yamagami et al. showed that spontaneous changes in $[Ca^{2+}]_i$ that occur in one cell will transmit to neighboring cells, possibly via gap junctions (Yamagami et al., 2002). Amperometry in glands from the rat has also been performed and release was stimulated both by electrical stimulation and by pressure ejection of high K^+ to an individual cell (Barbara et al., 1998). Barbara et al. also suggested that close proximity to the cell was required for electrical stimulation to evoke exocytosis. Recently, release in perfused murine adrenal slices has been compared to release from individual cells in culture using amperometry (Arroyo et al., 2006). The following description uses fast-scan cyclic voltammetry, FSCV, to monitor vesicular release.

MURINE ADRENAL SLICE PREPARATION

Wildtype C57 mice were used for experiments. Mice were anesthetized deeply by ether inhalation and subsequently decapitated. The adrenal glands were obtained and fatty

connective tissue was removed from the glands while in cooled artificial cerebral spinal fluid (aCSF) containing (in mM): NaCl, 126; KCl, 2.45; $NaHCO_3$, 25; $MgCl_2$, 1.2; HEPES, 20, NaH_2PO_4, 1.2; D-glucose, 11; $CaCl_2$, 2.4. The pH was adjusted to 7.4 using NaOH. Each gland was then placed in 3% low melting point agarose (Promega, Madison, WI) dissolved in aCSF without glucose and the agarose was allowed to congeal before slicing. Slices were cut to 200 μm thickness in aCSF with glucose using a vibratome (World Precision Instruments, Sarasota, FL) and were subsequently kept on ice in oxygenated adrenal buffer. The adrenal buffer contained (in mM): NaCl, 120; KCl, 2.7; $NaHCO_3$, 20; HEPES, 10; glucose, 10; $CaCl_2$, 5; the pH was also adjusted to 7.4 with NaOH.

CONFOCAL IMAGING OF MURINE ADRENAL SLICES

Images of adrenal slices from genetically engineered mice expressing human placental alkaline phosphatase (hPLAP) on cells expressing tyrosine hydroxylase (TH) (Puopolo et al., 2001) were collected. Confocal images of an adrenal slice are shown in Figure AII.1. The images illustrate the two distinct types of tissue found in adrenal glands: the cortex and the medulla. The cortex shows little labeling while the medulla is labeled by antibodies to TH and hPLAP (Figures AI.A and AI.B). In Figures AI.C and AI.D, clusters of cells are also apparent. Figures AI.E and AI.F also focus on one of these clusters. The size of the cluster is in reasonable agreement with previous work that suggested that chromaffin cell clusters were approximately 80 μm (Iijima et al., 1992). Labeling TH and hPLAP also exhibits high correlation. The co-localization of TH and hPLAP also demonstrate the potential utility of this mouse model in locating other catecholaminergic cells, such as dopamine neurons of the striatum. Moreover, imaging suggests that medullary tissue

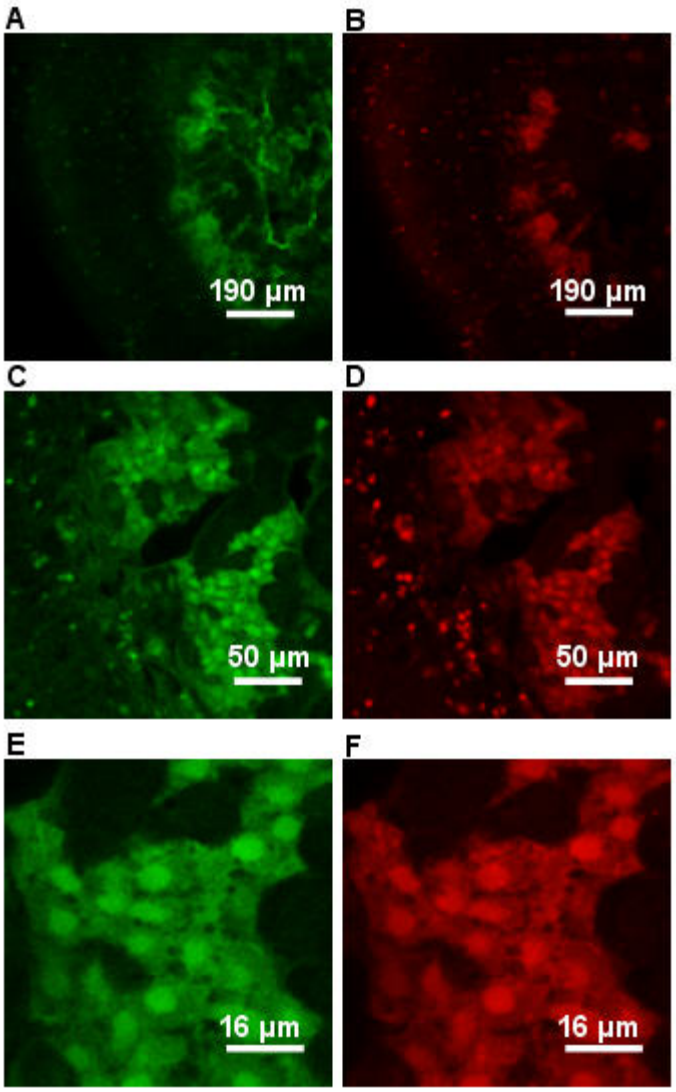

Figure AII.1. Confocal images of a murine adrenal slice labeled catecholamine-releasing cells. Left panel shows TH labeling; right panel shows hPLAP labeling. TH and hPLAP labeling exhibited high correlation. (A) and (B) show larger view of labeling. Note that cortex (to the left) shows very little labeling. A closer view is offered in (C) and (D), where cell clusters are visible. Images (E) and (F) show a closer view of an individual cell culture.

should be sampled closer to the edge of the medulla closer to the cortex as the middle of the slice appears to be damaged from the slice preparation.

MONITORING RELEASE WITH FSCV IN ADRENAL SLICES

Electrodes and electrochemistry

Carbon-fiber cylinder microelectrodes were prepared as previously described using T-650 carbon fibers (Amoco, Greenville, SC) (Kawagoe et al., 1993). Carbon fibers were aspirated into glass capillaries (A-M Systems, Inc, Carlsborg, WA), and the capillaries were subsequently heated and pulled to create a glass seal (Narishige, Long Island, NY). The extending carbon fiber was cut to allow 25-50 μm to extend beyond the glass seal; the seal was insulated further with epoxy (EPON resin 828, Miller-Stephenson, Danbury, CT; m-phenylenediamine, DuPont, Wilmington, DE). The electrodes were dipped in acetone briefly to eliminate epoxy on the surface of the protruding carbon fiber. Electrodes were cured at 100^{o}C for 12h and then cured at 150^{o}C for 2 h. Before use, electrodes were soaked for at least 10 min in 2-propanol purified with activated carbon (Bath et al., 2000). During experiments, fast scan cyclic voltammetry was used to monitor release events. The potential was ramped from -0.4 V to 1.0 V and back to the resting potential of -0.4 V at 300 V/s. vs. a Ag/AgCl reference electrode. The triangle waveform was scanned at 10 Hz. Carbon fiber electrodes were calibrated for concentration measurements using 10 μM dopamine in a flow cell with adrenal buffer containing no glucose.

Electrical stimulation via a biphasic waveform applied to a tungsten electrode was used to evoke exocyotic events in the adrenal tissue (Figure AII.2). Both the stimulating

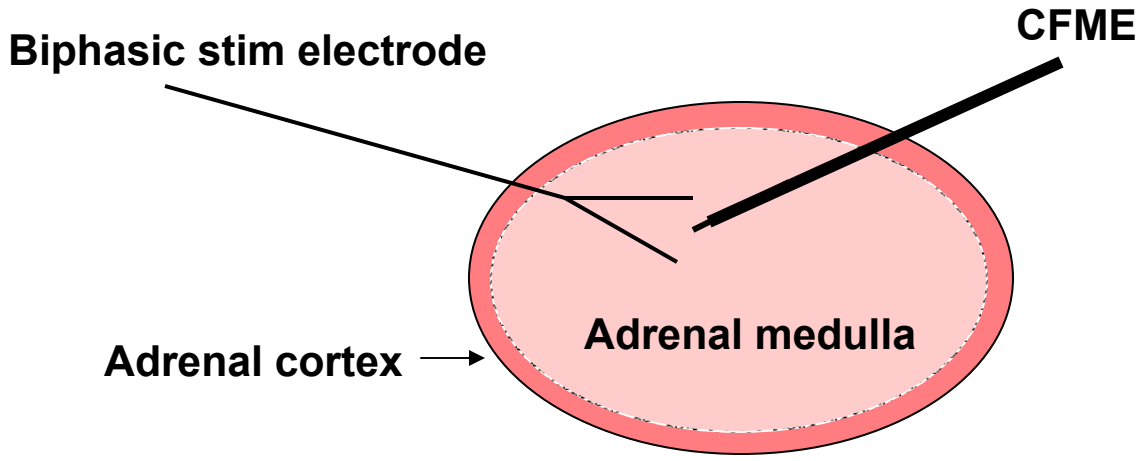

Figure AII.2. Diagram of adrenal slice preparation. Tissue is perfused with adrenal buffer and kept at 34^{o}C. Exocytosis is detected with carbon-fiber cylinder microelectrode (CFME). The widest part of the gland is approximately 2 mm in diameter.

electrode and the working carbon fiber electrode were positioned using micromanipuators (Sutter Instruments, Novato, CA). Adrenal buffer was flowed over the adrenal slices and maintained at 34^{o}C with a heated stage (Sutter Instruments, Novato, CA).

FSCV was used to detect exocytotic release. During FSCV, the potential range, in this case -0.4 V to +1.0 V, is scanned as a triangle waveform. Catecholamines can be detected by this technique as they are oxidized and reduced during the potential scan. Cyclic voltammograms were collected at 10 Hz. A plot of current versus potential, the cyclic voltammogram, can display the characteristic oxidation and reduction peaks of the analyte and can provide some selectivity in detection. For catecholamines detected at carbon-fiber microelectrodes, the oxidation peak is typically at +0.6 V and the reduction peak appears at -0.2 V (vs. a Ag/AgCl reference). FSCV is useful in identifying different analytes, but due to its limitations in selectivity, it is necessary to have knowledge of the tissue being tested to corroborate FSCV results. In this case, chromaffin cells are known to release epinephrine and/or norepineprhine (Moro et al., 1990). In order to distinguish the two compounds, it would be necessary to extend the waveform to +1.4 V, but this will be unnecessary for this work.

Catecholamine release in perfused adrenal slices

Release of catecholamine was detected in perfused adrenal slices. Varying stimulating currents were applied to the slice via a biphasic stimulating electrode. Typically, one 1.7-ms pulse was applied to the slice. Catecholamine release was seen to increase with increasing stimulation current. Interestingly, a group of slices showed an increase in catecholamine release with a slow decay over 60 s (Figure AII.3). The current did not return

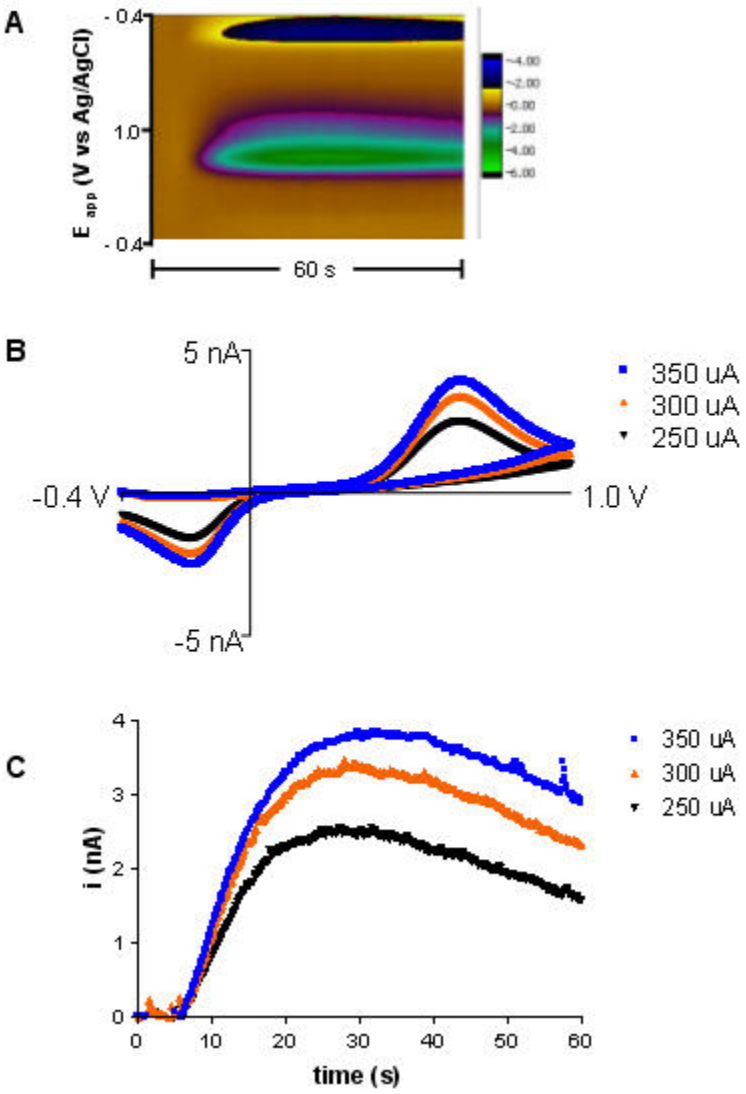

Figure AII.3. Stimulated catecholamine release in adrenal slices. One 1.7-ms stimulating pulse was applied to an adrenal slice at varying stimulating currents: 250, 300, and 350 µA. Data were collected using FSCV (A) Color plot depicting voltage along the ordinate and time along the abscissa. Current is shown as false color. (B) Cyclic voltammograms identifying catecholamine release due to epinephrine and/or norepinephrine. (C) Current (taken at the oxidation potential, +0.6 V) vs. time traces showing time course of catecholamine release.

to baseline in that time period. There has also been observation of stimulated current that did not exhibit this prolonged decay (Figure AII.4). The difference between these two responses may be a difference in sampling location and or differences in catecholamine uptake. Release that displayed the prolonged presence of catecholamine in the extracellular space may have been detected in a slice rich in cell clusters. The stimulating electrode essentially stimulates the entire slice; therefore, stimulating a slice abundant in chromaffin cell clusters may cause asynchronous release of the multiple clusters, which may explain the larger magnitude of current seen as well as the protracted presence of extracellular catecholamine. It is possible that the transporters in this area are unable to handle the amount of extracellular catecholamine present, which would result in the slow decay seen in the oxidative current. This prolonged release was also measured in the rat adrenal gland by Barbara et al. using amperometry (Barbara et al., 1998). On the other hand, the release exhibiting rapid decay may be due to measurement in an area in which only one cluster is located, thus showing synchronized release. Moreover, uptake may be more efficient in this type of location because the number of transporters available is sufficient to clear catecholamine from the extracellular space. The variability in cell cluster distribution may be attributed to heterogeneity in the medullary tissue or to disruption of the tissue during the slice preparation.

In Figure AII.5, an example of spontaneous release is shown. This may be due to the synchronous and efficient stimulation of a few chromaffin cell clusters as the current is also shown to decay rapidly. In some slices, this spontaneous release was noted with a frequency approximately every 5 min.

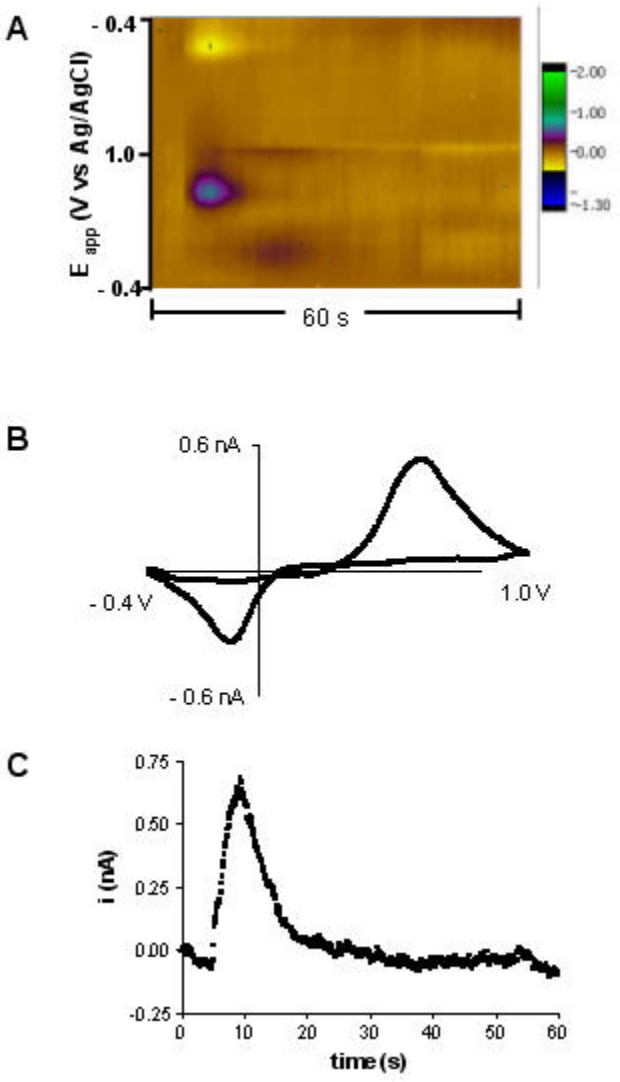

Figure AII.4. Stimulated catecholamine release exhibiting faster decay. One 1.7-ms stimulating pulse was applied to an adrenal slice at a stimulating current of 300 µA. Data were collected using FSCV (A) Color plot depicting voltage along the ordinate and time along the abscissa. Current is shown as false color. (B) Cyclic voltammogram identifying catecholamine release due to epinephrine and/or norepinephrine. (C) Current (taken at the oxidation potential, +0.6 V) vs. time trace showing time course of catecholamine release.

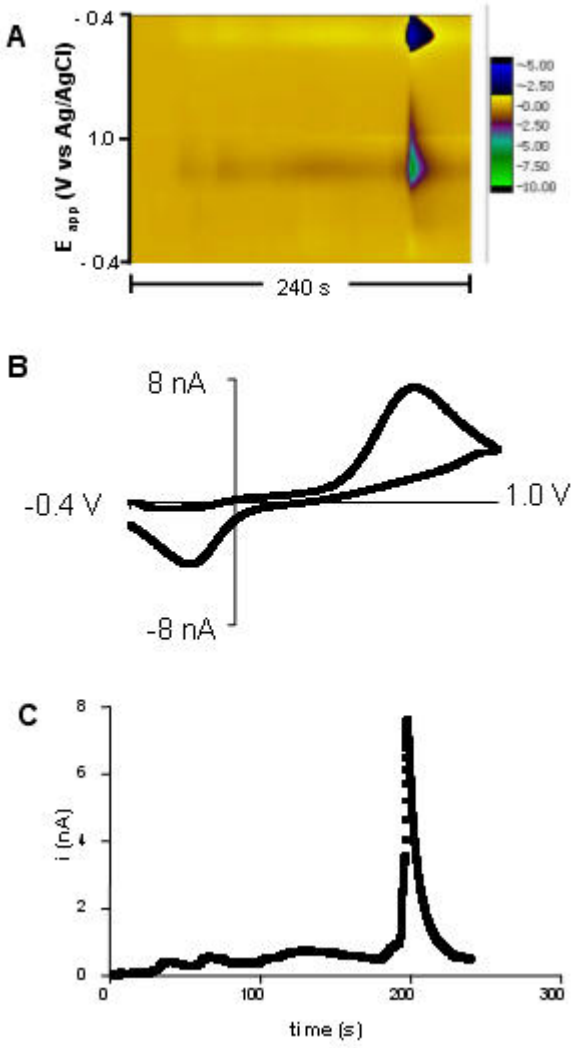

Figure AII.5. Spontaneous catecholamine release in adrenal slices. (A) Color plot depicting voltage along the ordinate and time along the abscissa. Current is shown as false color. (B) Cyclic voltammograms identifying catecholamine release due to epinephrine and/or norepinephrine. (C) Current (taken at the oxidation potential, +0.6 V) vs. time traces showing time course of catecholamine release. The nature of this release appears more synchronous that some of the previously measured stimulated release.

Murine adrenal slice preparations provide another avenue for studying exocytosis in chromaffin cells. Studies performed on perfused adrenal slices may provide complementary information to studies conducted on isolated cells to impart a fuller understanding of exocytosis in chromaffin cells. Knowledge of cellular mechanisms may contribute to a clearer insight to intercellular communication in chromaffin cells that may eventually be applied to exocytotic processes in neurons.

REFERENCES

Albillos A, Neher E, Moser T (2000) R-type Ca^{2+} channels are coupled to the rapid component of secretion in mouse adrenal slice chromaffin cells. Journal of Neuroscience 20:8323-8330.

Arroyo G, Fuentealba J, Sevane-Fernandez N, Aldea M, Garcia AG, Albillos A (2006) An amperometric study of the kinetics of exocytosis in mouse adrenal slice chromaffin cells: physiological and methodological insights. Journal of Neurophysiology in press.

Barbara J-G, Takeda K (1996) Quantal release at a neuronal nicotinic synapse from rat adrenal gland. Proceedings of the National Academy of Science 93:9905-9909.

Barbara J-G, Poncer JC, McKinney RA, Takeda K (1998) An adrenal slice preparation for the study of chromaffin cells and their cholinergic innervation. Journal of Neuroscience Methods 80:181-189.

Bath BD, Michael DJ, Trafton BJ, Joseph JD, Runnels PL, Wightman RM (2000) Subsecond adsorption and desorption of dopamine at carbon-fiber microelectrodes. Analytical Chemistry 72:5994-6002.

Iijima T, Matsumoto G, Kidokoro Y (1992) Synaptic activation of rat adrenal medulla examined with a large photodiode array in combination with a voltage-sensitive dye. Neuroscience 51:211-219.

Kajiwara R, Sand O, Kidokoro Y, Barish ME, Iijima T (1997) Functional organization of chromaffin cells and cholinergic synaptic transmission in rat adrenal medulla. Japanese Journal of Physiology 47:449-464.

Kawagoe KT, Zimmerman JB, Wightman RM (1993) Principles of voltammetry and microelectrode surface states. Journal of Neuroscience Methods 48:225-240.

Moro MA, Lopez MG, Gandia L, Michelena P, Garcia AG (1990) Separation and culture of living adrenaline- and noradrenaline-containing cells from bovine adrenal medullae. Analytical Biochemistry 185:243-248.

Puopolo M, Hochstetler SE, Gustincich S, Wightman RM, Raviola E (2001) Extrasynaptic release of dopamine in a retinal neuron: Activity dependence and transmitter modulation. Neuron 30:211-225.

Voets T, Neher E, Moser T (1999) Mechanisms underlying phasic and sustained secretion in chromaffin cells from mouse adrenal slices. Neuron 23:607-615.

Yamagami K, Moritoyo T, Wakamori M, Sorimachi M (2002) Limited intercellular spread of spontaneous Ca^{2+} signals via gap junctions between mouse chromaffin cells in situ. Neuroscience Letters 323:97-100.